THE PROCEEDINGS OF THE PHYSICAL SOCIETY

Section B

VOL. 63, PART 5 1 May 1950 No. 365 B

Summarized Proceedings of Symposium on Applications of Ultrasonics

BY G. BRADFIELD
National Physical Laboratory, Teddington, Middx.

Communicated by the Acoustics Group of the Society; *MS. received 26th July* 1949

ABSTRACT. A symposium of the Acoustics Group of the Physical Society, held on 18th February 1949, surveyed recent advances in (*a*) the investigation of the fundamental structure of matter; (*b*) telecommunication and allied applications; (*c*) use of mechanical forces set up by intense waves.

In (*a*) derivation of elastic constants of matter was an important field especially as small samples such as single crystals could be used. Losses incurred in propagating waves were surveyed with the help of an electrical transmission line model and simple versions of this were established to represent relaxation phenomena based on Maxwell's hypothesis of shear elasticity as a time function and on Kneser's treatment of loss due to delay in a storage process. There was excellent agreement of the latter with recent results on acetic acid.

Available sources of ultrasonic power were surveyed and the importance of barium titanate as a powerful and strongly coupled piezoelectric transducer was emphasized.

An expression for the receiver/transmitter power ratio in telecommunications systems was examined for gaseous, liquid and solid media and, from available data, optimum frequencies for various ranges were deduced. These were found to be in accord with experience in echo-sounding, earth exploration and in propagation in metals.

Accounts were given of experience with flaw detectors and echo-sounding which showed that these were becoming important industrially and in navigation; work on blind aids was unpromising. Advances in timing and time delay devices were described.

There is a dearth of important industrial applications of the use of intense waves in spite of the interesting phenomena which have been demonstrated in the laboratory. The importance of the study of cavitation was pointed out. Results were discussed for killing bacteria, disintegrating proteins, emulsifying, soldering aluminium and refining the crystalline structure in solidification of light alloys. Stress was laid on the wideness of the frequency spectrum over which these phenomena occurred and on the difficulties and importance of maintaining temperature constant and of measuring intensities during investigations.

§ 1. THE INVESTIGATION OF THE FUNDAMENTAL STRUCTURE OF MATTER

In this first section the simplest application is the derivation of elastic constants of solids and of adiabatic compressibility of fluids, through measurement of velocity. In solids an important case is that of small single crystals, the anisotropic properties of which can be more readily measured by ultrasonic waves than by alternative methods. Velocity and absorption tests in gases yield valuable information about molecular shape and spin and collision phenomena. Gaps in our knowledge exist of the performance of gases at high temperatures and the properties of mixtures of gases. In liquids the recent recognition of the error arising from neglect of dilatational viscosity has removed one serious divergence between theory and experiment.

Dr. Pinkerton emphasized the value of ultrasonic velocity and absorption measurements in determining relaxation times and thus providing information about molecular equilibria not otherwise obtainable. Three classes of relaxation phenomena may be distinguished: (i) the sharing of vibratory energy; (ii) changes in the local order of the molecules affecting the volume they occupy; (iii) chemical or quasi-chemical changes affecting the relative proportions of two or more molecular species.

The first and last effects were thought to be due to the temperature changes involving a relaxing specific heat while the second may be due either to this cause or to the vibratory changes or to both together.

It is convenient to consider the behaviour of a material propagating mechanical waves by using a model in the form of an electrical transmission line propagating an electromagnetic wave, the analogous expressions for the velocities v in these cases being

$$v_e = (LC)^{-\frac{1}{2}}, \qquad \ldots\ldots(1)$$

$$v_s = (\rho/n)^{-\frac{1}{2}} \text{ (shear wave in solid)}, \qquad \ldots\ldots(2)$$

$$v_l = \left\{\frac{\rho}{4n/3 + k}\right\}^{-\frac{1}{2}} \text{ (longitudinal wave in solid)}, \qquad \ldots\ldots(3)$$

$$v_l = (\rho\beta)^{-\frac{1}{2}} \text{ (longitudinal wave in liquid)}, \qquad \ldots\ldots(4)$$

where L, the inductance per unit length, corresponds with density ρ, and C the capacity per unit length corresponds with $1/n$, the reciprocal of the modulus of rigidity, or with $1/(4n/3+k)$, or with β, the adiabatic compressibility $(=1/k)$ respectively in (2), (3) and (4).

The attenuation of a line with a resistance R in series with C (Figure 1 (*a*)), $R \ll 1/\omega C$, is

$$\alpha = \tfrac{1}{2}\omega^2 R(LC^3)^{\frac{1}{2}}, \qquad \text{i.e.} \quad \alpha/\nu^2 = 2\pi^2 R(LC^3)^{\frac{1}{2}},$$

so that α/ν^2 is independent of frequency ν, and the model correctly represents the attenuation–frequency characteristic common to all fluids in the absence of relaxation phenomena.

Maxwell's hypothesis that viscosity be regarded as a shear elasticity diminishing exponentially with time leads, as suggested by Mason (1947), to Figure 1 (*b*), a condenser C_S shunting R with the normal relationship of α and ν at low frequencies but with a velocity increase to $[(1/C+1/C_S)/L]^{\frac{1}{2}}$ at high frequencies, when the attenuation is independent of frequency.

Liquids whose molecules are highly polymerized have been studied by Mason and his co-workers (1948). They found that polymers of isobutylene behave like solids at high frequencies in transmitting shearing waves and possessing shear elasticity. The velocity of longitudinal waves increased by 20% or more with increasing frequency. The shear elasticity possessed two components associated with different relaxation times, and the shorter time was found to vary with temperature in a manner similar to that in the case of acetic acid discussed below. These two components of shear elasticity are ascribed to two different types of relative motion between the long chain-like molecules of the polymers. The theoretical treatment given by Mason is in terms of an equivalent transmission line more complex than any of those discussed above; good agreement between theory and experiment was found.

During compression, energy is shared by various storage processes, so that a definite fraction is involved in any one relaxation process. The transmission line model can cover this case by adding to the simple network across R and C an additional pair of series elements R' and C' (see Figure 1 (*a*)), of time constant τ, where $C' \ll C$. It can readily be shown that α, the attenuation constant, is given by

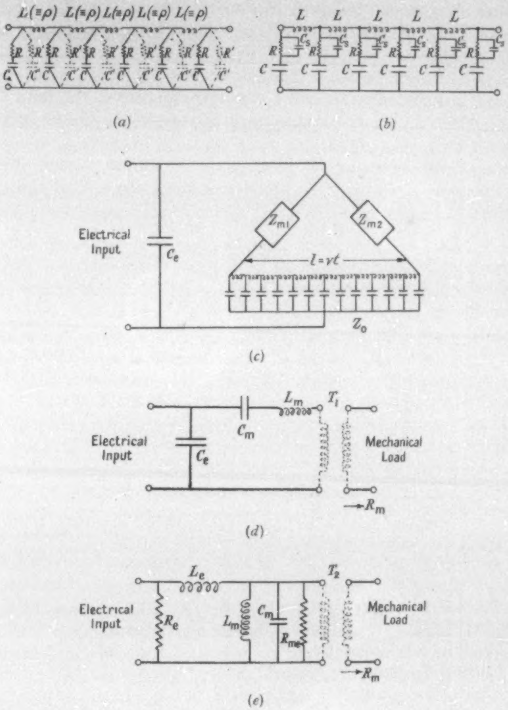

L(≡ρ) L(≡ρ) L(≡ρ) L(≡ρ) L(≡ρ)
R R′ C C′
(a)
L L L L L
R C C_s
(b)
Electrical Input
C_e
Z_m1
Z_m2
l = vt
Z_0
(c)
Electrical Input
C_e
C_m
L_m
T_1
Mechanical Load
R_m
(d)
Electrical Input
L_e
R_e
L_m
C_m
R_m
T_2
Mechanical Load
R_m
(e)

Figure 1.

$$\alpha = (C^1/2CV_\infty)\omega^2\tau/(1+\omega^2\tau^2), \qquad \ldots\ldots(5)$$

where V_∞ is the velocity at high frequencies. Maximum attenuation per wavelength μ_m, where $\mu = \alpha\lambda = \alpha v_1/\nu = 2\pi\alpha v_1/\omega$, occurs when $\tau = 1/\omega$, i.e.

$$\mu_m = \tfrac{1}{2}\pi C^1/C. \qquad \ldots\ldots(6)$$

Introduction of μ_m in (5) leads to the relation for α/ν^2 proposed by Kneser (1938). Similarly it is clear that at high frequencies such that $R^1 \gg 1/\omega C^1$ the velocity is independent of C^1 so that the total dispersion $(V_\infty - V_0)/V_\infty$ is, as given by Kneser,

$$(V_\infty - V_0)/V_\infty = C^1/2C = \mu_m/\pi. \qquad \ldots\ldots(7)$$

Equation (7) shows that the total molecular energy which is involved in the relaxation process can be found by measuring either μ_m or $(V_\infty - V_0)/V_\infty$; the measurements have necessarily to be carried out in the vicinity of the critical frequency $\omega = 1/\tau$.

In the case of those relaxation processes where the equilibrium is shifted by the adiabatic changes of temperature during propagation, the ratio C^1/C takes the form $(\gamma - 1)Ci/C_p$, where γ is the ratio of the specific heats and Ci is a relaxing specific heat.

Bauer's (1949) treatment of absorption in simple organic liquids with symmetrical molecules and no hydroxyl groupings shows that the abnormally high value is due to slow exchange of the vibratory energy, consonant with the weak intermolecular forces in these liquids. He predicts such high values for ν_m for typical liquids in this class, e.g. benzene and carbon tetrachloride, that the demonstration of relaxation effects in them would be very difficult in practice. Rapuano (1948), however, finds some evidence of abnormality in α/ν^2 between 10 and 75 Mc/s. in carbon disulphide.

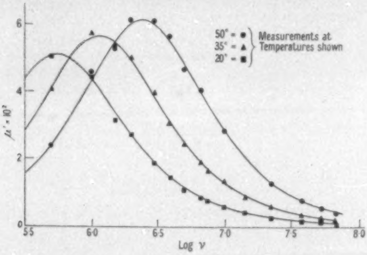

Figure 2. Absorption in acetic acid.

Plot of μ', the excess of absorption/λ over a constant term $A\nu^2$ for frequencies 0·5 to 67 Mc/s. (Lamb and Pinkerton 1949).

Curves were plotted from equation (5), using experimental values of contants.

In a class of liquids including water and the lower primary alcohols, the absorption is two or three times that expected from shear viscosity and is related to it, but no evidence for a relaxation process exists. In contrast with the previous class, absorption falls rapidly with temperature (Pinkerton 1949).

A relaxation process apparently arising from chemical dissociation or other change of molecular structure is evident in acetic acid, in aqueous solutions of its salts and in its methyl and ethyl esters. Investigation of acetic acid showed τ to be about 0·32 microsecond at 17° c., and Spakowski (1938) suggested that such a long time of equilibration corresponds to a chemical change connected with the linking and break-up of the dimer. The closeness of theory and experiment is shown in Figure 2, in which the excess absorption per wavelength is plotted against

$\log \nu$; the difference between the experimental points and the curves calculated from equation (5) by Lamb and Pinkerton (1949) is remarkably small.

The rapid change of τ with temperature evident in Figure 1 follows the law

$$\tau = \tau_0 \exp (\Delta E_a / \boldsymbol{R}T),$$

E_a, which is about 8,900 cal/gm. mol, can be regarded as an activation energy (cf. Hall 1948). Should the dissociation of the dimer of acetic acid be responsible for relaxation effects, then from the known heat of dissociation it should be possible to calculate the absorption and dispersion. Since this yields a value of absorption much less than that observed and also predicts a more violent variation of dispersion with temperature, the precise nature of the process remains somewhat obscure.

Dr. Pinkerton felt that there was little doubt that ultrasonic studies of the types outlined above were likely to reveal much that is fundamental about the liquid state.

§ 2. TELECOMMUNICATION AND ALLIED APPLICATIONS

As a preliminary to a review of applications in the fields of telecommunication and of high intensity irradiation, Mr. Bradfield discussed electromechanical transducer performance. The general network for the piezoelectric type is given in Figure 1 (*c*), where Z_{m_1} and Z_{m_2} are proportional to the terminating mechanical impedances on the element represented by a transmission line of travel time l/v, l being the length and v the mechanical wave velocity; near the half-wavelength resonance, this network simplifies to Figure 1 (*d*), where the transformer ratio of T_1 involves the dimensions and piezoelectric constant. The corresponding network for a magnetostrictive transducer is given in Figure 1 (*e*), but in this case the transformer T_2, besides involving a magnetostrictive constant, also inverts the mechanical load impedance. In Figures 1 (*d*) and (*e*), the ratios C_m/C_e and L_m/L_e represent the tightness of coupling of the electric and mechanical sides of the transducer and are proportional to the ratio of stored mechanical energy to stored electric (or magnetic) energy. In Table 1 performances are compared for typical materials, including also values for the moving conductor type of transducer.

The values for the hammer blow (i.e. last line on Table 1) obtainable from these materials show that barium titanate should be over 100 times better than quartz or nickel. The coupling factor C_m/C_e, which is a measure of bandwidth, was similarly about 100 times as good as for quartz. Although little detailed work has yet been done on the use of barium titanate for ultrasonic applications, its potentialities for this work seem to be very great.

The maximum intensity from various materials for c.w. operation will approximate to the expression $\Delta^2 E^{\frac{3}{2}}/\rho^{\frac{1}{2}}$, with a value of rather over 60 watts/cm^2 for a single-ended X-cut quartz transducer, which agrees well with practical experience.

High efficiency, though not of paramount importance in telecommunication applications, may prove vital for industrial applications requiring intense irradiation. Quartz transducers are good and barium titanate* should be similar but much more convenient in use. The efficiency of magnetostrictive transducers is

---

* *Note added in proof.* Whether its low Q (150–200) and consequent heating will be troublesome has yet to be seen.

Table 1. Comparison of Ultrasonic Sources

			Piezoelectric		Magnetostriction		Moving conductor	
		Note	Quartz X-cut	Barium Titanate (Mason 1948)	Nickel	Cobalt–Iron (50 : 50)	Copper	Aluminium
Density	ρ		2·66	5·5	8·9	8·2	8·9	2·7
Young's modulus in dynes/cm²	E		$7{\cdot}8\times10^{11}(=1/S_{11})$	12×10^{11}	20×10^{11}	22×10^{11}	$12{\cdot}3\times10^{11}$	$7{\cdot}1\times10^{11}$
Velocity (m/sec.)	$c=(E/\rho)^{\frac{1}{2}}$		5400	4700	4750	5200	3710	5120
Characteristic impedance (C.G.S. units)	$(E\rho)^{\frac{1}{2}}$		$1{\cdot}4\times10^{6}$	$2{\cdot}6\times10^{6}$	$4{\cdot}23\times10^{6}$	$4{\cdot}10\times10^{6}$	$3{\cdot}31\times10^{6}$	$1{\cdot}38\times10^{6}$
Electric or magnetic strain conditions	—	(3)	±130 kv/cm.	+30 kv/cm. to −7·5 kv/cm.	5500 lines/cm² 102 oersteds	20000 lines/cm² 66 oersteds	10000 amp/cm² 15000 lines/cm²	6600 amp/cm² 15000 lines/cm²
Mechanical strain (max.)	Δ		$\pm3\times10^{-5}$	6×10^{-4} total	3×10^{-5}	$4{\cdot}9\times10^{-5}$	—	—
Open-circuit pressure (dynes/cm²)	$P_{\max}=E\Delta$	(1)	47×10^{6}	720×10^{6}	60×10^{6}	105×10^{6}	—	—
(kg/cm²)	—		48	730	61	107	22	14
Short-circuit velocity (cm/sec.)	$c\Delta$	(1)	32	280	14	25	6½	10
Crushing strength (dynes/cm²)	—		10^{10}	—	$5{\cdot}3\times10^{9}$	—	$3{\cdot}5\times10^{9}$	$1{\cdot}8\times10^{9}$
Maximum intensity (watts/cm²)	$I_{\max}$	(1) (2)	38	5000	21	63	3½	3½

(1) Complete reversal for quartz. 30 to −7·5 kv/cm. for barium titanate. Zero to maximum current for moving conductor.

(2) $I_{\max}=\frac{1}{4}\Delta^2(E^3/\rho)^{\frac{1}{2}}$ into matched load at each end.

(3) 102 oersteds is for half-hard nickel. Decreases to about 20 oersteds for soft nickel.

lower but, for lower frequencies, about 65% efficiency can be attained by good design using nickel radiating into water; a somewhat higher efficiency is possible for cobalt–iron for alloys.

For generating or receiving waves in air, transducers with solid elements are disadvantageous because of the low characteristic impedance of the medium, and although bilamellar elements help, especially for reception, a high power transmitter of the siren type (Allen and Rudneck 1947) is much more promising. The source intensity is here around 400 watt/cm² and efficiency about 20%, while powers up to 2 kw., or even more, do not seem difficult to obtain.

In telecommunication and allied applications, absorption plays as important a part as geometrical spreading in limiting the range of ultrasonic propagation. The overall attenuation of the system is the product of factors representing radiating and receiving array gains, geometrical spreading and absorption loss together with a scattering or reflection coefficient in the case of echoes of radar type. For fluids in the absence of relaxation phenomena the attenuation can be expressed

$$\frac{P_r}{P_g} = \text{const.}\,\frac{D^4}{\lambda^2 x^2}\exp\left(\frac{-2ax}{\lambda^2}\right), \qquad \ldots\ldots(8)$$

where P_r is the electrical power from the receiving transducer, P_g the electrical power input to the transmitting transducer, $D(\gg\lambda)$ is the diameter of the transmitting and receiving arrays, x is the total path length and $a = \alpha\lambda^2$ and is independent of frequency.

Equation (8) can apply to solids if the index 2 of λ in the exponential term be replaced by m, the value of which varies from unity for material of fine grain at lower frequencies to about 4 for coarser grains and higher frequencies. The index of x shown as 2 applies to extensive specularly reflecting surfaces. For extensive scattering surfaces this index rises to 4.

These expressions lead to optimum wavelengths λ_0 for propagating over any given path length with minimum attenuation:

$$\text{for fluids } (m=2), \qquad \lambda_0 = (2ax)^{\frac{1}{2}}, \qquad \ldots\ldots(9)$$

$$\text{for solids } (m=1), \qquad \lambda_0 = a'x, \qquad \ldots\ldots(10)$$

where the exponent in (8) is $-2a'x/\lambda$.

Some modification has to be made in the case of echoes from small targets. The optimum wavelength λ_0' then equals about $0{\cdot}43\,\lambda_0$.

In this way various media and various distances have appropriate optimum frequencies as in Table 2.

Table 2

		Optimum frequency for given distance				
Medium	a or a'	1 ft.	10 ft.	100 ft.	1000 ft.	10000 ft.
Nitrogen	$1{\cdot}9\times10^{-4}$	—	98 kc/s.	31 kc/s.	9·8 kc/s.	3·1 kc/s.
Pure water	$5{\cdot}5\times10^{-6}$	8 Mc/s.	2·5 Mc/s.	800 kc/s.	250 kc/s.	80 kc/s.
Sea-water	3×10^{-4}	Relaxation region			35 kc/s.	11 kc/s.
Mudstone	$a'=\alpha\lambda=0{\cdot}08$ $(m=1)$	120 kc/s.	12 kc/s.	1200 c/s.	120 c/s.	12 c/s.
Aluminium	$a'=4\times10^{-4}$ $(m=1)$	$m\neq1$	5·4 Mc/s.	540 kc/s.	54 kc/s.	—

It follows that it is impracticable to explore in a mudstone medium with extensive radiators as they would become impossibly unwieldy. But clearly exploration, or flaw detection, in a metal such as aluminium is readily possible at a frequency of a few megacycles per second.

The above relationships appear to agree well with practical results and hold for a wide range of variables. For instance, the frequency of about 30 c/s. can be shown to be about optimum for range of about 5,000 feet in geophysical survey. Where the medium is anomalous, as for example air, the choice of optimum frequency is more difficult but for the rather unfavourable case of air at 90% humidity, frequencies are about one-third of those in Table 2.

One of the most important applications of ultrasonics in the telecommunication and allied fields is the provision of precision timing elements, such as quartz frequency standards, the quartz crystal 'clock' and the provision of loss-free electromechanical filter elements for band-pass networks. It may be noted that in these fields a new substance, ethylene diamine tartrate, seems to promise distinct advantages over quartz because of its higher C_m/C_e ratio, and its loss is quite low—about two or three times that of quartz. Flaw detection or ultrasonic non-destructive testing competes with echo-sounding for leading place among other applications, and several speakers described experience with the British system of flaw detection. In this country attention has been concentrated on pulse systems, but in Germany the C.W. systems of Trost and Pohlmann seem to have had some success and may be superior for certain specialized tasks. The British system scans the body by movement of the transmitting and receiving elements, but consideration is now being given to means for steering the beams to curtail labour in scanning. Other minor improvements include the direct indication of the efficiency of contact between transducer and specimen, a matter of great importance if any quantitative estimate of flaw magnitude is attempted.

Mr. D. O. Sproule described the principle and operation of a commercial flaw detector using the pulse method. The equipment normally operated at 2½ Mc/s., but modified modes of working enabled frequencies down to ½ Mc/s. to be used with the same X-cut quartz crystal probes or transducers. The use of high frequencies permits the radiation to be concentrated in a beam, the half-amplitude semi-angle of the beam at 2½ Mc/s. being about 5°. The beams can be reflected and scattered rather like light beams and, since the wavelength in steel at this frequency is about 2½ mm., flaws of this order of size or even smaller can, in suitable circumstances, be readily detected. The equipment has many points of similarity with radar; a short electrical wave train is converted to mechanical waves and transmitted by one crystal probe, the received waves are picked up by a similar probe and, after amplification and rectification, displayed on an amplitude–range trace. The general schematic diagram of the system and the overlap of the polar diagrams for transmitting and receiving are shown in Figures 3 (*a*) and (*b*); Figure 3 (*b*) shows how short-range operation can be achieved with special probes in which the crystals transmit through metal wedges. Typical results on a special 1⅞ in. thick steel test piece are given in Figure 4 (Plate I). In this case the 'flaws' were long drilled holes parallel to the surface and 1¼ in. below it, their axes being normal to the line joining the wedge-mounted transducers.

Mr. Sproule said that testing with an oil film was satisfactory on plane surfaces but not with a 'rough-as-rolled' surface. In the latter case some improvement

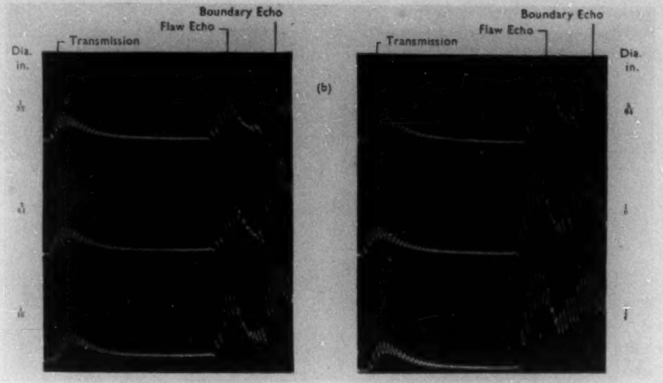

Figure 4. Echoes from cylindrical flaws.

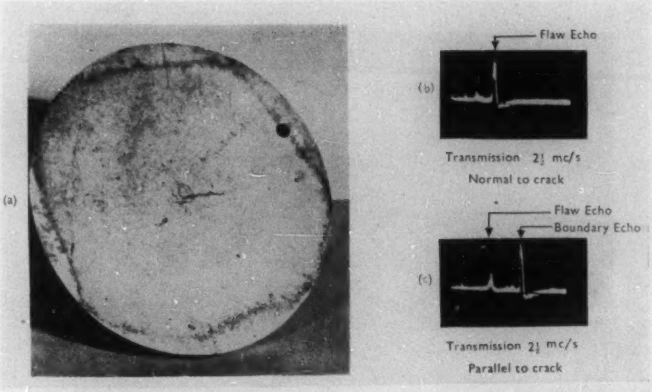
(a)
Flaw Echo
(b)
Transmission 2½ mc/s
Normal to crack
Flaw Echo
Boundary Echo
(c)
Transmission 2½ mc/s
Parallel to crack

Figure 5. Cast aluminium billet 18 inches dia. showing effect of orientation of large shrinkage crack.

PLATE I.

To face page 312

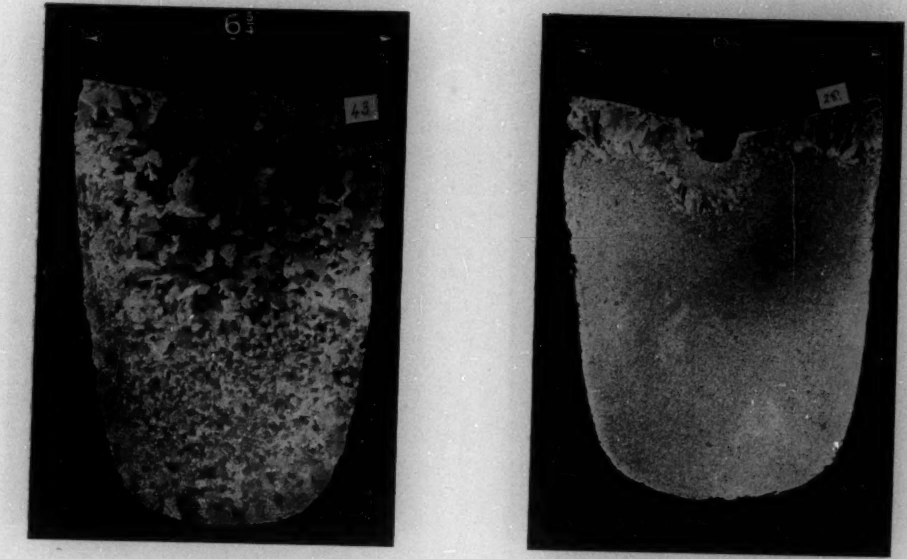

Solidified normally.

Solidified under the influence of ultrasonic agitation.

Figure 7. Solidification under ultrasonic agitation.

20 lb. melts of aluminium 4% copper alloy.

PLATE II.

resulted from a reduction of frequency from 2¼ to 1¼ Mc/s., but better results were obtained at 2¼ Mc/s. with an amalgam film. Shaped probe surfaces were often helpful.

Rolled and extended materials were generally better than cast, and excellent resnlts were obtained on such materials as aluminium alloys. On porous materials a reduction to 1½ Mc/s. often revealed faults much more distinctly. With care some very good results were achieved: see, for example, Figure 5 which shows even the orientation of a certain flaw in a cast aluminium bar.

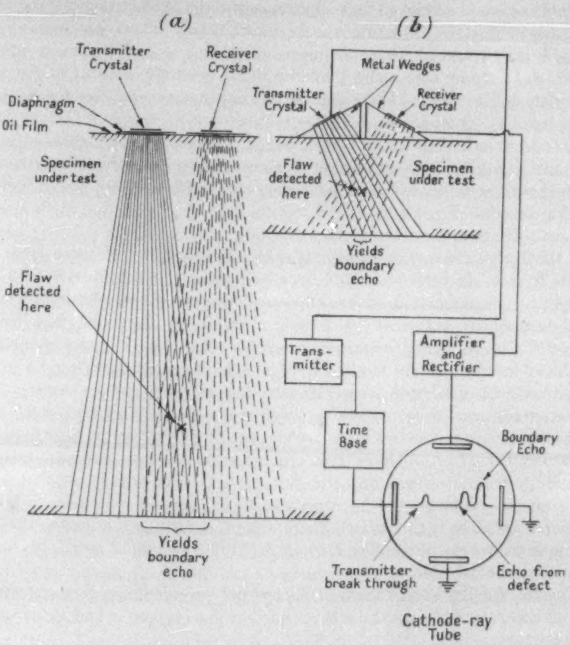
(a)
Transmitter Crystal
Receiver Crystal
Diaphragm
Oil Film
Specimen under test
Flaw detected here
Yields boundary echo
(b)
Metal Wedges
Transmitter Crystal
Receiver Crystal
Flaw detected here
Specimen under test
Yields boundary echo
Trans-mitter
Amplifier and Rectifier
Time Base
Boundary Echo
Transmitter break through
Echo from defect
Cathode-ray Tube

Figure 3. British flaw-detection system.

Mr. G. T. Harris described the use of the flaw detecting equipment for the routine inspection of many thousands of costly austenitic alloy steel forgings for gas turbine rotors which had to withstand very great stress in use at speeds up to 30,000 r.p.m. and temperatures up to 750° c. The rotor blanks were 6 in. thick and 9 in. to 40 in. in diameter, the flat faces being carefully surfaced for application of the probes. This thickness was too great for normal x-ray testing; as the blanks had been flattened, no guidance was obtainable from examination of the surface so that the ultrasonic method seemed without rival. It was found that porosity or defects of the order of half a millimetre or even less could be detected by this means, although it was impossible to differentiate between the presence of a single serious defect and a patch of pinhole porosity or non-metallic inclusions. However, a grading scheme was successfully adopted for defects and the grading achieved checked consistently on re-examination. Besides examination of the blanks, the original ingots were successfully inspected from machined 45° flats on the corners, the indications of primary and secondary piping and of axial porosity correlating well with subsequent sectioning. The blooms used, which were up to 2 feet diameter, were provided with three or four lengthwise machined flats at 90°, inspection then being carried out by the usual echo method, by observation of the bottom echo or by side-to-side transmission.

Mr. Heselwood described four applications of the above described equipment to the steel industry. The first was to detect 'hairline' cracks, once a serious trouble but now less so owing to improved techniques. The cracks are disc-shaped, about 6 mm. across and ¼ micron thick, generally parallel to the surface of the plate, billet or bar. These were readily detected except when few in number and as small as ½ mm. across.

Defects of the lamination type could often be detected with the same equipment but transmitting through from side to side. Quite extensive sheets could be searched with suitable lead arrangements; water with a little wetting agent was used for contact. For plates of sufficient thickness, the reflection method proved more sensitive than the transmission method.

A third application was for testing cold-rolling rolls which were from about 2 in. to 20 in. in diameter and were made by forging to shape followed by a heat treatment. The hardening of the skin was accompanied by high internal stresses often dangerously enhanced by flaws. Ultrasonic inspection has been so successful that no breaks occurred in service after this system was instituted. Finally, an interesting case was described of a 4½ in. square steel ingot which had crystallized with dendrites normal to each face meeting at the diagonal planes. The latter appeared to reflect the rays well while the crystals apparently guided the rays. This structure prevents normal use of ultrasonics in ingots, and such effects together with the 'looseness' often present in steel castings, made flaw detection difficult. Discussing the future, Mr. Heselwood felt that besides improvement (which should be applicable to all types of materials) to facilitate flaw detection close to the surface, there was room for much improvement in the technique for testing iron and steel castings, while a system of rapid scan for large areas would be valuable.

Mr. H. W. Taylor summarized four years' experience in flaw detection on aluminium alloy extrusions and cast billets; routine inspection had been instituted for these cases.

Extrusions required no surface preparation beyond the application of a thin oil film before inspection. Rectangular extrusions could be inspected at the rate of five feet per minute. In the case of extruded bar, which had to be rotated during traversal, the inspection rate dropped to two feet per minute. In rectangular bars he considered that it was possible to deduce the size and configuration of a defect from the flaw detector indications, but correlation was not so good with round bars even with shaped crystal mountings, and the difficulty increased with bars as small as two inches in diameter, although increase in transmitter power was helpful. To avoid misleading results, the probes needed to be in a common tangential plane with the bar. In only one instance was an area of segregate located by ultrasonic inspection.

Cast materials were more difficult to test, and it was often necessary to lower the test frequency. It was generally essential to cut or grind flats on the billets to provide reasonable test surfaces. It was better to test billets from the cylindrical surfaces as effects believed to arise from the orientation of crystals prevented successful testing from the ends. A high-power transmitter was needed when absorption occurred, as in high zinc content alloys, but even these could be tested up to diameters of sixteen inches. Porosity appeared as a mass of reflections varying with small movements of the probes and in such cases a low frequency helped to distinguish defects, although skill was needed to interpret the flaw detector indications. The ultrasonic inspection of cast material was very valuable in detecting gross defects before extrusion, and in monitoring the casting process

Before describing the next important application, i.e. echo-sounding for ships, mention should be made of the possibilities of this technique in air. Two main applications might be vehicular guidance in fog and an aid to the blind.

In considering the possible use of an ultrasonic guiding device for blind people, it was emphasized that the generation and pick-up of the ultrasonic beam constituted a relatively simple part of the problem, the major difficulties arising from the specular nature of most reflections, the need for extreme lightness and the need to present the picked-up information in a form which could be easily assimilated. Publicity had been avoided for fear of raising the hopes of blind people prematurely. Mr. Beurle said any easy use of ultrasonic devices was unlikely and first described the way in which audible noises were used, surprisingly effectively, to guide blind people. Ultrasonic means might give three advantages, firstly in being inconspicuous, secondly in being less disturbed by ambient noises, and thirdly by increasing the scattering signal from slightly rough surfaces such as walls. A compromise at 50 kc/s. to avoid excessive absorption in air had been found reasonable, and bilamellar or 'bimorph' piezoelectric generating and receiving crystals in parabolic reflectors had worked well. Using a pulse length of about $\frac{1}{2}$ msec. and rate of about 20 p.p.s., it had been found best to combine the rectified transmitted and received pulses after limiting and then to present them aurally to the blind man. Often it was even possible to distinguish between a wall, a fence and a hedge in this way. Although development is not far advanced, the narrow beam ultrasonic device has a strong competitor in a wide-angle device, using binaural direction-finding and operating at the higher audible frequencies. Mr. Beurle felt that, at present, the latter device showed more promise.

Mr. D. O. Sproule discussed echo-sounding for ships with special reference to a modern magnetostriction type echo-sounding recorder (Figure 6). A toroidal ring of nickel laminations is used as transmitting transducer in the usual pulse system, reception being on a similar transducer. The signal after amplication is marked by a moving stylus on chemical recording paper, the delay in the return of the signal due to its travel time in the water being indicated by the displacement of the mark produced with reference to a datum line. In considering the choice of frequency for transmission, practical considerations may modify somewhat the optimum value deduced from Mr. Bradfield's fundamental equations (8) and (9): high accuracy in range might be required or freedom from the influence of the ship's rolling or of the slope of the sea-bed might be needed, and the water itself might be salt or fresh, aerated or emulsified with mud; the ship's noise spectrum may also play a part. The equation gives a frequency of 15 kc/s. for 800 metre depth in sea-water, and experience shows this to be about right. A compromise has to be struck as regards the effect of rolling of the ship, since at 15 kc/s., with the equipment sketched in Figure 6, the main lobe semi-angle is about 20° (using 12 to 14 in. aperture), and consequently in heavy weather a record is only obtained for part of the time.

One of the main practical difficulties is the impedance of the skin of the hull which is at least $\frac{3}{8}$ in. thick and in the case of the *Queen Mary* is $1\frac{1}{4}$ in. thick. Furthermore, this thick skin transmits machinery noise which tends to obscure echoes. The high noise level and thick skin reduced range on this ship to 600 fathoms (1,200 yd.) using a frequency of 15 kc/s. and a 5 joule condenser discharge through the magnetostrictive transducer. In some other trials it was found that a range of 1,800 fathoms would be reduced to about 260 fathoms in a storm due to aeration of the water and to noise. As an example of the use of lower frequencies

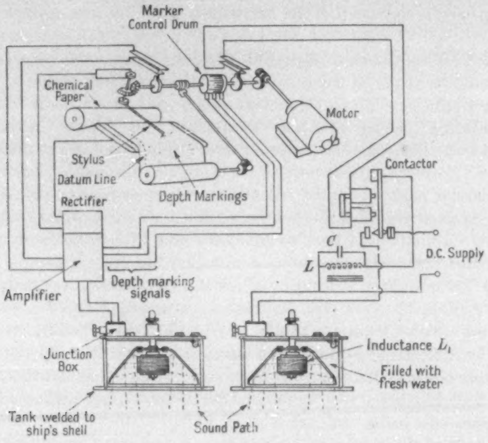
Marker
Control Drum
Chemical
Paper
Motor
Stylus
Datum Line
Rectifier
Depth Markings
Contactor
C
L
D.C. Supply
Amplifier
Depth marking
signals
Junction
Box
Inductance L_1
Filled with
fresh water
Tank welded to
ship's shell
Sound Path

(*a*) Schematic diagram of equipment.

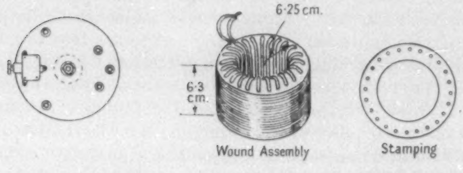
6·25 cm.
6·3
cm.
Wound Assembly
Stamping

(*b*) Plan view of oscillator mounted in tank.

(*c*) 15 kc/s. magnetostriction transducer.

Figure 6. Echo-sounding recorder of magnetostriction type.

for greater range, a 9,000 metre range was obtained at 10 kc/s., using a 10 joule condenser discharge. It is interesting to note that, for short ranges, say 40 feet, even using 15 kc/s., it is possible to measure to an accuracy of 3 inches, which is just under a wavelength in water.

Mr. Sproule concluded by giving details of the equipment employed (see also Wood *et al.* 1935). A motor system drives stylus, paper, marking drum and transmitting and receiving cam-operated contacts roughly as shown in Figure 6 (*a*). When the contactor is operated, the energy in the high-inductance choke L surges into the condenser C, by which time the contactor connects the transmitter to the transducer and a damped train results at $7\frac{1}{2}$ kc/s., the mechanical wave being, however, at 15 kc/s. For a typical discharge of 2 joules, a magnetostrictive transducer as in Figure 6 (*b*) will have a contraction of about 0·004 mm. on the diameter, with radiation about 540 watts at 2 watt/cm^2, and mechanical Q about 10. The receiver transducer is similar but operated with polarization (the residual flux after saturation). The bandwidth of the amplifier is about $1\frac{1}{2}$ kc/s.; its gain is controlled by an exponentially falling grid bias (initiated by a cam-operated contact) to lessen overloading by the stronger signals occurring at short range.

An ultrasonic application unique in its way is the delay line where times of the order of a millisecond and waves with bandwidths of 1 Mc/s. or more are involved. In television phraseology it was possible to store about 2,000 picture points and change these 500 times a second.

Successful ultrasonic delay lines have been made, using either solid or liquid propagating media, the former being longer, less troublesome in use but more difficult to design. Carrier frequency operation was universally adopted to obtain a uniform phase shift–frequency rate over the wide-frequency band transmitted.

Mr. H. Grayson gave an account of water delay lines pointing out that the $1\frac{1}{2}$ metres required for a millisecond delay corresponded to the travel time in 200 miles of electrical cable. The frequency used, which was always such that the transducer had an aperture of many wavelengths, depended on the bandwidth required. A compromise was necessary between the higher path absorption at the higher frequency, and the higher losses occurring with complex electrical terminating networks when a wide bandwidth with low carrier frequency is essential. Other factors in this choice are the objectionable tilt occurring on the attenuation–frequency characteristic for the high frequencies and the danger of multiple path effects if the attenuation is too low with low frequencies. Using quartz transducers working on one face only, water provides a bandwidth of about 10% with simple terminating networks. Although water has an absorption of about 30 db. at 10 Mc/s. for 1 millisecond delay at normal temperatures, refraction effects have been found troublesome, and it has been found better on this account to work at about 73° c., where the temperature–velocity gradient was zero; fortunately the absorption is also lower there.

Mercury lines were similar in length to water lines; they had the advantage of much greater bandwidth and lower attenuation, but their design and maintenance presented serious difficulties.

Mr. Bradfield said that these accounts did not by any means exhaust applications in this field. He touched on such applications as echo methods in rock and concrete, echo exploration of liquid-filled underground cavities and measurement of velocity and absorption in fluids, hydrosols and aerosols as an aid to analysis.

§3. APPLICATIONS OF THE MECHANICAL FORCES SET UP BY INTENSE RADIATION

Mr. Bradfield then introduced the discussion on high-intensity ultrasonics pointing out that, though spectacular experiments had been made, little industrial application had taken place in this field. In early days effects such as the killing of bacteria had been obscured by the simultaneous heating which occurred, but this complication was now avoided.

In approaching this subject, four points should be borne in mind. (i) Particle sizes did not seem to be critical; for instance, protozoa at say $20\,\mu$, bacteria a few microns in size and protein molecules of, say, 100 A. all seem vulnerable to a wavelength of 2 mm., i.e. 100 to 200,000 times greater. (ii) There is little evidence of optimum frequencies; indeed effects often persist down to audible frequencies. (iii) The accelerations involved are astonishingly great. (iv) Cavitation, which occurs when the intensity exceeds a few watts/cm^2, certainly plays a very important part.

Dr. B. E. Noltingk agreed that cavitation was very important in high intensity irradiation, and that nuclei appeared necessary for this to occur so that the effect of impurities would need to be studied closely. As a point of interest, he reported some experimental evidence that cavitation voids may be more like 'hairline' cracks than spherical hollows. Cavitation was not pronounced at a frequency of about 1 Mc/s. and oscillatory pressures of about 5 atmospheres but was violent at about 20 kc/s. frequency at 3 atmospheres pressure, subsiding into mere bubble formation at 1 atmosphere. Emulsification was especially easy at low frequencies and any pair of immiscible liquids could be emulsified at 20 kc/s. (except those having a metal as one constituent).

Mr. G. M. Wells remarked that, in spite of the number of interesting possibilities, there was a dearth of actual industrial application of intense ultrasonic waves. There was a serious lack of precise information as to the way in which actions such as emulsification, dispersion and sterilization depend on frequency. The widespread adoption of the frequency range of 200 to 1,000 kc/s. was largely due to the convenience of generation from quartz vibrators. High intensities were readily obtainable in this way, and he had used quartz up to 50 watts/cm^2. Cavitation was clearly of importance and its variation with frequency should be studied. The assumption that its onset coincided with negative pressure in the liquid implied invariance of threshold intensity with frequency, a prediction not borne out by experience, since it had been found easier to produce cavitation at 50 kc/s. than at 1 Mc/s. Experiments in America by Knapp and Hollander (1948) also showed that the growth of bubbles often lasted some milliseconds, suggesting the periodic time of the wave is important, and the higher intensity with shorter pulses found by Briggs and Johnson (1947) and Mason (1947) provided evidence of rather similar nature. The fact that von Ardenne (1940, 1941, 1943) had found emulsions prepared by violent shaking at 100 c/s. to be apparently identical with those prepared ultrasonically showed the wide field of frequency variation which needed to be explored.

Miss M. Thornley described experimental work on bacteriological effects, pointing out first that published work seemed to indicate that oxidation was unimportant (Flosdorf *et al.* 1936, Rouyer and Grabar 1947), but that cavitation increased mortality. It was thought that shock waves were started which were highly lethal. Such a process might well yield a logarithmic survival curve, and she had indeed found, using 1 Mc/s. radiation up to 2 watts/cm³ (ratio of R.F. input power to sample volume) on *Bacterium coli* in dilute casein solution, that a constant proportion of viable cells was killed per unit time though this proportion sometimes decreased slowly with time. The decrease might be due to some of the organisms being tougher than others. Care was needed to keep temperature constant in spite of heating. Her tests at Imperial College showed evidence at 1 Mc/s. of a threshold, then an increased killing rate as intensity increased; Shropshire (1947), though working at 9 kc/s. and admittedly using a different suspending medium, had found no such threshold. Suspending media played an important part (Beckwith *et al.* 1936) and milk, perhaps on account of the fats it contained, was difficult to sterilize.

On account of the wide variations in conditions reported in published work (Païc *et al.* 1935, v. Euler *et al.* 1944, Chambers *et al.* 1932, Yen *et al.* 1934 and Grabar *et al.* 1945), it was impossible to say whether high or low frequency irradiation was more lethal, though negative results were sometimes reported at high frequencies.

There might be a valuable application in extracting enzymes (Stumpf *et al.* 1946) without damaging them and also in releasing virus from tissue cells (Chambers *et al.* 1936). On the whole, small scale work, especially on valuable materials, seemed most promising, industrial applications having yet to be justified since they might prove uneconomical.

Mr. A. W. Cronshaw reported on bacteriological and emulsifying effects. He used a frequency of 200 kc/s., with 44 watts/cm² intensity at the 2 in. diameter crystal; transformer oil of viscosity 0·2 poise was used. Irradiation of both cultures of *Bacterium coli* and of *Staphylococcus albus* in a test tube held above the crystal for 10 minutes gave no lethal results. He found that emulsification took place far more rapidly at 10 kc/s. than at 200 kc/s.

Mr. C. J. Bradish described his investigations, which were mainly on the irradiation of proteins with ultrasonics. The experiments were carried out at about 700 kc/s. with a power–volume ratio of 6 watts/cm³, very careful precautions being taken to avoid appreciable temperature rise. The first reaction studied was coagulation, and it was found that several proteins had the same coagulation rate of 15% per hour: human serum proteins, human carboxy haemoglobin, egg albumin and *Helix pomatia* haemocyanin. This was a much higher rate than would arise through a simple increase in air–solution interface. The reaction products appeared to be the same as those which would result from coagulation by simple heating; moreover the uncoagulated residue was apparently unchanged. Irradiation was not accompanied by change of gross physical properties, for instance, denaturation which is believed to entail an uncoiling of the constituent polypeptide chain. On the other hand, it has been reported that irradiating normal horse serum for a few hours at 1 to 2 watts/cm³ altered the soluble-fraction.

In contrast to some of the above proteins, with molecular weights around 75,000, was fibinogen with molecular weight five times as large and length about 0·07 μ. This is an essential agent in the clotting of blood. Irradiation for one hour was sufficient to prolong clotting times tenfold. An even larger molecule, *Helix pomatia* haemocyanin, with a molecular weight of 9×10^6, length nearly

0·1 micron and diameter one-sixth of this, has the property of longitudinal cleavage to $\frac{1}{2}$, $\frac{1}{4}$ or $\frac{1}{8}$ the size, but Mr. Bradish has been quite unable to confirm Brohult's claim (Brohult 1940) that irradiation caused an increase in the relative concentration of the half molecule. There was, however, a notable polydispersion of the one-eight molecule due to irradiation.

These reactions have appeared to proceed at a rate proportional to watts/cm³, and there was no evidence of a threshold effect. Increased size seemed to be accompanied by increased rate of disintegration; for example, the protozoon *trichomonas foetus* (approximately 15 μ diameter) at 6 watts/cm³ suffers 50% mortality in 15 seconds compared with 50% protein coagulation in 3 hours. Mr. Bradish thought that any large unit was subject to considerable frictional forces because it was too bulky to follow the motion of the medium faithfully. Cavitation also plays a part and below $\frac{1}{2}$ micron particle size is probably the most powerful agency in disintegration.

Mr. Maguire described a process which had been successfully used for two years for joining aluminium, especially in the form of fine wires, using 10 kc/s. vibrations, and a power of 50 watts. The vibrator was a hard drawn pure nickel tube 9 in. × $\frac{7}{8}$ in. o.d. with 1/16 in. wall supported at its centre with the axis vertical. It was slotted at the lower end and was surrounded there with a coil carrying 10 kc/s. and D.C. polarizing currents. The upper end was closed by a brazed steel disc $\frac{1}{8}$ in. thick mounting a 1 in. × 5/32 in. diameter rod surmounted by a $\frac{1}{4}$ in. × $\frac{5}{8}$ in. diameter brass cylinder. The latter had a bead of 70% tin 30% zinc solder on top which was kept molten by a gas jet. The intensity of vibration was adjusted to give a striated appearance to the solder. The aluminium, or aluminium and copper wires to be soldered were twisted loosely and, without cleaning, were immersed in the solder globule for somes econds. Wires down to 0·006 in. diameter had been used. There was no subsequent change in the resistance at the joint.

Larger wires and flat aluminium objects could be tinned by being pressed on to the cylinder top, avoiding pitting from too prolonged contact. Subsequently such tinned parts could be joined with ordinary solder at a low temperature with the operation shortened to avoid loss of the special solder surface.

Mr. A. N. Turner discussed the effects which ultrasonic irradiation might cause in metallurgy and described experimental work along three lines involving aluminium alloys. A 120 watt generator of 26 kc/s. vibrations was used and the melts each weighed about 20 lb. The melt at 100° C. superheat was transferred to a refractory lined crucible open at the bottom where it rested on a heavy cast steel base plate. Vibrations were introduced at 50° C. above liquidus and solidification took 15 to 20 minutes. The degassing effect in an aluminium–4% copper alloy was compared with that from degassing with chlorine, the criterion being a test based on the density of specimens taken from the metal after subjection to a special reheating and vacuum cooling treatment; it was found to be equally efficacious.

The second effect investigated was reduction of grain size. Excellent results were obtained on the alloys aluminium–4% copper, aluminium–12% silicon, aluminium–9% silicon and aluminium–0·5% manganese. It was especially noteworthy that the dendrites in the microstructure were broken up by the vibrations and a proposed explanation of the refining action on grain size was that newly formed dendrites in a metastable region during solidification were shattered by irradiation and so produced showers of new nuclei for the formation of new crystallites. Figure 7 (Plate II) shows a typical irradiated 4% copper alloy compared with a non-irradiated control.

The third effect was the tendency to increase segregation of alloy components. In a silicon alloy, since the specific gravity of aluminium and silicon (at room temperature) are 2·7 and 2·4 respectively, there is a strong tendency for primary silicon in a hyper-eutectic alloy (the eutectic is 12% silicon) to float while there is little tendency for primary aluminium in a hypo-eutectic alloy to sink. Even in the latter alloys, ultrasonic irradiation produces appreciable segregation. This effect is also strongly marked in copper alloys which had been investigated up to the aluminium–33% copper eutectic.

In the course of this work it was felt that an improved method of monitoring the intensity of the vibrations in the melt was greatly to be desired.

Mr. Bradfield summarized by saying that, as a general rule, it was more profitable to use ultrasonic waves for irreversible actions such as killing microbes, cleansing, wetting fine particles, dislodging oxide films and scales, freeing dissolved gases, refining the grain of metals, precipitation of aerosols and drying paper pulp, while for reversible actions such as emulsification and coagulation of hydrosols the method seemed less promising. Care also had to be taken that two effects might not interfere, for instance, segregation of components in irradiating molten metals might take place as well as refinement of the grain. Finally, the effects of standing waves must not be overlooked, and for this and other reasons, it was highly desirable that methods of measuring intensity of irradiation easily and reliably should soon be established and become widely used in investigations.

REFERENCES

Allen, C. H., and Rudneck, I., 1947, *J. Acoust. Soc. Amer.*, **19,** 847.

von Ardenne, M., 1940, *Colloid Z.*, **93,** 158; 1941, *Angew. Chem.*, **54,** 144; 1943, *Chem. Tech.*, **16,** 177.

Bauer, E., 1949, *Proc. Phys. Soc.* A, **62,** 141.

Beckwith, T. D., and Weaver, C. E., 1936, *J. Bact.*, **32,** 361.

Briggs, H. B., and Johnson, J. B., 1947, *J. Acoust. Soc. Amer.*, **19,** 4, 665.

Brohult, S., 1940, *Nova Acta Soc. Sci. Upsal.*, 4, **12,** 4.

Chambers, L. A., and Flosdorf, E. W., 1936, *Proc. Soc. exp. Biol. N.Y.*, **34,** 631.

Chambers, L. A., and Gaines, N., 1932, *J. Cell. Comp. Physiol*, **1,** 451.

von Euler, H., and Skarzynski, B., 1944, *Arch. Kemi. Min. Geol.*, **17 B,** 15.

Flosdorf, E. W., and Chambers, L. A., 1935, *J. Immunol.*, **28,** 297.

Flosdorf, E. W., Chambers, L. A., and Malisoff, W. M., 1936, *J. Amer. Chem. Soc.*, **58,** 1069.

Grabar, P., and Rouyer, M., 1945, *Ann. de l'Inst. Pasteur*, **71,** 154.

Hall, L., 1948, *Phys. Rev.*, **73,** 775.

Knapp, R. T., and Hollander, A., 1948, *Trans. Amer. Soc. Mech. Engrs.*, **70,** 5, 419.

Kneser, H. O., 1938, *Ann. Phys., Lpz.*, **32,** 277.

Lamb, J., and Pinkerton, J. M. M., 1949, *Proc. Roy. Soc.* A, **199,** 114.

Loiseleur, J., 1945, *Ann. de l'Inst. Pasteur*, **71,** 378.

Mason, W. P., 1947, *Trans. Amer. Soc. Mech. Engrs.*, **69,** 359; 1948, *Phys. Rev.*, **74,** 1134.

Mason, W. P., Baker, W. O., McSkimmin, H. J., and Heiss, J. H., 1948, *Phys. Rev.*, **73,** 1074.

Païc, M., Deutsch, V., and Borcila, I., 1935, *C.R. Soc. Biol.*, **119,** 1063.

Pinkerton, J. M. M., 1949, *Proc. Phys. Soc.* B, **62,** 129.

Prudhomme, A. O., and Grabar, P., 1947, *Bull. Soc. Chim. biol., Paris*, **29**, 122.
Rapuano, R. A., 1948, *Phys. Rev.*, **72**, 78.
Rouyer, M., and Grabar, P,, 1947, *Ann. de l'Inst. Pasteur*, **73**, 215.
Shropshire, R. F., 1947, *J. Bact.*, **53**, 685.
Spakowski, B., 1938, *C.R. Acad. Sci., U.R.S.S.*, **18**, 169.
Stumpf, P. K., Green, D. E., and Smith, F. W., 1946, *J. Bact.*, **51**, 487.
Wood, A. B., Smith, F. D., and McGeachy, J. A., 1935, *J. Instn. Elect. Engrs.*, **76**, 461, 550.
Yen, A. H., and Liu, S. C., 1934, *Proc. Soc. exp. Biol., N.Y.*, **31**, 1250.

APPENDIX

List of Authors and Titles of Papers summarized (sequence as in summarized proceedings).

Author	Title of Paper
G. Bradfield	Applications of Ultrasonics.
J. M. M. Pinkerton	On the Study of Fundamental Properties of Liquids and Solids by Ultrasonic Methods.
D. O. Sproule	Flaw Detection in Metals.
G. T. Harris	An Industrial Application of Ultrasonic Testing.
W. C. Heselwood	Flaw Detection in Steel.
H. W. Taylor	Flaw Detection in Light Alloys.
R. L. Beurle	Ultrasonic Guiding Devices for Blind People.
D. O. Sproule	Echo Sounding.
H. Grayson	Ultrasonic Time Delays.
B. E. Noltingk	Cavitation.
G. M. Wells	Use of High Intensity Ultrasonics in Liquids.
Miss M. Thornley	Bacteriological Applications of Ultrasonics.
A. W. Cronshaw	Bacteriological Effects, Preparation of Emulsions.
C. J. Bradish	Ultrasonic Vibrations and the Protein Molecule.
C. R. Maguire	Soldering Aluminium.
A. N. Turner	Achieving a Fine Crystalline Structure during Solidification.

Measurement of the Equivalent Electrical Circuit of a Piezoelectric Crystal

By A. C. LYNCH
Post Office Engineering Research Station, London, N.W. 2

MS. received 17*th August* 1949, *and in amended form* 7*th November* 1949

ABSTRACT. A new method for measuring the reactances in the circuit requires measurements of equivalent capacitance at several frequencies around that of resonance, preferably differing from the resonance frequency by from ½ to 5%; the accuracy is unaffected by capacitance in parallel with that of the specimen. The measurements can be made with a suitably screened substitution Schering bridge; it should be suitable for frequencies between about 50 and 600 kc/s., and the only unusual component needed for it is a variable condenser which can be read to 0·001 pF. If there are no unwanted modes of vibration, the equivalent circuit can be measured to within 0·1%.

The piezoelectric coefficient *d* is sometimes calculable from the equivalent circuit and the dimensions of the crystal, but there are difficulties which limit the accuracy of *d* to about ½%. Results obtained include, for example, d_{11} for quartz at 20° C. $= 6{\cdot}9_5 \times 10^{-8}$ cm/E.S.U. of potential.

§ 1. INTRODUCTION

PIEZOELECTRIC effects can be measured with comparable accuracy by either electrostatic or dynamic methods. The latter require observations on bars or plates vibrating in resonance with an alternating electric field. Similar resonance effects are used in the application of crystals in carrier-frequency telephone systems. This paper describes a new dynamic method of obtaining the electrical data which are needed either for deducing the piezoelectric coefficients or in designing and constructing crystal filters for telephone systems.

A bar or plate of piezoelectric material mounted between electrodes, and at a frequency near that of resonance, is equivalent electrically to a circuit containing capacitance, inductance and resistance all in series, shunted by a capacitance approximately equal to the electrostatic capacitance of the specimen (see Figure 1). For two reasons we may need to measure these components.

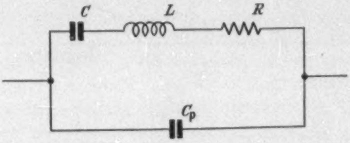

Figure 1. Equivalent circuit of a piezoelectric crystal.

First, when a filter circuit is to include a crystal, data are needed for choosing the orientation and dimensions of the crystal so that it has the required equivalent circuit. Second, the equivalent capacitance C and the resonance frequency f_0 can sometimes be used to deduce the piezoelectric coefficient d (for example, if the specimen is a narrow bar in longitudinal vibration). For specimens of convenient size f_0 will usually be of the order of 100 kc/s. and C of the order of 0·01 pF.

Most of the methods previously used (Cady 1946, p. 387) are based on measurements of both series and shunt resonance frequencies of the crystal. The latter is dependent on the electrostatic capacitance C_p, and on any stray capacitance which may appear in parallel with it. Such stray capacitance is almost unavoidable, particularly if one terminal of the crystal is connected to earth. These methods therefore require an accurate measurement of total parallel capacitance; the present method does not. Few of the published descriptions state the accuracy attainable; for some of the methods it appears to be of the order of within 1% in C. The wide variations between published values of piezoelectric coefficients (see, for example, Cady 1946, p. 220) may be the result either of poor specimens or of errors in the electrical measurements.

The original object of the present work was to obtain an accuracy of within about 1% in C. Since d is derived from C by use of formulae of the type $d^2 = kC/f_0^2$, where k involves the dimensions and density of the crystal and also a numerical constant, this would permit accuracy within $\frac{1}{2}$% in d. Later, better accuracy in C was obtained, and this was used to determine the change in C with temperature.

§ 2. PRINCIPLE OF METHOD

At any one frequency f, the impedance of the crystal is equivalent to that of a capacitance C_x and a conductance G in parallel. At frequencies near that of a resonance of the crystal, the change of the capacitance C_x with frequency is of the type shown in Figure 2. The central part of the curve (especially between the points P and Q) is controlled by the resistance R; the remainder, which is nearly hyperbolic, is controlled by the capacitance C and inductance L. The curve can, and usually does, cross the horizontal axis, corresponding to negative values of the capacitance C_x. The capacitance difference $(C_x - C_p)$ is introduced by the branch of the equivalent network which includes L, C, and R; it will be written as K. The capacitance C can be deduced from a group of values of K at suitable frequencies; these frequencies should be in the range for which the curve of Figure 2 is nearly hyperbolic.

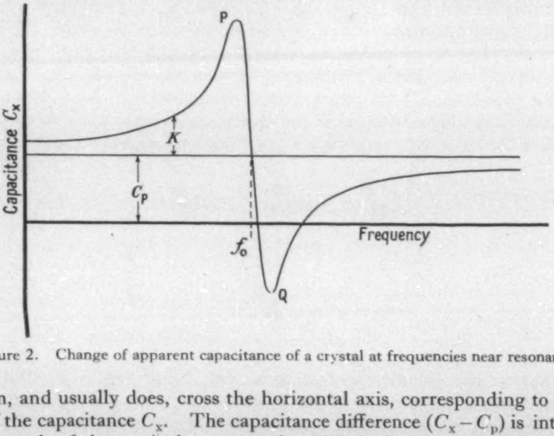

Figure 2. Change of apparent capacitance of a crystal at frequencies near resonance.

If the effect of the resistance R can be neglected, the relation between K and C is simple. At any frequency f, the susceptance of the L-and-C branch of the network is $1/(j\omega L+1/j\omega C)$, where $\omega=2\pi f$, and this is equal to the measured susceptance $j\omega K$. Hence

$$K=C/(1-\omega^2 LC). \qquad \ldots\ldots(1)$$

For two values K_1, K_2, observed at frequencies f_1, f_2, near the frequency of resonance,

$$\frac{1}{K_1}-\frac{1}{K_2}=\frac{\omega_2^2 LC-\omega_1^2 LC}{C}$$

or, since $\omega_0^2 LC=1$, where $\omega_0=2\pi f_0$ and f_0 is the frequency of series resonance,

$$\frac{1}{K_1}-\frac{1}{K_2}=\frac{\omega_2^2-\omega_1^2}{\omega_0^2 C} \qquad \ldots\ldots(2)$$

$$\simeq\frac{2\Delta f}{f_0 C} \qquad \ldots\ldots(3)$$

where $\Delta f=f_2-f_1$, the difference between the two frequencies of measurement. Hence

$$C\simeq\frac{2\Delta f}{f_0(1/K_1-1/K_2)}. \qquad \ldots\ldots(4)$$

If in equation (3) we put $f_2=f_0$, so that $1/K_2=0$, we find that the relation between $1/K_1$ and (f_0-f_1) is nearly linear. Here, then, is a useful method of measuring f_0: if f_1 and f_2 are on opposite sides of f_0, we make a linear interpolation between them:

$$f_0\simeq f_1+\frac{1/K_1}{1/K_1-1/K_2}(f_2-f_1). \qquad \ldots\ldots(5)$$

Thus, for the present method, the frequencies at which measurements are made can all be integral multiples of a standard frequency (e.g. 1 kc/s.).

If there is more than one resonance frequency, the various equivalent circuits (one for each frequency) can be found separately by successive approximations. By rearranging equation (1), and introducing $\omega_0^2 LC=1$, we find that the measured capacitance due to a resonance at a frequency greater by F than the frequency of observation is approximately

$$\frac{C'f_0'}{2F(1+F/f_0')}$$

or, if $F\ll f_0'$, $C'f_0'/2F$ where f_0' is the frequency of that resonance and C' the capacitance in its equivalent circuit. By use of this formula we can correct the observed results for the effect of irrelevant resonances. Graphical methods can also be used.

§ 3. DISCUSSION OF APPROXIMATIONS

We shall now justify the approximations which have been made; one of them requires the frequencies f_1, f_2 to be disposed nearly symmetrically about f_0, and so this condition will be assumed throughout. Put h for the difference between ${}_0$ and the mean of f_1 and f_2, expressed as a fraction of f_0; i.e., $h=[\frac{1}{2}(f_2+f_1)-f_0]/f_0$. h need not exceed 0·01, even if f_1 and f_2 are restricted to integral numbers of kilocycles per second and f_0 is as low as 50 kc/s. For convenience we shall write $g=\Delta f/f_0$; g may reach 0·2.

There are three approximations to consider:

Approximation (i). We repeat the calculation leading to equation (2), allowing for the effect of resistance R in series with L and C. The measured susceptance must now be equal to the imaginary part of the admittance of L, C, and R in series; it follows that

$$K=\frac{C(1-\omega^2LC)}{(1-\omega^2LC)^2+(\omega CR)^2}$$

or, writing a for $(1-\omega^2LC)$ and b for ωCR,

$$K=Ca/(a^2+b^2).$$

For two values K_1, K_2, and corresponding values a_1, a_2, b_1, b_2,

$$1/K_1-1/K_2=(a_1-a_2+b_1^2/a_1-b_2^2/a_2)/C,$$

and this can be shown to be equal to

$$(a_1-a_2)(1-b_0^2/a_1a_2)/C,$$

where b_0 is the value of b at frequency f_0.

But $a_1a_2 \simeq (g^2-4h^2)(1+h) \simeq g^2$, so that we must consider the likely magnitude of b_0^2/g^2. Now b is $1/Q$, where Q is the ratio reactance/resistance, and it can be determined either from measurements with the bridge described below or, more conveniently, by a separate experiment. It rarely exceeds 0·001. Hence, for accuracy in C to within 0·1%, this correction should be used if g is less than 0·03. In practice, consistent results are obtained for smaller values of g; apparently the representation of the crystal by the circuit of Figure 1 is not quite satisfactory when the loss is greater than usual. This is reasonable: for whereas damping by air should be represented by a series resistance as in Figure 1, internal friction or a flaw in the crystal would probably introduce a parallel resistance across part of the inductance and capacitance. Now a parallel resistance, if across the whole circuit, would cause no error in equation (2); so that we expect in practice to find that, in making this correction, b_0 should be given more nearly the value appropriate to an unflawed crystal, which is less than 0·0001. Hence no correction is needed even if g is as small as 0·003.

Approximation (ii). In deriving equation (3) we have put $f_1+f_2 \simeq 2f_0$. For greater accuracy we could multiply the right-hand side of equations (3) and (4) by $(1+h)$; but see below.

Approximation (iii). An error may arise in determining the constant capacitance C_p, from which the changes with frequency are measured, because the capacitance of the crystal tends above the resonance frequency towards C_p, but below it towards C_p+C. In practice, therefore, we measure K from an initial value between zero and C. Suppose we find this initial value by taking the mean of measurements at frequencies $f_0(1+m)$, where m is of the order of $\frac{1}{4}$. The mean of these two values of K is $C/(4-m^2)$, or nearly $\frac{1}{4}C$.

This gives a correcting factor, for the right-hand side of equation (4), of

$$1-h+\tfrac{1}{8}g^2h+\tfrac{1}{64}g^4-\tfrac{1}{4}m^2h+\tfrac{1}{32}m^2g^2,$$

ignoring higher powers than h^2 and g^4.

Approximations (ii) *and* (iii) *combined.* The product of these two factors is

$$1-h^2+\tfrac{1}{8}g^2h+\tfrac{1}{64}g^4-\tfrac{1}{4}m^2h+\tfrac{1}{32}m^2g^2 \qquad \ldots\ldots(6)$$

and some smaller terms. As m is conveniently about $\frac{1}{4}$, then if $h<0{\cdot}01$ and $g<0{\cdot}2$ none of the small terms in (6) exceeds 0·00015; and so, for accuracy in C to within 0·1%, no corrections to equation (4) are needed.

§ 4. EXPERIMENTAL APPARATUS

The capacitances can conveniently be measured in a substitution Schering bridge (see, for example, Hague 1943, p. 353). The earth connection should be made to the junction of the resistive arms; thus we exclude from the measured quantity any stray capacitance to earth.

In the apparatus used, the capacitance of the crystal was measured with condensers of either 85 pF. range and 0·01 pF. scale-reading accuracy, or 4 pF. range and 0·001 pF. scale-reading accuracy. These condensers were double-screened. The ratio arms of the bridge were wire-wound, of 100 ohms each. With these values, frequencies from 50 to 650 kc/s. could be used.* The oscillator was of good short-period stability, and its frequency was adjusted to integral multiples of 1 kc/s., or of 250 c/s. if necessary, by comparison with a standard 1-kc/s. supply (accurate to 1 part in 10^7), using stationary patterns on a cathode-ray oscillograph. Balance was observed with a heterodyne detector and telephones. With about 5 v. input to the bridge, balancing to 0·001 pF. was possible. The balance of the bridge, with no specimen connected, was nearly independent of frequency; any variation of the balance could therefore be regarded as caused by the crystal, and there was no need for balancing both with and without the specimen at every frequency used. In both quartz and ethylene diamine tartrate, the variation of C_p with frequency was found to be negligible, so that, for these materials at least, K is given directly by the change in bridge readings between the test frequency and a frequency remote from that of resonance.

The specimens carried their own electrodes, deposited by evaporation of silver; they were held at their centres between springs carrying silver contacts. The effect of any likely bad centring was negligible (since mounting at two-fifths of the length, a very obvious error, was found to cause an error in equivalent capacitance of only $-0{\cdot}8\%$). The crystal was screened by a copper box of dimensions 10 cm. × 10 cm. × 5 cm. Temperature control was necessary only for measurements of variation of piezoelectric coefficient with temperature, for which the box was heated by a current of warm air. When the ambient humidity was high slight heating was used, to reduce the damping of the specimen.

§ 5. BRIDGE ERRORS

The Schering bridge measures the effective series capacitance of the specimen, not the parallel capacitance which we need. Also, capacitance permanently in parallel with the resistance R_0 of each of the ratio arms causes an error; and capacitance or inductance of the ratio arms themselves will increase or decrease this parallel capacitance. (Possible values of these capacitances would be 200 pF. due to screened leads, transformer windings, and minimum settings of variable condensers, and ± 100 pF. for capacitance or inductance of the ratio arms themselves.) Together these corrections amount to a capacitance

$$C_{\mathrm{b}} = \omega^2 R_0^2 C_2 C_4 \Delta C_4$$

to be subtracted from that observed: C_4 is the capacitance in the arm opposite to the specimen, ΔC_4 the change in C_4 on connecting the specimen and re-balancing, and C_2 the total capacitance in the arm containing the specimen.

But $b \simeq \omega R_0 C_2 \Delta C_4 a^2/C$; so that $C_b \simeq \omega R_0 C C_4 b/a^2$. Hence for two values a_1, a_2, such that $a_1 \simeq -a_2$, C_b is nearly constant; its change $\simeq (8h/g^2 - 1)\omega_0 b_0 R_0 C_4 K$, which is normally less than $10^{-5} \times K$ and therefore negligible.

---

* Even if the ratio arms are not purely resistive, the accuracy of measurement of capacitance in a substitution bridge is almost unaffected.

Table 1

(A) Measurements, and values of K:

Frequency (kc/s.)	Bridge settings: In parallel with crystal: C_1 (pF.)	Bridge settings: In parallel with ratio arm: C_4 (pF.)	Hence K (pF.) (measured from the mean of settings at 120 and 166 kc/s.)
134	2·754	150	0·770
135	2·852	150	0·868
136	2·977	150	0·993
137	3·147	150	1·163
138	3·383	150	1·399
148	0·631	149	−1·353
149	0·857	149	−1·127
149·5	0·950	149	−1·034

Frequency (kc/s.)	Bridge settings*: In parallel with crystal: C_1 (pF.)	Bridge settings*: In parallel with ratio arm: C_4 (pF.)	Hence K (pF.) (measured from the mean of settings at 120 and 166 kc/s.)
149·75	1·017	150	−0·967
150	0·986	150	−0·998
150·25	1·035	150	−0·949
151	1·127	150	−0·857
152	1·223	149	−0·761
120	2·279	150	mean 1·984
166	1·689	150	

Frequency f_1 (kc/s.)	K_1 (from above) (pF.)	Correction for other resonance (pF.)	Corrected K_1 (pF.)	Frequency f_2 (kc/s.)	K_2 (from above) (pF.)	Correction for other resonance (pF.)	Corrected K_2 (pF.)	$\frac{1}{K_1}$ (pF.)$^{-1}$	$\frac{1}{K_2}$ (pF.)$^{-1}$	$\frac{1}{K_1}-\frac{1}{K_2}$ (pF.)$^{-1}$	Δf (kc/s.)	$\frac{1/K_1-1/K_2}{\Delta f}$ (pF. kc/s.)$^{-1}$
(B) First approximation for main resonance:												
138	1·399			**148**	−1·353			0·714$_8$	−0·739$_1$	1·454	10	0·1454
Hence $f_0 \simeq 138+\frac{0\cdot715}{1\cdot454}.\,10=142\cdot9$ kc/s. and $C \simeq \frac{2}{0\cdot1454\times142\cdot9}=0\cdot0963$ pF.												
(C) Approximation for minor resonance, using the values of f_0 and C just found:												
149·5	−1·034	1·056	0·022	**150·25**	−0·949	0·940	−0·009	45	−110	155	0·75	210
149·75	−0·967	1·009	0·042	**150**	−0·998	0·964	−0·034	24	−29	53	0·25	210
Hence $f_0' \simeq 149\cdot75+\frac{24}{53}\times0\cdot25=149\cdot86$ kc/s. and $C' \simeq \frac{2}{210\times149\cdot86}=0\cdot00006$ pF.												
(D) Final calculation for main resonance:												
134	0·770	<0·001		**152**	−0·761	0·002	−0·759	1·29$_9$	−1·31$_8$	2·61$_7$	18	0·145$_4$
135	0·868			**151**	−0·857	0·004	−0·853	1·15$_2$	−1·17$_2$	2·32$_4$	16	0·145$_2$
136	0·993			**150**	−0·998	0·034	−0·964	1·00$_7$	−1·03$_7$	2·04$_4$	14	0·146$_0$ †
137	1·163			**149**	−1·127	−0·005	−1·132	0·859$_8$	−0·883$_4$	1·743$_2$	12	0·145$_3$
138	1·399			**148**	−1·353	−0·003	−1·356	0·714$_8$	−0·737$_5$	1·452$_3$	10	0·145$_2$

$$\text{Hence } f_0=138+\frac{0\cdot715}{1\cdot452}.\,10=142\cdot93 \text{ kc/s. and } C=\frac{2}{0\cdot1453\times142\cdot93}=0\cdot0963 \text{ pF.}$$

---

* Both of these are from arbitrary zeros. The condenser used for C_1 has a reversed scale.

† This high value is the result of inaccuracy in the rather large correction to K at 150 kc/s., and it has been ignored in taking the mean. If we sacrifice the symmetry about f_0, and use the 150·25 kc/s. measurement instead of that at 150 kc/s., we find [illegible]

Table 2

Type of crystal	Dimensions (cm.)	Frequency at 20° c. (kc/s.)	Capacitance at 20° c. (pF.)	*Ct/lb*		Piezoelectric coefficients × 10^8 (cm/E.S.U. of potential)	
				from present work (pF/cm.)	from previously-published work* (pF/cm.)	in direction given by specimen	Hence d_{11}
X-cut bars	$3\cdot622 \times 0\cdot503_5 \times 0\cdot187_8$	$74\cdot86$	$0\cdot0328_6$			$\pm 6\cdot9_5$	$6\cdot9_8$
	$3\cdot627 \times 0\cdot504_0 \times 0\cdot199_5$	$74\cdot83$	$0\cdot0296_0$			$\pm 6\cdot7_9$	
Bars in X-plane :							
45° from Y-axis	$2\cdot001 \times 0\cdot300_5 \times 0\cdot204_3$	$138\cdot71$	$0\cdot0045_5$			$\pm 4\cdot5_9$	$6\cdot9_7$
135° ,, ,,	$2\cdot001 \times 0\cdot300_5 \times 0\cdot204_0$	$174\cdot25$	$0\cdot00194$			$\pm 2\cdot3_8$	
CT plates −37° 20′ from axis	$2\cdot128 \times 2\cdot136 \times 0\cdot053_6$	$145\cdot3_8$	$0\cdot098_6$	$0\cdot00116_3$	$0\cdot00117_0$		
	$2\cdot168 \times 2\cdot168 \times 0\cdot054_3$	$142\cdot9_3$	$0\cdot100_2$	$0\cdot00115_8$			
DT plates : 52° 20′ from axis	$2\cdot305 \times 2\cdot305 \times 0\cdot049$	$89\cdot49$	$0\cdot116_6$	$0\cdot00107_5$	$0\cdot00108_0$		
	$2\cdot306 \times 2\cdot306 \times 0\cdot049_5$	$89\cdot45$	$0\cdot118_1$	$0\cdot00109_5$			

* Deduced from results given by Bechmann (1943) for plates of similar orientation.

If condensers were used in series with the resistors in the ratio arms instead of in parallel with them, the bridge would measure parallel capacitances and the first of these errors would not arise. But, with any practical condensers, the error due to the initial impurity of the ratio arms would become many times larger.

§ 6. EXAMPLES OF RESULTS

Each of the following examples illustrates both successful use of the method and a difficulty in the measurements. Table 1 gives the results of measurements of a CT-cut quartz plate at 50° c. This plate had two resonances, and the Table shows the method of dealing with the effect of a weak resonance in the presence of a strong one. If there had been a single resonance, the measurements at 149·5, 149·75 and 150·25 kc/s. would not have been needed, and neither would sections B and C of the table, nor the part of section D between the vertical lines.

The results for f_0 and C of a suitable specimen may be used in finding the piezoelectric coefficient for a particular direction—e.g. along the length of a bar (the necessary formulae for narrow bars are well known: see, for example, Cady 1946, pp. 88, 297). These results can then be combined if necessary to give piezoelectric coefficients referred to the customary axes.

Table 2 shows some results for quartz at 20° c. The results for the two X-cut bars did not agree as closely as was expected: the second bar was afterwards found to be partially twinned. The + sign has been used for d_{11}, in agreement with the I.R.E. convention (Cady 1946, p. 409). The coefficients for the 45° and 135° bars must be given − signs, for otherwise they could not be combined to give a reasonable value for d_{11}. The results for d_{11} may be compared with the value $6 \cdot 9 \times 10^{-8}$, recommended by Cady (1946, p. 219) in his review of published results. There are no published formulae for deriving d from the C of plates in contour-shear vibration; the results are therefore compared with those for plates of similar orientations measured by Bechmann (1943) by a different method. The results for both bars and plates are in good agreement with the earlier work.

§ 7. CONCLUSION

The consistency obtained in measurement of the equivalent capacitance C is usually of the order of within 0·1%, provided that C is at least 0·02 pF. and that there is no other resonance close to that being studied. The method has been used to measure C's of from 0·0002 to 0·7 pF., at frequencies ranging from 50 to 650 kc/s.

On the evidence of Table 2, and similar groups of results for other materials, both at 20° c. and at 50° c., it seems reasonable to claim an accuracy reaching to within about ½% in the piezoelectric coefficient. With an idealized specimen the error in d would be only half that in C. The additional error found in practice is caused by departure of the experimental conditions from those assumed in the formulae giving C in terms of dimensions etc. There may, for example, be imperfections in the shape and mounting of the crystals, multiple resonances, or, in quartz, twinning. When measurements are made at two temperatures the effect of these imperfections is usually fairly constant, and, if so, the temperature coefficient of d can be found with the accuracy available in measurements of C, or even better. Some results obtained by this method have already been published (Bechmann and Lynch 1949) and others are awaiting publication.

ACKNOWLEDGMENTS

Acknowledgment is made to the Engineer-in-Chief of the General Post Office for permission to make use of the information contained in this paper. The author is indebted to members of the Radio Branch of the Post Office Engineering Department for providing many accurately made specimens.

REFERENCES

Bechmann, R., 1943, *Hochfrequenztech. u. Elektroakust.*, **61,** 1.
Bechmann, R., and Lynch, A. C., 1949, *Nature, Lond.*, **163,** 915.
Cady, W. G., 1946, *Piezoelectricity* (New York : McGraw-Hill).
Hague, B., 1943, *Alternating-current Bridge Methods* (5th edition) (London : Pitman).

Surface Effects and the Plasticity of Zinc Crystals

By S. HARPER and A. H. COTTRELL
Metallurgy Department, University of Birmingham

MS. received 16*th October* 1949

ABSTRACT. The effects of various surface treatments on the plastic properties of zinc crystals are examined. Roscoe's observation of the hardening effect of a surface film of oxide is confirmed ; electrolytically polished specimens have critical shear stresses of about 33 gm.mm^{-2} whereas oxidized specimens have values up to 65 gm.mm^{-2}. Similar effects are observed on the rate of creep under constant stress. The Rehbinder effect—softening crystals by immersing them in paraffin and oleic acid—can be produced on oxidized specimens but not on others. Oxidized specimens do not respond instantly to immersion and the time of response is proportional to the viscosity of the liquid. It is suggested that the liquid penetrates the oxide film and reduces its ability to harden the metal; the action of the oxide film itself is not yet clear.

§ 1. INTRODUCTION

The success of Griffith's theory of cracks in explaining the low breaking strength of brittle solids has encouraged occasional attempts to explain the low yield strength of plastic crystals in a similar manner, although interest has mostly been diverted in recent years to the theory of dislocations. One result of efforts to obtain evidence for the action of cracks has been the observation that the plastic properties of some metal crystals are affected by the surface condition of the specimens. Roscoe (1936) showed that oxide films of about 1,000 atoms thickness on cadmium crystals raised the critical shear stress of these to 2·4 times that of freshly cleaned crystals. This has been confirmed recently by Cottrell and Gibbons (1948). In explanation Roscoe suggested that molecules of oxide sealed up surface cracks and strengthened the outer layers of the crystal. Using crystals of zinc and tin, Rehbinder, Lichtmann and Maslenikov (1941) observed that the yield strength was the same for specimens tested in air and in a non-polar paraffin oil, but that, when 0·2% of oleic acid was added to the oil, the strength was halved. Similarly, the rate of flow in a creep test could be increased five to ten times by the addition of oleic acid. These effects were accompanied by an increase in the number of glide lamellae and a decrease in their size. It was suggested that the oleic acid acted by penetrating surface cracks, causing them to open and expand.

Although these observations show that plastic properties are affected by surface conditions they do not go far towards indicating the mechanism involved. It was felt that further investigations were needed and the work on zinc crystals reported below was started. While this was in progress the results of two other investigations became known. Andrade and Randall (1948) reported experiments in which clean cadmium crystals were heated in air or *in vacuo*, or were immersed in solutions of cadmium and other salts. Heating in air for 20 hours at 200° c. produced hardening and this was attributed to the formation of a surface film, in agreement with Roscoe's work. This hardening was produced more rapidly when the specimen was first contaminated locally with cadmium nitrate solution. In general, immersion in salt solutions caused the specimen to soften, although in the case of cadmium nitrate this was followed by a considerable hardening effect. Kemsley (1949) has recently attempted to reproduce the Rehbinder effect on tin crystals ; although the technique used in the original work was followed he was unable to obtain an observable response to treatment in oleic acid solution.

§ 2. EXPERIMENTAL DETAILS

All experiments were made on a sample of spectroscopically pure zinc supplied by Messrs. Johnson Matthey and Co., in the form of 1 mm. wire. A modification of the Kapitza method due to Andrade and Roscoe (1937) was used to grow crystals. By cleaning each wire before growth, using baked silica quills to support the wires while molten and an atmosphere of argon to reduce oxidation and volatilization, crystals could be prepared which had smooth, clean surfaces and which could be removed easily from their quills. Each crystal was cut into three pieces with the aid of a fine gas flame, care being taken to localize the heating and to minimize distortion. Two of the pieces, each 4 cm. long, were used for mechanical tests and the remaining one for determining the crystal orientation. Barrett and Levenson's (1940) etch-pit method was used for orientation measurements, with an accuracy within about 1°. Some of the specimens for mechanical testing were electropolished, using the chromic acid solution suggested by Rodda (1943). These were each immersed in the solution along the axis of a nickel tube, which served as the cathode and an E.M.F. of 6 volts was applied for 10 seconds. This gave a highly polished surface free from irregularities and reduced the diameter by about 0·1 mm.

In the early part of the investigation, the effect of the surface condition on the critical shear stress was studied. Most of these experiments were made on an apparatus of the type described by Andrade and Roscoe (1937). The load-extension curve was recorded photographically and it was possible to extend specimens at fairly fast rates, about 10^{-2} cm.sec^{-1}. A few experiments were also made at lower rates of extension, $10^{-4}-10^{-5}$ cm.sec^{-1}, with an apparatus similar to that described by Polanyi (1925). As is usual in critical shear stress measurements a large scatter was observed, amounting occasionally in extreme cases to 20% of the average value. However, more reproducible results were obtained among specimens taken from the same crystal than from different crystals, suggesting that the scatter was due to some uncontrolled variation, for example in the gas content, among the crystals. To reduce the effect of the scatter repeated tests on several specimens were always made and their results averaged.

Later experiments were made by creep testing, using an apparatus which enabled constant shear stress to be maintained on the glide plane in the glide direction (Cottrell and Aytekin 1947, 1950). Creep testing had the advantage that the surface condition of a specimen could be changed while the test was in progress, so that difficulties due to variations in the properties of different specimens were avoided.

§ 3. COMPARISON OF VARIOUS SURFACE CONDITIONS

Table 1 summarizes the measurements of the critical shear stress after applying various surface treatments.

Untreated specimens (Series A) possessed light-grey oxidized surfaces and an average critical shear stress of 56 gm.mm^{-2}. Series B and C represent various treatments, the common feature of which was a light attack by dilute hydrochloric acid. Apart from the C5 specimens, a critical shear stress of about 43 gm.mm^{-2} was observed in all cases, independently of whether the specimen was tested while immersed in the acid, made the electrode in a cell, or removed from the acid

Table 1. Critical Shear Stresses of Zinc after various Surface Treatments (Rate of Strain $\simeq 10^{-2}$ sec^{-1})

Serial number		Surface treatment	Number of tests	Average stress for 0·5% extension gm.mm^{-2}
A		Freshly grown, untreated	15	56
B	1	Tested in 10% HCl solution	10	42
	2	As B1, with specimen as anode of electrolytic cell	6	42
	3	As B1, with specimen as cathode	6	42
C	1	Etched in HCl, washed, dried, exposed to air for 5 minutes	6	46
	2	As C1, exposed for 30 minutes	7	42
	3	As C1, exposed for 1 hour	4	45
	4	As C1, exposed for 18 hours	7	44
	5	As C1, exposed for several days	8	56
D	1	Electrolytically polished, washed, dried, exposed to air for 5 minutes	8	33
	2	As D1, exposed for 1 hour	12	33
	3	As D1, exposed for 18 hours	6	33
	4	As D1, exposed for several days	3	32
E	1	Polished, immersed in $FeSO_4$ solution, dried, exposed to air for 5 minutes	6	41
	2	As E1, exposed for 1 hour	12	46
	3	Polished, immersed in HCl, dried, exposed to air for 5 minutes	6	46
	4	As E3, exposed for 30 minutes	12	44
	5	Polished, dried without washing, exposed to air for 5 minutes	6	41
	6	Polished, immersed in $ZnCl_2$ solution, dried, exposed to air for 5 minutes	6	44
F	1	Polished, etched in HCl, steamed for 1 hour	6	65
	2	Polished, washed, dried, steamed for 1 hour	6	33
	3	Polished, etched in HCl, steamed for 1 hour, repolished	3	36

and washed and dried before testing. On all the specimens the acid removed the original film and gave the surface a bright matt appearance. The specimens in C5, on the other hand, were exposed to the atmosphere for several days, after etching, until their surfaces resembled those of untreated specimens.

The effect of electrolytic polishing is shown by series D in which specimens were polished, washed, dried and exposed to the atmosphere for various periods of time. Polishing produced brilliant, mirror-like surfaces which resisted atmospheric attack remarkably well, remaining unchanged in appearance for several weeks. This is reflected by the critical shear stresses which were about 33 $gm.mm^{-2}$ in all cases.

Series E summarizes attempts to increase the critical shear stress of polished specimens by the subsequent application of aqueous solutions of various agents, including the chromic acid solution used in the polishing process (E5). The critical shear stress in all cases was, within experimental error, the same as for those specimens treated only in hydrochloric acid (Series B and C). Thus the value of 43 $gm.mm^{-2}$ appears to be characteristic of the lightly attacked condition, independently of the details of the treatment.

Finally, the specimens in Series F were exposed to steam with the object of producing thick oxide coats. Thick, grey coats were formed when etched specimens were treated in steam and the critical shear stress was raised to 65 $gm.mm^{-2}$; in the case of polished specimens the treatment had no effect on either the surface appearance or the critical shear stress, again demonstrating the high resistance of the polished surface.

The last result, F3, shows that the high strength produced by treating an etched specimen in steam does not survive a subsequent polishing treatment, and hence that it is caused by the surface state of the crystal rather than by any internal metallurgical changes which might conceivably be produced.

§ 4. SURFACE EFFECTS AT THE START OF PLASTIC FLOW

The above experiments show that the hardening effect of a surface film occurs also with zinc, as well as with cadmium, crystals. In explanation, one might suggest that molecules of oxide or other corrosion products fill surface cracks and thereby reduce the ability of these to concentrate stress. In this case the effect ought to be most marked at the start of a mechanical test, before enough plastic flow has occurred to smooth out stress concentrations. Roscoe (1936) showed that the increased strength of an oxidized specimen persists for large deformations (300% extension), which makes this explanation doubtful, but did not examine the very early stages of plastic flow in detail.

Accordingly, a study was made of the early part of the stress–strain curve, critical shear stress measurements being taken at extensions of 0·05, 0·1, 0·5 and 1%. Electrolytically polished and lightly etched specimens were studied and, to ensure a reliable comparison, the specimens were selected so that, of each pair taken from the same crystal, one was etched and the other polished. Six crystals were examined, using a rate of strain of about 10^{-2} sec^{-1}, and the sets of critical shear stress values for the two surface conditions were averaged to give the results in Table 2. These show that the critical shear stresses start at about the same value and that the greater strength of the etched specimens does not appear until some plastic deformation has occurred. These experiments were repeated at a lower rate of strain, 10^{-5} sec^{-1}, and the results of these in Table 2 show that the difference between the polished and etched specimens is no longer detectable at this rate of strain. Considering also the first result, it thus appears

Table 2. Critical Shear Stresses of Polished and Etched Zinc Crystals at various Extensions

Approximate rate of strain sec^{-1}	Surface treatment	Average stress, gm.mm^{-2}, for an extension of			
		0·05%	0·1%	0·5%	1·0%
10^{-2}	Etched	30	32	40	44
	Polished	28	29	33	36
10^{-5}	Etched	21	22	24	25
	Polished	21	22	24	25

that the greater strength of the etched specimens is a dynamical effect connected with the amount and rate of plastic flow, rather than with the stress required to start flow.

§ 5. CREEP EXPERIMENTS

A few creep experiments were made at room temperature to confirm the critical shear stress results. It has been shown (Cottrell and Aytekin 1947, 1950) that the flow of zinc crystals, under constant shear stress on the glide planes in the glide direction, obeys the equation

$$\gamma=\gamma_0+\beta t^{1/3}+\kappa t,$$

where γ is the shear strain, t is the time and β and κ are coefficients. This equation is essentially the same as that proposed by Andrade (1910) for the creep of polycrystalline metals. In the present work fairly short durations of loading (2–3 hours) were used so that most of the flow was of the transient, β-flow, type. When a specimen had settled down after loading to a well-defined transient flow, its surface condition was changed by immersing it in a suitable fluid, and the effect on the creep curve was studied. The apparatus was arranged so that the fluid could be brought round the specimen without interrupting the creep test or disturbing the specimen.

Figure 1 shows the strain–time curve of a specimen which was heavily oxidized in steam and then subjected to a resolved shear stress of 70 gm.mm^{-2}. After flow had occurred for 37 minutes the specimen was immersed in dilute hydrochloric acid. The rate of flow immediately increased; a large instantaneous strain took place and was followed by a fast transient flow. The large reduction in the critical shear stress caused by removing the oxide film is thus reflected by the creep behaviour.

The results of a similar experiment on a polished specimen stressed to 39 gm.mm^{-2} are shown in Figure 2. Immersion in hydrochloric acid, after 40 minutes under load, produced a perceptible but small decrease in the rate of flow. Since the latter is a much more sensitive property than the critical shear stress, it is thus hardly surprising that the measurements summarized in Table 2 showed no difference between the polished and etched specimens at low rates of strain. A third creep specimen was etched in hydrochloric acid, washed, dried and then made to flow under a stress of 42 gm.mm^{-2}. Hydrochloric acid was introduced after 30 minutes, but in this case it caused no observable change in the rate of flow.

§ 6. THE REHBINDER EFFECT

An examination of the effects of paraffin and oleic acid on the creep behaviour of specimens given various surface treatments proved interesting. Polished or etched crystals were made to flow under constant stress as before and then, at a suitable stage in the test, they were immersed in B.P. liquid paraffin either with or without 0·2% oleic acid in solution. In all cases, no change in the creep curve could be detected; Figure 3 shows a typical example with a polished specimen

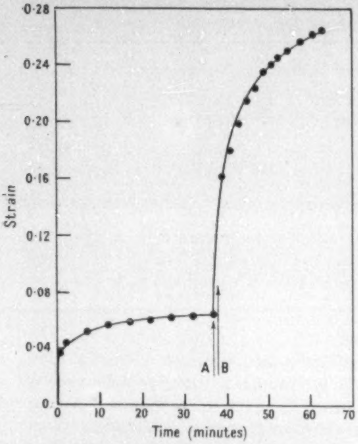

Figure 1. Creep curve of an oxidized crystal. Hydrochloric acid was applied at A and removed at B.

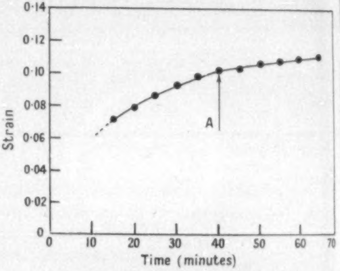

Figure 2. Creep curve of a polished crystal. Hydrochloric acid was applied at A.

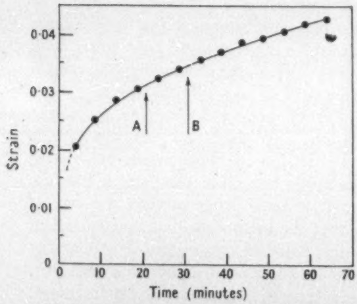

Figure 3. Creep curve of a polished crystal. Paraffin was applied at A and oleic acid solution at B.

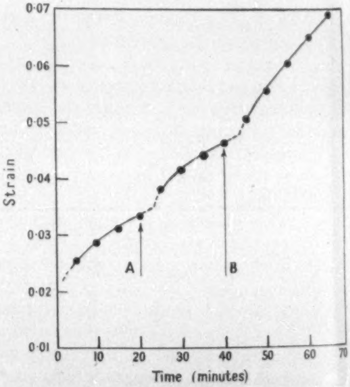

Figure 4. Creep curve of an oxidized crystal. Paraffin was applied at A and oleic acid solution at B.

stressed to 32 gm.mm^{-2}. On the other hand, specimens that had been heavily oxidized in steam responded to the paraffin treatment. Figure 4 shows the creep curve of one such specimen cut from the same crystal as that of Figure 3 under a stress of 63·5 gm.mm^{-2}. At the point A paraffin was introduced round the specimen and, within five minutes of immersion, the rate of flow increased. A second increase occurred when the paraffin was replaced by the solution of oleic acid (point B). Paraffin by itself produced a response only in heavily oxidized specimens and with lightly oxidized ones it was necessary that oleic acid should be present.

It was observed that the creep rate of heavily oxidized specimens could be increased by immersing them in kerosene or ethyl alcohol, whereas polished or etched specimens showed no response to these agents. Also, the creep rate of an oxidized specimen increased almost immediately when the specimen was immersed in kerosene or alcohol; when paraffin was used, on the other hand, a period of about five minutes elapsed before the specimen responded.

§7. RELATION OF TIME OF RESPONSE TO VISCOSITY OF MEDIUM

The facts that the Rehbinder effect could be produced only on specimens with thick oxide coats and that, with a viscous agent such as paraffin, it appeared some five minutes after immersion, while mobile agents such as kerosene or alcohol produced an almost immediate response, suggested that the effect was concerned with the penetration of the surface film by the agent. This would mean that the time for the response to appear should be related to the viscosity of the agent.

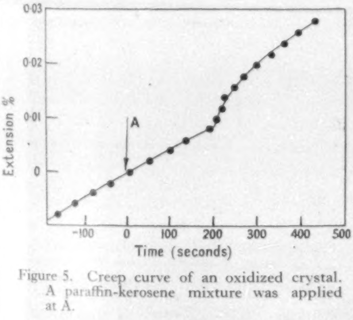

Figure 5. Creep curve of an oxidized crystal. A paraffin-kerosene mixture was applied at A.

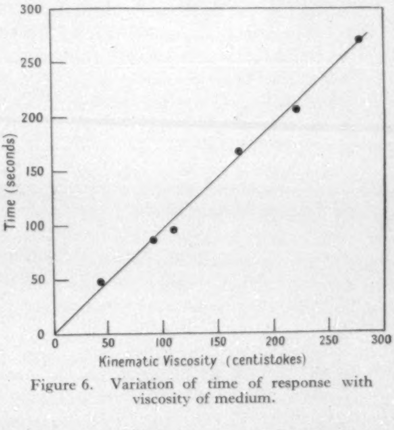

Figure 6. Variation of time of response with viscosity of medium.

Some experiments were made to examine this point using specimens that were standardized, as far as possible, by oxidizing them together in steam. A series of liquids of different viscosities was prepared by mixing paraffin and kerosene in various proportions and their kinematic viscosities were measured at room temperature with the aid of standard U-tube viscometers. Creep experiments were then made and the time interval between immersion in each liquid and the subsequent increase in the creep rate was determined. Figure 5 shows the response of a specimen to immersion, at the point A, in a liquid of high viscosity (220 centistokes); the creep rate remained unaltered for about 200 seconds and then quite suddenly increased. The results of these experiments are given in Figure 6 which shows that the experimental points lie reasonably well on a straight line through the origin, and hence that the time of response varies linearly with the viscosity.

§ 8. DISCUSSION

The above results provide a possible basis for correlating the observations of Roscoe, Rehbinder and Kemsley. It appears that the primary surface effect is the hardening produced by a film of oxide, or of other products of corrosion, and that paraffin and oleic acid produce a secondary effect by modifying the action of the film. If the surface film is sufficiently thin to be fairly ineffective, on its own account, the oleic acid solution produces no response; this may be the reason why Kemsley was unable to produce the Rehbinder effect.

The response of oxidized specimens to paraffin or similar liquids is not instantaneous and the time of response increases linearly with the viscosity of the liquid. It is thus reasonable to suppose that these liquids act by penetrating the oxide film, presumably through cracks, and weakening its adherence to the surface of the metal, thereby reducing its hardening effect. The mechanism by which the film hardens the metal remains obscure. It is difficult to reconcile a simple explanation, in terms of the ability of surface cracks to concentrate stress, with the observation that the effect appears to be related more to the progress than to the start of plastic flow. Roscoe's suggestion that the outer layers of the metal become hardened by included filaments of oxide is more reasonable.

The recent theory of Frank (1948) concerning the formation of slip-bands by the multiplication of fast dislocations suggests that the surface condition may affect the development of slip-bands and, therefore, the coefficient of strain hardening. This offers the possibility of an alternative explanation, but more work is needed before the effect of the oxide film can be properly understood.

ACKNOWLEDGMENTS

This research was carried out in the Metallurgy Department of the University of Birmingham under the general supervision of Professor D. Hanson, to whom the authors' thanks are due for interest and help. The work forms part of a programme supported by the Department of Scientific and Industrial Research through the National Physical Laboratory, to whom grateful acknowledgment is made.

REFERENCES

Andrade, E. N. da C., 1910, *Proc. Roy. Soc.* A, **84**, 1.

Andrade, E. N. da C., and Randall, R. F. Y., 1948, *Nature, Lond.*, **162**, 890.

Andrade, E. N. da C., and Roscoe, R., 1937, *Proc. Phys. Soc.*, **49**, 152.

Barrett, C. S., and Levenson, L. H., 1940, *Trans. Amer. Inst. Min. Met. Engrs.*, **137**, 76, 112.

Cottrell, A. H., and Aytekin, V., 1947, *Nature, Lond.*, **160**, 328; 1950, *J. Inst. Met.*, in press.

Cottrell, A. H., and Gibbons, D. F., 1948, *Nature, Lond.*, **162**, 488.

Frank, F. C., 1948, *Report on the Strength of Solids* (London: Physical Society), p. 46.

Kemsley, D. S., 1949, *Nature, Lond.*, **163**, 404.

Polanyi, M., 1925, *Z. tech. Phys.*, **6**, 121.

Rehbinder, P., Lichtmann, V. I., and Maslenikov, V. M., 1941, *C.R. Acad. Sci., U.R.S.S.*, **32** (2), 125.

Rodda, J. L., 1943, *Min. and Met.*, **43**, 323.

Roscoe, R., 1936, *Phil. Mag.*, **21**, 399.

Yield Points in Zinc Crystals

By H. L. WAIN and A. H. COTTRELL
Metallurgy Department, University of Birmingham

MS. received 16*th October* 1949

ABSTRACT. It is shown that sharp yield points can be produced in crystals of zinc containing nitrogen. The gas is introduced in a preliminary melting operation, either by bubbling it through the metal or by allowing it to be absorbed from the atmosphere, using a flux to keep the surface clean. Strain ageing treatments are needed to develop the yield point clearly, but once it is developed it returns at the same level after each successive treatment at the same temperature. Ageing experiments at room temperature show that overstrained zinc crystals soften by recovery before the yield point returns; zinc differs from iron in this respect. General conditions for producing yield points in metals of common crystal structures are briefly discussed.

§ 1. INTRODUCTION

THE phenomenon of the sharp yield point, familiar in mechanical tests on mild steel, is now recognized as a property of some metals containing certain other elements. It appears prominently in iron if the metal contains small amounts of carbon or nitrogen, but not otherwise (Edwards, Phillips and Jones 1940, Snoek 1941, Low and Gensamer 1944). It has also been observed in single crystals of cadmium (Smith 1947, Cottrell and Gibbons 1948) and in polycrystals of molybdenum (Túry and Krausz 1936, 1937), and in both cases nitrogen has been shown to be effective in producing the yield point. A recent theory (Cottrell 1948, Nabarro 1948, Cottrell and Bilby 1949) suggests that the yield point is caused by the segregation of solute atoms to dislocations. The attraction of the dislocations to the segregated atoms provides a bond which has to be broken by a larger force than is necessary to maintain freed dislocations in motion; the material thus gives way suddenly and softens, at the start of plastic flow, producing a sharp yield point. The theory also explains the observed removal of the yield point by plastic overstrain and its return on strain ageing. A freshly strained specimen contains freed dislocations and does not show a yield point, but on ageing these dislocations become anchored by the migration of solute atoms to them and the yield point returns.

Some time ago, Orowan (1934, 1940) observed a yield point of a very similar kind to that described above in single crystals of zinc. Because the effect appeared in crystals that were annealed after overstraining, he called it 'thermal hardening'. However, it seems preferable to retain the terms 'yield point' and 'strain ageing' since these are familiar and adequate, and since the term 'thermal hardening' has also been applied to another effect, the hardening produced by surface oxidation (Andrade and Randall 1948).

Orowan's observation has so far remained unconfirmed. Accordingly, the attempt described below was made to produce yield points in zinc crystals and to ascertain whether the effect required the presence of a specific additional element.

§ 2. METHOD

Two grades of zinc were used, the first being a sample of spectrographic purity kindly presented by the National Smelting Company, and the second a sample of commercially pure zinc. The spectrographic analyses of 1 mm. diameter wires, extruded from these materials, are given in the Table.

Analyses of Zinc Wires

Sample	% Pb	% Cd	% Cu	% Fe
Pure zinc	0·001	0·0001	0·0005	0·001
Commercial zinc	0·010	0·010	0·003	0·003

Single crystals were grown from the wires by Andrade and Roscoe's (1937) fusion method and their orientations were determined by optical measurements of the reflections from etch-pits (Barrett and Levenson 1940). Mechanical tests were made with a machine of the Polanyi (1925) type, using incremental loading, in which 3 cm. wire specimens were strained in tension by means of hooks which engaged with loops of copper wire welded to the ends of the specimens. A standard strain ageing treatment was always given before testing for the presence of a yield point. The specimen was extended a small amount (~0·3%) and, while still mounted in the machine, was annealed in a paraffin bath for 40 minutes at 180° c., after which it was cooled to room temperature. The test for the yield point was made before the bath was removed, in order not to disturb the specimen between annealing and testing, because of the possibility that mechanical shocks might overstrain the material locally and thereby prevent the observation of a yield point.

The straining, ageing and testing cycle was applied several times to each specimen. The absence of a yield point in the first test or so was considered to be inconclusive since it was not possible to be sure that the crystal was sufficiently straight, that the load was applied axially or that the concentrations of stress near the ends of the specimen were negligible. A high localized stress can cause yielding to take place prematurely, before the mean stress has reached the level of the lower yield point, in which case a smooth stress–strain curve may be observed. However, after a few repetitions of the testing cycle, inhomogeneities in the stress are usually smoothed out by plastic flow and the yield point will then appear in a susceptible material. The criteria adopted as being indicative of a true yield point were that the onset of plastic flow should be abrupt and accompanied by a fall in stress, and that the yield point should be absent in a freshly overstrained specimen and should return on ageing or annealing. Together, these distinguish the yield point phenomenon from other effects which have some similar features, e.g. hardening produced by surface oxidation (Andrade and Randall 1948) and geometrical softening produced when the glide planes are orientated at large angles to the axis of extension (Boas and Schmid 1929, Andrade and Roscoe 1937).

§ 3. ATTEMPTS TO PRODUCE YIELD POINTS

Since it has been shown that crystals of cadmium grown in nitrogen possess yield points (Cottrell and Gibbons 1948), the first attempts to produce yield points in zinc were made by growing crystals in various gases. Nitrogen, carbon dioxide, hydrogen and argon were tried, but in the case of pure zinc no yield points could be developed. Smooth stress–strain curves, with a critical shear stress of 20–30 gm. mm^{-2}, were always observed even after repeated strain ageing treatments Curves 1 and 2 of Figure 1 are examples taken from a crystal grown in nitrogen.

Similar experiments with commercial zinc showed that yield points could always be produced irrespective of the gas in which the crystals were grown. Two strain ageing treatments were usually necessary before the yield point became pronounced. Curves 3, 4 and 5 of Figure 1, taken from a crystal grown in argon, show the formation of a yield point after two strain-ageing treatments. Once formed, the yield point occurred repeatedly after each successive treatment, except when the specimen was disturbed by dismounting it from the machine. The removal of the yield point by plastic overstrain is illustrated by curve 5, which was taken immediately after curve 4. The upper yield point usually occurred at a resolved shear stress of 80–110 gm.mm^{-2} and the lower yield point at 70–95 gm.mm^{-2}.

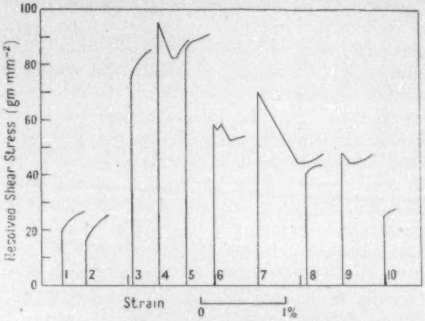

Figure 1. Stress–strain curves on zinc crystals.

Curve 1. Initial test on pure zinc, crystal grown in nitrogen.
,, 2. As curve 1, after four strain-ageing treatments.
,, 3. Initial test on commercial zinc, crystal grown in argon.
,, 4. As curve 3, after two strain-ageing treatments.
,, 5. Taken immediately after curve 4.
,, 6. Commercial zinc, partly degassified, crystal grown in argon, after two strain-ageing treatments.
,, 7. Pure zinc, melted in air with flux, crystal grown in nitrogen, after three strain-ageing treatments.
,, 8. Taken immediately after curve 7.
,, 9. Pure zinc, treated with nitrogen, crystal grown in nitrogen, after one strain-ageing treatment.
,, 10. Pure zinc, melted in argon with flux, crystal grown in argon, after four strain-ageing treatments.

These experiments showed not only that yield points could be produced in zinc crystals but also that the effect was associated with impurities in the metal. To identify the impurity element responsible, some crystals were made from pure zinc to which had been added traces of other metals, e.g. 0·01% cadmium. No yield points could be developed, however, and so attention was next directed to gaseous impurities. A small ingot of commercial zinc was melted and solidified several times, *in vacuo*, in an attempt to degassify the metal. Crystals grown in argon from wires extruded from this ingot showed yield points (curve 6, Figure 1), although these were less marked and the yield stress was reduced to 50–60 gm.mm^{-2}. This indicated that the effect was related to gas in the metal. It was known that the commercial zinc had been melted in air, under a flxn of ammonium and zinc chlorides, and it seemed possible that this procedure might have affected the gas content of the metal. Accordingly, a 50 gm. sample of pure zinc was melted in air in an open combustion boat for 30 minutes, during which time its surface was kept clean by sprinkling it occasionally with pure ammonium chloride. The ingot was then extruded to wire and crystals were grown in nitrogen. These showed the yield phenomenon very strikingly, with a fall in stress of 20–30% at the yield point. Curves 7 and 8 of Figure 1 are examples. In general the upper yield point occurred at 60–80 gm.mm^{-2} and the lower yield point at 40–50 gm.mm^{-2}.

During the preliminary melting operation the ammonium chloride appeared to remove the oxide film completely from the molten metal, which would presumably allow the latter to absorb gases, particularly nitrogen, from the atmosphere more easily. On the other hand, it was possible that ammonium chloride or one of its decomposition products had dissolved in the metal. Two experiments showed that the first possibility was more probable. If dry, oxygen-free nitrogen was bubbled through molten pure zinc, with no flux present, yield points could then be developed in crystals of the metal (curve 9, Figure 1). Secondly, yield points could not be developed in crystals made from pure zinc which had been melted under flux in an atmosphere of argon (curve 10, Figure 1).

Zinc is thus similar to cadmium in that single crystals possess yield points when they contain nitrogen. However, whereas sufficient nitrogen to develop the yield point is absorbed by cadmium during growth of the crystals in a nitrogen atmosphere, in the case of zinc nitrogen has to be introduced in a preliminary melting operation.

§4. CHARACTERISTICS OF THE YIELD POINT IN ZINC

The fact that in the above experiments the nitrogen was introduced before the metal was extruded almost disposes of the possibility that the yield point might be a result of a special surface condition, such as, for example, the formation of a nitride on the surface. The indifference of the yield phenomenon to the surface condition was confirmed by experiments on crystals of pure zinc containing nitrogen which were electro-polished before being tested. The polishing was carried out in chromic acid solution (Rodda 1943) and removed a layer about 0·025 mm. deep from the surface. The yield point could be developed very clearly in these specimens (Figure 2) which shows, in agreement with theory, that the effect is due to nitrogen within the metal rather than at its surface.

Figure 2 also illustrates the development of the yield point after successive strain-ageing treatments. It is remarkable how closely the yield point can be reproduced, once it has been clearly developed by the early strain-ageing treatments. In curves 6, 8 and 10 the upper yield occurs consistently at 84–85 gm.mm^{-2} and the lower yield at 67–68 gm.mm^{-2}. This is quite different from the behaviour of iron and steel, where the yield point returns at a higher level of stress after each successive treatment (Muir 1906).

The reason for this became apparent after a series of experiments in which a crystal was aged, after overstraining, at room temperature for various periods of time. Figure 3 shows the results. For short times of ageing the elastic limit decreases due to recovery and the yield point does not appear. Recovery is rapid at first and after two to four hours the elastic limit reaches a minimum. It then remains constant until the yield point first appears, after eight to nine hours; ageing for progressively longer times causes the yield point to increase. Interpreted theoretically, two phenomena have to be considered, recovery, involving the

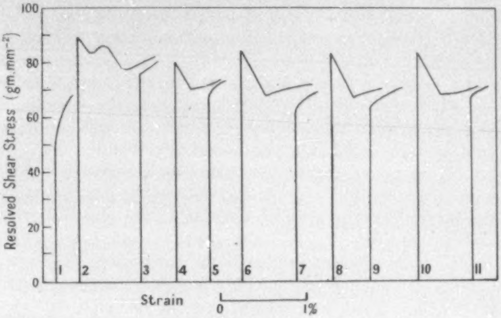

Figure 2. Stress-strain curves on an electrolytically polished crystal made from pure zinc melted in air under ammonium chloride.

Curve 1. Initial test.
,, 2. After one strain-ageing treatment.
,, 3. Taken immediately after curve 2.
,, 4. After two strain-ageing treatments.
,, 5. Taken immediately after curve 4.
,, 6. After three strain-ageing treatments.
,, 7. Taken immediately after curve 6.
,, 8. After four strain-ageing treatments.
,, 9. Taken immediately after curve 8.
,, 10. After seven strain-ageing treatments.
,, 11. Taken immediately after curve 10.

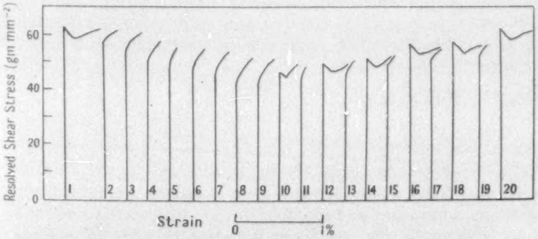

Figure 3. Stress-strain curves, after various ageing treatments at room temperature, on a crystal made from pure zinc melted in air under ammonium chloride.

Curve No.	1	2	3	4	5	6	7	8	9	10
Time of ageing (hours)	48	0	0·25	0·5	1	2	3·75	6	8	8·5
Curve No.	11	12	13	14	15	16	17	18	19	20*
Time of ageing (hours)	0	10	0	11	0	17	0	24	0	48

* Curve 1 repeated.

movement and annihilation of dislocations, and strain ageing, involving the migration of nitrogen atoms to dislocations. It is hardly possible for strain ageing to occur during the early stages of recovery when the dislocations are moving rapidly; however, when recovery is almost completed the solute atoms have a reasonable chance of migrating to the dislocations and fixing them in position. Further evidence on this point was given by ageing a specimen while it was subjected to an applied stress. It was not possible to make the yield point return except when the stress was well below the lower yield value. Higher stresses evidently cause creep by the continued movement of freed dislocations, so that strain ageing can hardly occur.

The rapid recovery of these specimens can be attributed to the high purity of the metal, which allows free dislocations to be highly mobile. In the case of iron, however, the metal is much less pure and it is well known that thermal softening only becomes rapid at temperatures approaching 500°. As a result, strain ageing occurs before the strain hardening is removed; the increase in the yield point, with successive straining and ageing treatments, can thus be traced to the accumulation of strain hardening in the material. In pure zinc, on the other hand, recovery occurs almost completely during each strain-ageing treatment so that the yield point returns at the same level.

The experiments summarized in Figure 3 were repeated, using slightly elevated ageing temperatures, and showed that the rate of ageing increased with temperature. Thus, at 30, 40 and 50° c., the times taken for the first appearance of the yield point were 140, 45 and 15 minutes, respectively. It may be deduced from these results that the process is thermally activated, with an activation energy of 21,000 cal. per mol.

Smith (1947) reported that the magnitude of the yield point in strain-aged cadmium crystals depended upon λ, the angle between the axis of tension and the glide direction, being very small when this angle was about 40–45°; this was not confirmed by Cottrell and Gibbons (1948) who obtained large yield points in cadmium crystals of all orientations. In the present work no dependence of the yield point of zinc on orientation was found although it was noticed that more strain-ageing treatments were usually needed to develop the yield point fully in crystals with $\lambda \simeq 45^\circ$ than in others. For a given critical shear stress, a crystal having this orientation is softer and more easily overstrained than any other; it is possible that more strain-ageing treatments were needed because such specimens are more easily bent during preparation and mounting prior to testing.

§ 5. DISCUSSION

In each of the four metals iron, molybdenum, cadmium and zinc in which the yield phenomenon has been clearly established, it has been shown that nitrogen is an effective solute element for producing the yield point. Carbon is also effective in iron, but its behaviour in the other metals has not so far been studied. Theoretically, the conditions for a solute atom to produce the yield phenomenon are that it should distort the lattice severely and be able to migrate fairly rapidly, conditions which are known to be fulfilled in the case of carbon and nitrogen in iron. The behaviour of these elements in the other metals has not been sufficiently studied, but it seems probable that they dissolve interstitially, in which case they may be expected both to distort the lattice and to be highly mobile.

In no metal of face-centred cubic structure has a yield point been established so clearly as in the above metals. Frank (private communication) has suggested that the comparative rarity of the effect may be because most solute atoms probably interact weakly with screw dislocations. The hydrostatic stress round a screw dislocation is ideally zero, so that the dislocation may not attract solute atoms that produce only spherically symmetrical distortions. Solute atoms that produce non-symmetrical distortions are needed to anchor this type of dislocation, since these can interact with its shear stress field. Carbon and nitrogen are known to produce this type of distortion in α-iron and probably in other body-centred cubic transition metals (Dijkstra 1947, Kê 1948), but not in face-centred cubic metals; this is a consequence of the shapes of the interstitial positions occupied by these atoms in the two types of lattice. In the case of the close packed hexagonal structure the presence of a crystallographically unique axis obviously favours a non-symmetrical distortion round solute atoms.

Strongly marked yield points may therefore be rare in face-centred cubic metals because of the difficulty of anchoring screw dislocations in this type of lattice. This does not mean, of course, that edge dislocations will not be anchored; the strong hydrostatic component in their stress fields should enable them to attract many types of solute atoms, but this can hardly lead to a yield point while the screw dislocations remain free.

ACKNOWLEDGMENTS

The authors wish to thank Professor D. Hanson, under whose general supervision this work was carried out, for his interest and support, and Mr. D. F. Gibbons and Dr. A. T. Churchman for many useful discussions. The spectrographic analyses were kindly made by the laboratories of the Imperial Smelting Corporation.

REFERENCES

Andrade, E. N. da C., and Randall, R. F. Y., 1948, *Nature, Lond.*, **162,** 890.
Andrade, E. N. da C., and Roscoe, R., 1937, *Proc. Phys. Soc.*, **49,** 152.
Barrett, C. S., and Levenson, L. H., 1940, *Trans. Amer. Inst. Min. Met. Engrs.*, **137,** 76, 112.
Boas, W., and Schmid, E., 1929, *Z. Phys.*, **54,** 16.
Cottrell, A. H., 1948, *Report on the Strength of Solids* (London : Physical Society), p. 30.
Cottrell, A. H., and Bilby, B. A., 1949, *Proc. Phys. Soc.* A, **62,** 49.
Cottrell, A. H., and Gibbons, D. F., 1948, *Nature, Lond.*, **162,** 488.
Dijkstra, L. J., 1947, *Philips' Res. Rep.*, **2,** 357.
Edwards, C. A., Phillips, D. L., and Jones, H. N., 1940, *J. Iron and Steel Inst.*, **142,** 199.
Kê, T. S., 1948, *Phys. Rev.*, **74,** 9.
Low, J. R., and Gensamer, M., 1944, *Trans. Amer. Inst. Min. Met. Engrs.*, **158,** 207.
Muir, J., 1906, *Proc. Roy. Soc.* A, **77,** 277.
Nabarro, F. R. N., 1948, *Report on the Strength of Solids* (London : Physical Society), p. 38.
Orowan, E., 1934, *Z. Phys.*, **89,** 634; 1940, *Proc. Phys. Soc.*, **52,** 14.
Polanyi, M., 1925, *Z. Tech. Phys.*, **6,** 121.
Rodda, J. L., 1943, *Min. and Met.*, **43,** 323.
Smith, C. L., 1947, *Nature, Lond.*, **160,** 466.
Snoek, J. L., 1941, *Physica*, **8,** 734.
Túry, P., and Krausz, S., 1936, *Nature, Lond.*, **138,** 331; 1937, *Ibid.*, **139,** 30.

A Simple Constant Stress Apparatus for Creep Testing

By L. M. T. HOPKIN*
British Non-Ferrous Metals Research Association, London

Communicated by A. G. Quarrell; MS. received 16*th November* 1949

ABSTRACT. A simple device is described which can maintain the stress on a creep specimen constant to within 0·8% during uniform extensions up to 100%. The apparatus is suitable for slow rates of strain. Examples are given of creep curves obtained with this device from tests on lead and a lead–tin alloy extending to 1,000 and 400 hours respectively; good agreement with the Andrade creep equation is observed in both cases.

Long time creep tests are usually performed under conditions of constant load for the sake of simplicity, although this method has the disadvantage that the stress increases as the cross-sectional area of the specimen decreases during extension. The change in stress is insignificant when the extension is small, but it becomes important in tests on materials which undergo large extensions before failure. In consequence Andrade, in his classic work on the creep of metals (Andrade 1910), carried out his tests at constant stress and was able to derive a general equation for the creep curves so obtained. Most subsequent fundamental investigations of the phenomenon of creep in ductile materials have been carried out under conditions of constant stress.

In a long-term investigation of the influence of metallurgical factors on the creep of lead and lead alloys now in progress in the laboratories of the British Non-Ferrous Metals Research Association, the tests are being made at constant stress to simplify interpretation of the results and to enable the creep curves to be analysed mathematically. The results obtained should increase the knowledge of the mechanism of flow in metals as it will be possible, for example, to test the validity of the Andrade equation in creep tests of long duration. In this investgation up to 150 specimens will be tested simultaneously and many of the tests will be continued for several years. It was therefore essential that the constant stress device employed should be simple in construction, relatively inexpensive, and suitable for slow rates of strain by being as frictionless as possible in operation. These considerations ruled out the designs which have already been described in the literature (Andrade 1910, 1914, 1948, Andrade and Chalmers 1932, Pearson 1934, Fisher and Carrker 1949, Ward and Marriott 1948), but a simple apparatus has been designed and tested which fulfils all requirements.

The apparatus is shown in Figure 1, and is a modification of the lever used by Andrade and Chalmers (1932). The method of suspension by knife edges used by these workers has been replaced by an arrangement of steel tapes. Figure 2 shows a creep testing frame containing specimens of lead and lead alloys loaded by means of these constant stress levers.

As the specimen extends, the moment of the applied weights about a point in the line of action of the anchoring tapes is inversely proportional to the length of the specimen, and hence directly proportional to the cross-sectional area of the specimen assuming the specimen does not change its volume during extension. Like other constant stress devices, this new apparatus maintains a constant stress only if the specimen extends uniformly.

---

* Investigator, B.N.F.M.R.A., London.

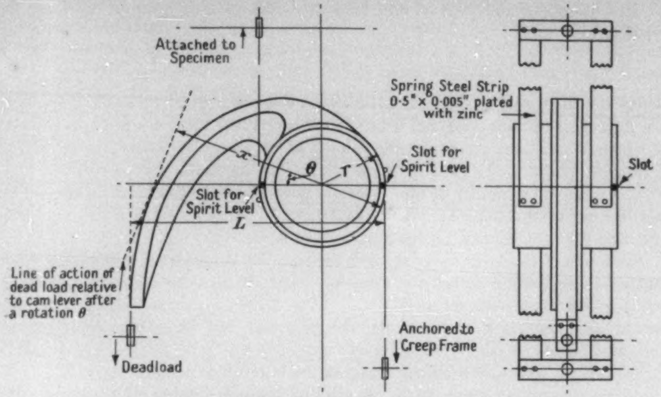
Attached to Specimen
Spring Steel Strip 0·5" x 0·005" plated with zinc
x
θ
r
T
Slot for Spirit Level
Slot for Spirit Level
Slot
L
Line of action of dead load relative to cam lever after a rotation θ
Anchored to Creep Frame
Deadload

Figure 1. Constant stress cam lever.

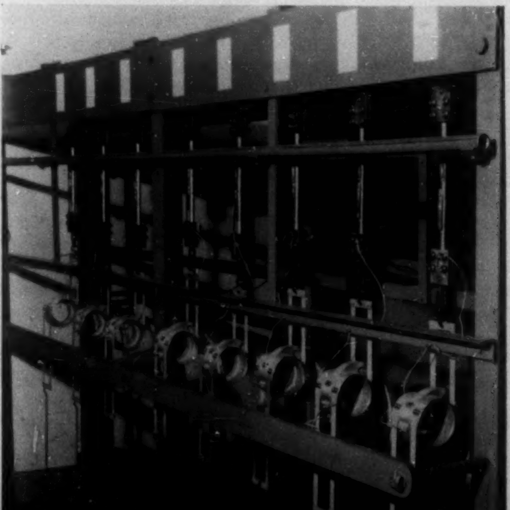

Figure 2. Creep frame containing specimens of lead and lead alloys loaded by means of the constant stress levers.

The shape of the cam of the lever was determined graphically from the relationship

$$\frac{x}{L}=\frac{a}{a+2r\theta}, \qquad \ldots\ldots(1)$$

where a is the initial length of the specimen, θ is the angular rotation of the lever, r is the radius of the cylindrical drum of the lever, and x is the arm of the moment of the weights about a point in the line of action of the anchoring tapes after an angular rotation of θ; L is the initial arm of the moment when $\theta=0^\circ$.

Equation (1) is similar to that given by Andrade and Chalmers except for the factor 2 in the denominator. This is introduced because, in the present case, the effective fulcrum falls as the specimen extends.

The size of the lever was determined from the dimensions $L=6$ in., $a=7$ in. and $r=1\cdot5$ in., which permit the stress on a specimen to be maintained constant for uniform extensions up to 100%. After 100% uniform extension the test continues under constant load. It will be noted that the initial lever ratio is 2:1 when $\theta=0$.

The lever, which was designed so that the maximum initial force of 225 lb. wt. could be exerted on a specimen, consists of a single casting of a high strength aluminium alloy machined to the required dimensions. The connections from the lever to the weights, to the specimen, and to the point of anchor on the creep testing frame are made with spring steel tape, 0·5 in. wide and 0·005 in. thick, electrolytically plated with zinc, 0·0005 in. thick on each side, to prevent corrosion. Any hydrogen embrittlement of the tapes which may have resulted from the plating process was removed by a suitable heat-treatment. The weight of a complete lever is 1 lb.

For accurate and reproducible results the inclination of the centre line of the lever to the horizontal at the beginning of a test must be known and capable of adjustment. This inclination is determined by a small spirit level mounted so that it can be readily fitted, when required, into two slots milled on the horizontal centre line of the apparatus (see Figure 1). An adjustable anchorage for the tapes on the creep-testing frame enables the inclination of the lever to be adjusted as required.

When arranging the inclination of the lever relative to the horizontal at the beginning of a test, allowance is made for the rotation of the lever which occurs on loading as the result of the elastic extension of the tapes. The relationship between the rotation and the applied load can be determined experimentally as follows, and is the same for all the levers. The lever is set up as it is used in practice with the exception that the creep specimen is replaced by a steel bar of such dimensions that its elastic extension is negligible under the maximum load used in the creep tests. A suitable load is attached to the lever and the anchoring connection is adjusted until the centre line of the lever is horizontal. The load is removed with the exception of a small weight sufficient to keep the tapes taut, and the new position of the bubble of the spirit level is marked. This procedure is repeated for several of the loads to be used in the creep tests. When starting a creep test the lever, loaded with the same small weight sufficient to keep the tapes taut, is adjusted so that the bubble of the spirit level is at the mark corresponding to the load to be used for the particular creep test.

The major error of the device arises from the force applied to the specimen by the moment of the weight of the casting about the effective fulcrum. This error, together with any others, can be determined by calibrating the lever in a tensile testing machine. Over the range of forces of 100–225 lb. wt. which could be applied to a specimen at the beginning of a test, it was found that at any strain up to 100% the error in the force would not be greater than 0·8% of the theoretical value. For initial forces between 40–100 lb. wt. it was found that at any strain up to 15% the error in the force on a specimen would not be greater than 0·3% of the theoretical value, although for strains between 15% and 100% the error increased to 0·8%.

If necessary, the error due to the weight of the lever can be minimized for small strains by making suitable additions to weights to the body of the lever so that the centre of gravity of the apparatus falls near the effective fulcrum at the beginning of a test.

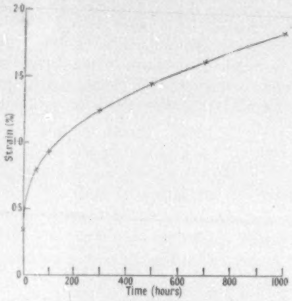

Figure 3. A creep test at a constant stress of 300 lb/in² on lead of 99·999% purity.

Experimental curve shown by continuous line. The points shown by crosses were calculated from the constants:

$l_0=1\cdot0034,\quad \beta=1\cdot2\times10^{-3}\ \mathrm{hr}^{-1/3},$
$K=3\cdot0\times10^{-6}\ \mathrm{hr}^{-1}.$

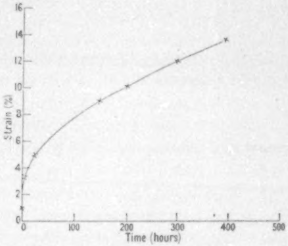

Figure 4. A creep test at a constant stress of 1,000 lb/in² on an alloy of lead containing 1% of tin.

Experimental curve shown by continuous line. The points shown by the crosses were calculated from the constants:

$l_0=1\cdot0097,\quad \beta=1\cdot29\times10^{-2}\ \mathrm{hr}^{-1/3},$
$K=7\cdot4\times10^{-5}\ \mathrm{hr}^{-1}.$

The creep curves shown in Figures 3 and 4 were obtained from tests carried out on lead of 99·999% purity and the same lead alloyed with 1% of tin using the constant stress device. In both figures the continuous line passes through the experimentally determined points, which have been omitted for the sake of clarity. The crosses indicate the points calculated from the Andrade equation $l_t=l_0(1+\beta_t^{1/3})e^{Kt}$ where l_t is the length of the specimen at time t and l_0, $\beta(\mathrm{hr}^{-1/3})$ and $K(\mathrm{hr}^{-1})$ are constants.

ACKNOWLEDGMENTS

The author wishes to thank the Director and the Council of the British Non Ferrous Metals Research Association for permission to publish this paper. The method of suspension of the lever was evolved from a suggestion made by Mr. R. May, A.R.S.M.

REFERENCES

Andrade, E. N. da C., 1910, *Proc. Roy. Soc.* A, **84,** 1; 1914, *Ibid.*, **90,** 329; 1948, *Proc. Phys. Soc.*, **60,** 304.

Andrade, E. N. da C., and Chalmers, B., 1932, *Proc. Roy. Soc.* A, **138,** 348.

Fisher, J. C., and Carrker, R. P., 1949, *J. Metals*, **1,** 178.

Pearson, C. E., 1934, *J. Inst. Metals*, **54,** 111.

Ward, A. G., and Marriott, R. R., 1948, *J. Sci. Instrum.*, **25,** 147.

Surface Tensions in the System Solid Copper–Molten Lead

By G. L. J. BAILEY and H. C. WATKINS*
The British Non-Ferrous Metals Research Association, London

MS. received 21*st October* 1949

ABSTRACT. A method is described by which the surface tension of surfaces occurring in the systems copper–hydrogen or argon and copper–lead–hydrogen or argon is determined. At temperatures round 850° c. the surface tension between copper grains is 640 dyne/cm. and between copper and the equilibrium lead–copper liquid phase 340 dyne/cm. The surface tension of a copper–gas surface is the same whether the gas is hydrogen or argon, within the limits of precision of the experiment, and has the value 1,800 dyne/cm. When lead vapour is present in the gas atmosphere at a partial pressure of the order of 0·1 mm. Hg the surface tension of the copper–gas surface has the much lower value of 780 dyne/cm. It is suggested that the reduction is due to the adsorption of lead at the copper–gas surface. The failure of the liquid phase to exhibit a contact angle of zero against solid copper surfaces is thereby understood.

§ 1. INTRODUCTION

THE wetting of a solid by a liquid may be regarded formally as being determined by the surface tensions at the three surfaces solid–liquid, liquid–gas and solid–gas. If the contact angle exceeds zero its value shows the balance of these three tensions, but generally the absolute magnitude of only one of them, the liquid–gas surface tension, is known or readily ascertainable. The present paper describes an attempt to measure the two unknown surface tensions using methods inspired by the work of C. S. Smith (1948) on the rôle of surface tensions in determining the structure of fully annealed alloys.

In the course of the British Non-Ferrous Metals Research Association's investigation of soldering and brazing, simple experiments were made in which the angle at which the surface of a liquid lead–copper alloy met a solid surface of copper was estimated, at a series of temperatures up to 950° c., the metals being heated in an atmosphere of purified cylinder hydrogen. It was noted that, especially at the higher temperatures employed, the grain-boundaries of the exposed copper surfaces rapidly became etched and filled with liquid. Further experiments, in which electropolished specimens of oxygen-free copper were heated in an atmosphere of hydrogen or argon with or without the presence of unsaturated lead vapour showed that marked thermal etching of the grain-boundaries occurred when lead vapour was present, the effect in hydrogen or argon alone being comparatively small.

The interpretation placed upon these observations was that proposed by Chalmers, King and Shuttleworth (1948), that the development of grain-boundary grooves represents an approach to an equilibrium condition of minimum surface free energy, the mechanism probably being that of surface migration of copper ions.

Surface tension is often regarded as equivalent, and numerically equal, to specific surface free energy. Gurney (1949) has recently discussed the conditions under which such an assumption is justified. In his view surface tension and specific surface free energy are numerically equal only when surface migration of atoms has occurred to the extent required for the establishment of thermal equilibrium, so that both are minimal. In the experiments to be described, the attainment of equilibrium was always sought. The terms surface tension and specific surface free energy are therefore taken to be equivalent.

---

* Now with Messrs. H. J. Enthoven & Sons, Ltd., London.

It seemed likely that the surface tension of copper is lower in the presence of lead vapour than in the presence of argon or hydrogen alone, since the boundary grooves were deeper. Such a decrease might possibly result from the adsorption of lead from the vapour phase, but, whatever the reason, it could explain why the contact angle of lead–copper liquid against a copper surface is greater than zero. The value of the contact angle is determined by the surface tensions of the solid–gas, liquid–gas and solid–liquid interfaces. The surface tension of a clean copper surface in contact with its own vapour and hydrogen is expected to be greater than 1,000 dyne/cm., since that of liquid copper just above the melting point has been found to exceed this value. The liquid–gas surface tension is not likely to be greater than 500 dyne/cm., and, according to Smith (1948), the solid–liquid surface tension is about one-half that of the surfaces between grains of the solid, which is itself several times smaller than that of the solid–gas surface. Thus the liquid phase would be expected always to exhibit a contact angle of zero against a copper surface cleaned in hydrogen. This is not, in fact, observed.

It appeared that absolute values for the surface tension of copper in hydrogen or argon, and also of copper in hydrogen or argon containing lead vapour, might be determined, together with values for the copper–lead surface and for the surface between grains in solid copper. These would be derived, in terms of the surface tension of the liquid phase, from measurements of the angles at the root of the etched grain-boundaries and of the contact angle between the liquid lead–copper alloy and copper, together with some of the measurements quoted by Smith. The derivation of these absolute values is described below.

§ 2. PRINCIPLE OF THE METHOD

Smith (1948) has proposed that the grain structure of many well-annealed alloys reveals an approach to equilibrium between phase and grain interfaces whose surface tensions balance each other at the points and along the lines where they meet. In a particular case of a well-annealed two-phase alloy, for example of copper containing a small percentage of lead, a normal cross section of a boundary between three copper grains might appear as in Figure 1, the lead being present as a prismatic filling along the edges where the copper grains would otherwise meet. At each corner of the prism the balance of surface tensions is represented by the equation

$$\gamma_{11} = 2\gamma_{12} \cos \theta/2 \qquad \ldots\ldots (1)$$

in which γ_{11} is the surface tension between copper grains, γ_{12} the surface tension between copper and lead phases, and the angle θ is called by Smith the 'dihedral angle'. Smith suggests that the values of γ_{11} and γ_{12} are substantially independent of crystallographic orientation and, from measurements of the dihedral angle θ, quotes values for the ratio γ_{12}/γ_{11} of a number of alloys at several temperatures.

The equilibrium configuration of grain-boundaries exposed in a solid–gas surface is similarly determined by the balance of surface tensions (Chalmers, King and Shuttleworth 1948). Figure 2 represents a normal cross section through a grain-boundary groove produced by thermal etching, for example of copper. The balance of surface tensions is given by the equation

$$\gamma_{11} = 2\gamma_{13}\cos\phi/2 \qquad \ldots\ldots(2)$$

in which γ_{11} is the surface tension between copper grains, γ_{13} the surface tension between copper and gas phase, and ϕ the dihedral angle.

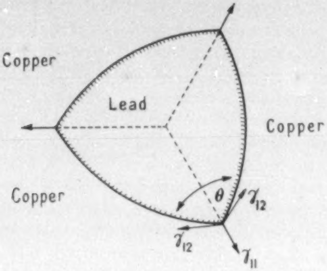

Figure 1.

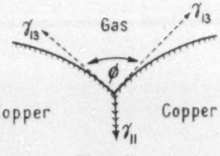

Figure 2.

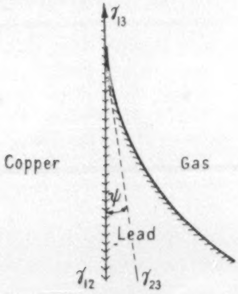

Figure 3.

It is assumed that γ_{12} is independent of relative orientation.

From Figure 3 it is clear that the balance of surface tension forces determining the contact angle exhibited against a smooth solid surface is given by the expression

$$\gamma_{13} = \gamma_{12} + \gamma_{23}\cos\psi \qquad \ldots\ldots(3)$$

where γ_{23} is the surface tension of lead–copper liquid, ψ the angle of contact, and γ_{12}, γ_{13} have the meanings previously assigned.

The values of γ_{11}, γ_{12}, γ_{13}, γ_{23} must all be considered to depend on temperature, and, since adsorption may have important effects, on the components of the gas phase and their partial pressures. It will be assumed that γ_{11} (copper–copper), γ_{12} (copper–lead) and γ_{23} (lead–gas) are independent of the nature of the gas phase, which affects only the solid–gas surface tension, γ_{13}. Then, from measurements of the angles θ, ϕ and ψ, the values of γ_{11}, γ_{12} and γ_{13} may be readily determined in terms of the surface tension of the liquid lead–copper alloy, γ_{23}.

Fig. 4

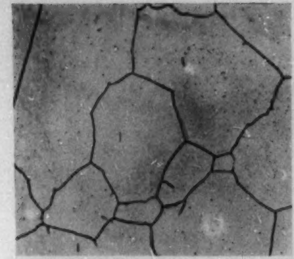

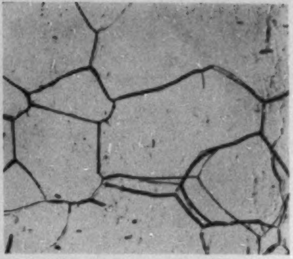

Fig. 5

Fig. 6

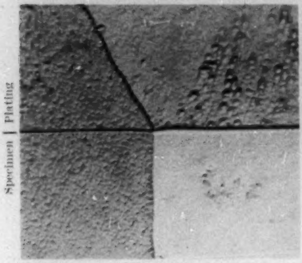

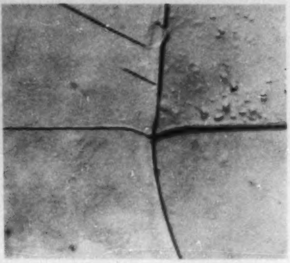

Fig. 7

Fig. 8

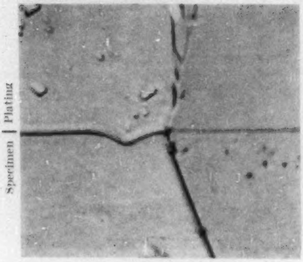

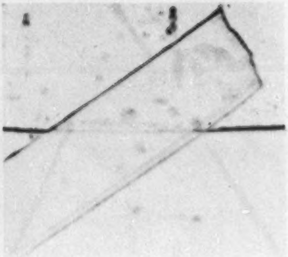

Fig. 9

Figure 4. Grain boundary etching of electrolytically polished copper surface heated in argon for two hours at 900° c. ×50.

Figure 5. Grain boundary etching of electrolytically polished copper surface heated in argon with unsaturated lead vapour for two hours at 900° c. × 50.

Figure 6. Section of groove produced at grain-boundary by thermally etching electrolytically polished copper in hydrogen for two hours at 900° c. × 2500.

Figure 7. Section of groove produced at grain-boundary by thermally etching electrolytically polished copper in hydrogen with unsaturated lead vapour for two hours at 900° c. × 2500.

Figure 8. Same treatment as for Figure 7. Section showing detached groove and grain-boundary. × 2500.

Figure 9. Same treatment as for Figure 7. Section showing intersection of twin boundaries with surface. × 2500.

§ 3. EXPERIMENTAL

(i) *Thermal Etching Technique*

The materials used were oxygen-free high-conductivity copper and high-purity (99·998%) lead. The copper specimens, 25 mm. × 5 mm., cut from 16-gauge sheet, were electrolytically polished in phosphoric acid after preliminary polishing on emery papers. After this treatment the copper surface appeared smooth and featureless when examined microscopically at ×2,500.

Annealing was carried out in a silica tube heated in a furnace which could be withdrawn after the experiment so as to promote rapid cooling from the temperature of treatment. The furnace atmosphere was either cylinder hydrogen or argon at atmospheric pressure, freed from residual oxygen by passage over heated platinized asbestos, followed by a series of drying tubes and further through a second similar train. When argon was used the specimens were subjected to a de-oxidizing treatment in hydrogen before switching over to the argon supply.

Preliminary experiments indicated that the development of grain-boundary grooves in hydrogen atmosphere was rather slow at temperatures below 800° c., and the investigation was confined to a relatively narrow temperature range, viz. 800–900° c.

In the experiments using an atmosphere containing lead vapour the lead was contained in a small silica boat placed in the silica tube upstream of the copper specimen. It was arranged that when the furnace was in position the specimen temperature was always about 50° c. higher than the temperature of the lead, so that the lead vapour was unsaturated above the specimen. No attempt was made in these experiments to control the vapour pressure rigidly. Its value was taken to be of the order of 0·1 mm. Hg.

After the grain-boundary etching treatment the specimens were cooled by withdrawing the furnace, and the surfaces were protected by plating in an acid copper bath. The plated specimens were sectioned, mounted in bakelite, and polished in the normal manner for metallographic examination. The best etch was found to be a mixture of equal volumes of 0·88 ammonium hydroxide and 10 vol. hydrogen peroxide. The surface appearance of boundary grooves developed in the absence and presence of lead vapour is shown in Figures 4 and 5 (see Plate) respectively, and etched sections through typical grooves appear in Figures 6 and 7.

It is of interest to note that the surfaces of specimens exposed to lead vapour afterwards showed little tendency to tarnish in the laboratory atmosphere, in comparison with similar specimens treated in hydrogen only.

(ii) *Measurement of Dihedral Angle ϕ (Solid–Gas)*

Dihedral angles of the proper value will be observed on a section through the surface only if the following conditions are met:

(*a*) The plane of the microsection is normal to the surface of the specimen.

(*b*) The plane of the grain boundary is perpendicular to the surface of the specimen.

(*c*) The plane of the grain boundary is perpendicular to the plane of the microsection.

Care was taken to cut sections perpendicular to the surface of the specimen, and no serious error is likely to have been introduced from this cause. It was observed that most of the boundaries were substantially perpendicular to the surface of the specimen. Any showing deviations of more than a few degrees were neglected in the measurement of dihedral angle.

Compliance with condition (*c*) above is clearly impracticable when polycrystalline specimens are used. The effect of a departure from perpendicularity between the plane of the grain-boundary and that of the microsection is to enlarge the dihedral angle; thus to obtain a true value only the smallest observed value should be taken. The directions of the grain-boundaries upon the thermally etched surface are random, so that the probability that the plane of a boundary will lie within a given angular range about a particular angle to the plane of the normal section examined is the same for all angles. By inspection it was found that the lowest angle obtained on any specimen was about 120°. With a true dihedral angle of this value it may readily be shown that, if the plane of the boundary is within $\pm 22{\cdot}5^\circ$ of the normal to the plane of section, the apparent dihedral angle does not exceed the true value by more than 3°, and the probability that a given angle is within 3° of the true value is thus 1:4. The error of measurement was expected to be of this order.

It is reasonable to suppose that the equilibrium dihedral angle, ϕ, is established as soon as thermal etching begins, and that, as etching proceeds, the grooves merely become deeper, while maintaining the same root angle. The flanks of a groove are cylindrically curved surfaces, intersecting at its root, and the measurement of root angle on a section requires that tangents shall be drawn to the traces of these surfaces at their point of intersection. The deeper the groove, the more accurate is this process likely to be. However, the depth of grooves did not increase proportionately to time of anneal after the first two hours. The reason for this is probably that grain-growth took place during annealing, so that boundaries were in general moving slowly and equilibrium tended to be established between the rate of boundary migration and depth of groove, determined by the rate of surface migration of copper atoms. A sudden increase in rate of boundary migration could supposedly result in a boundary becoming detached from its groove, which should then begin to heal. Such a detached groove and boundary are shown in section in Figure 8, and surface scars resulting from a change in rate of movement may be seen in Figure 5. The difficulty could no doubt be overcome, for example, by using bicrystal specimens; by this means also the dependence of surface tensions on crystallographic orientation could be ascertained.

However long the annealing time, the depth of grooves did not exceed that typified in Figures 6 and 7, in which the magnification is 2,500 times.

Tangents at the root of selected grooves were drawn in by eye on prints of such micrographs enlarged a further five times.

A best value for the dihedral angle was derived in the following way. A large proportion of the boundaries observed were between twins, and did not develop grooves (Figure 9), and some of the remaining boundaries were not perpendicular to the surface of the specimen. These were all discarded. Of the remainder, some were not deep enough to be measurable reliably, or were ill-defined, but on most of them measurement could have been attempted. From all these a selection was made of that quarter of the total appearing to have the lowest angles. These were photographed and measured as described above. It was assumed that in all these cases the plane of the boundary was normal to that of the section, and the most frequently occurring angle was taken as the best value for the true angle.

An analysis of observations made on a typical specimen is given in Table 1, and in Table 2 are set out the values of the angle measured for each of the twelve grooves photographed, as stated in Table 1.

Table 1. Analysis of Observations on Typical Specimen

(Copper heated for 8 hours at 800° c. in hydrogen with unsaturated lead vapour)

Discarded boundaries :	
Twin boundaries	154
Boundaries not perpendicular to surface of specimen	12
Selected boundaries :	
Dihedral angles not measurable or too large	34
Dihedral angles photographed	12

Table 2. Measured Values of Dihedral Angle on Typical Specimen

Number	1	2	3	4	5	6	7	8	9	10	11	12
Angle (deg.)	119	123	124	128	128	128	129	129	132	132	144	157

From the greater frequency of occurrence of the angles 128–129°, it was considered that the value 129° could be taken as the true dihedral angle in this case. A similar procedure was applied in the remaining cases, and the results are summarized in Table 3.

Table 3. Estimated Values of Dihedral Angle, ϕ

Gas phase	Temperature (° c.)	Annealing time (hr.)	Dihedral angle (deg.)
Argon	900	2	160
Hydrogen	800	14	158
	900	2	160
Lead vapour–Argon	900	2	142
Lead vapour–Hydrogen	800	8	129
	900	2	129

To enable these values of dihedral angle ϕ to be used in calculating absolute values for the surface tensions, estimates are required of the value, at 800° and 900° c., of the microstructural dihedral angle θ, as measured by Smith, and also of the contact angle ψ, and of the surface tension of liquid lead containing equilibrium proportions of copper. These estimates are made below.

(iii) *Estimation of Dihedral Angle θ, (Solid–Liquid)*

The following values of the dihedral angle θ are given by Smith for two-phase copper–lead alloys for temperatures 600°, 700° and 900° c. respectively: 70°, 65°, 50°; by interpolation the angle at 800° c. is 57°.

(iv) *Estimation of Surface Tension of Liquid Phase*, γ_{23}

Values of the surface tension of lead over a range of temperatures have been given by Bircumshaw (1934) and by Sauerwald and Drath (1927). Values for copper between 1,131° and 1,215°c. are also given by Sauerwald and Drath. From an extrapolation of the values for copper to the temperatures of interest the surface tensions of the liquid phase at 800° and 900°c. are estimated, using a simple mixtures rule, to be 435 and 466 dyne/cm. respectively.

(v) *Estimation of Contact Angle* ψ (*Solid–Liquid–Gas*)

The contact angle ψ is that angle which would be observed at the line of contact of liquid and solid surfaces if the solid surface were perfectly smooth. Real surfaces are seldom smooth, however, and, according to Wenzel (1936), when the ratio of actual surface area to the nominal area is r the angle actually established is λ, where $\cos\lambda = r\cos\psi$.

It has been shown by Shuttleworth and Bailey (1948), however, that this is true only when the roughness takes the form of interlacing grooves. When it has the character of isolated depressions, the observed contact angle is no longer uniquely determined by the roughness. When the liquid advances over the surface the contact angle exceeds the true value, and when it recedes the observed angle is less than the true value, i.e. hysteresis of the contact angle is exhibited. Hysteresis is normally encountered in metallic systems, in which intermetallic diffusion frequently results in the roughening of initially polished surfaces.

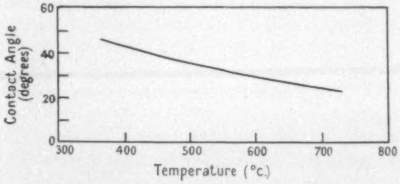

Figure 10. Contact angle vs. temperature: copper–lead system.

Even when electropolished copper is dipped into a liquid copper–lead alloy of equilibrium composition at the temperature of experiment some roughening rapidly occurs at the solid–liquid interface and hysteresis is observed, although the unwetted surface remains smooth for a longer time. It is probable, however, that the advancing contact angle is in this case near to the true value. Measurements have been made of this angle, using the well-known Wilhelmy plate method (Wilhelmy 1863), in the temperature range 350–750° c., the furnace atmosphere being purified hydrogen. The results are shown in Figure 10. Observation by eye at temperatures up to 950° c. suggests that it is reasonable to extrapolate the curve of Figure 10 to estimate values for the contact angle at 800° and 900° c.; these estimated values are 25° and 15° respectively. Observation by eye of the angle exhibited in an argon atmosphere shows that it cannot differ greatly from the values at corresponding temperatures when a hydrogen atmosphere is used, and these estimates are therefore used for both conditions.

The use of the advancing contact angle is appropriate in view of the possible occurrence of adsorption hysteresis in addition to the roughness hysteresis already mentioned.

§ 4. CALCULATION OF SURFACE TENSIONS

The estimates of angle ϕ, θ and ψ and of the surface tension of the liquid phase at temperatures of 800° and 900° c. are inserted in the appropriate equations, (1) to (3), to calculate values for the surface tensions γ_{11}, γ_{12} and γ_{13}. These are given in Table 4.

There are two numerical values for the solid–gas surface tension of copper, one appropriate to a lead-free atmosphere and one to atmosphere containing lead vapour.

Table 4. Evaluation of Surface Tensions

Temp. (° c.)	Gas phase	γ_{23} (dyne/cm.)	θ (deg.)	ψ (deg.)	ϕ (deg.)	γ_{13} (dyne/cm.)	γ_{12} (dyne/cm.)	γ_{11} (dyne/cm.)
800	Hydrogen	—	—	—	158	1750	—	670
	Hydrogen +lead	435	57	25	129	780	380	
900	Hydrogen	—	—	—	160	2000	—	700
	Hydrogen +lead	466	50	15	129	810	360	
900	Argon	—	—	—	160	1600	—	560
	Argon +lead	466	50	15	142	740	290	

§ 5. DISCUSSION OF RESULTS

In view of the assumptions and approximations made, the accuracy of the values obtained cannot be great, and discussion of the variations of individual surface tensions would be unprofitable. Average values of all the results are as follows:

Clean copper:	1,800 dyne/cm.
Between copper grains:	640 dyne/cm.
Between copper and lead:	340 dyne/cm.
Copper with adsorbed lead:	780 dyne/cm.

The value of 1,800 dyne/cm. obtained for the surface tension of clean copper is in fair agreement with that recently found by Udin, Schaler and Wulff (1949) using another method. Their value is 1,370 dyne/cm. at the melting point of copper. Using their quoted temperature coefficient of −0·46 dyne/cm. per degree, the value at 850° c. would be about 1,500 dyne/cm. A recent theoretical estimate by Huang and Wyllie (1949) gives a value of 1,820 dyne/cm. for solid copper at its melting point. The surface tension between grains of copper is, as expected, much lower than the surface tension of clean copper, though still surprisingly high, and its ratio with that of the copper–lead phase boundary is, of course, that given by Smith. The substantial reduction of the surface tension of a copper surface exposed to lead vapour is evident.

Clearly, lead vapour at a very low partial pressure is extremely effective in this respect, whereas hydrogen, which is soluble in copper, and therefore liable to become adsorbed, has little effect. The effect of hydrogen alone is little more marked than that of argon alone, where adsorption is not expected and the copper surface should be clean.

From the experimental values of contact angle given in Figure 10 it is possible, with the aid of equation (3) and assuming γ_{12} and γ_{23} to remain constant with temperature, to estimate the surface tension of a copper surface exposed to lead vapour in a hydrogen atmosphere throughout the temperature range 350–750° c. The results are shown in Table 5.

Table 5. Estimated Surface Tension of Copper in presence of Lead Vapour

Temperature (° c.)	350	450	600	750
Surface tension (dyne/cm.)	420	570	640	730

It is interesting to note that at a temperature just above the melting point of lead the surface tension of copper exposed to lead vapour at low pressure is on this basis roughly the same as the surface tension of liquid lead. It seems probable that the lead exerts its effect on the contact angle through adsorption on to the solid surface, and possible that, at temperatures round 350° c., the copper surface is just covered by a complete layer of lead.

§ 6. CONCLUSION

Several approximations and assumptions have been made in deriving the absolute surface tension values quoted. Many of these could doubtless be eliminated by further experiment. The results obtained are, however, of value in pointing to the reason why liquid lead does not spread completely over copper surfaces, and in showing the approximate magnitudes of the surface tensions of the various surfaces.

The failure of lead to spread readily upon copper appears to be a fundamental feature of the lead–copper system, and is not, for example, due to adventitious contamination of the surface.

The results are of wider interest in demonstrating the strongly marked reduction in the surface tension of a solid metal surface which may be brought about by the adsorption upon it of atoms of another metal, and it follows that a knowledge of the surface tension of the clean solid metal could not be used to facilitate the study of spreading when it is in contact with different liquid metals.

ACKNOWLEDGMENTS

The authors wish to express their thanks to the Director and Council of the British Non-Ferrous Metals Research Association for permission to publish this paper, which was released to members of the Association in September 1949.

REFERENCES

Bircumshaw, L. L., 1934, *Phil. Mag.*, **17**, 181.

Chalmers, B., King, R., and Shuttleworth, R., 1948, *Proc. Roy. Soc.* A, **193**, 465.

Gurney, C., 1949, *Proc. Phys. Soc.* A, **62**, 639.

Huang, K., and Wyllie, G., 1949, *Proc. Phys. Soc.* A, **62**, 180.

Sauerwald, F., and Drath, G., 1927, *Z. anorg. Chem.*, **162**, 301.

Shuttleworth, R., and Bailey, G. L. J., 1948, *Discussion, Faraday Soc.*, No. 3.

Smith, C. S., 1948, *Amer. Inst. Min. Met. Engrs., Tech. Pub.* No. 2387.

Udin, H., Schaler, A. J., and Wulff, J., 1949, *J. Met.*, **1** (2), 186.

Wenzel, R. N., 1936, *Ind. Eng. Chem.*, **28**, 988.

Wilhelmy, L., 1863, *Ann. Phys., Lpz.*, **119**, 177.

The Construction of Interference Filters for the Transmission of Light of Specified Wavelengths

By K. M. GREENLAND and C. BILLINGTON
British Scientific Instrument Research Association, Chislehurst, Kent

MS. received 16*th August* 1949, *and in final form* 28*th December* 1949

ABSTRACT. Optical interference filters are composed of thin films deposited on a glass base by volatilization in a high vacuum. The narrowness of the transmission bands characteristic of these filters demands a high degree of accuracy in the regulation of the thickness of the films if maximum transmission is to occur at a specified wavelength. A method of observing the optical thickness of transparent films during deposition is described and it is concluded that its accuracy is sufficient, for instance, to enable the centre of a fourth-order transmission band to be placed within 20 A. of any wavelength in the visible spectrum.

§ 1. INTRODUCTION

The interference filter is composed of two partially reflecting metal films separated by a film of transparent material (Geffcken 1942, 1948, 1949). A full mathematical and experimental analysis of their properties is given in two papers by Hadley and Dennison (1947, 1948). In the construction of an interference filter intended to transmit light of a particular wavelength, it is essential that the thickness of the transparent film should be adjusted as accurately as possible to the value determined by that wavelength. The films are deposited on a glass base by slowly volatilizing the materials in a high vacuum; methods of control of film thickness may therefore depend either on the evaporation of a predetermined amount of material (measured by weight or by time and temperature of evaporation) or on an observed indication of the film thickness as the film grows.

Methods of the first kind rely on a degree of constancy in the conditions of volatilization which is in practice almost impossible to obtain. We have, therefore, devised an optical system by means of which the increasing optical thickness of the film in the vacuum chamber may be estimated visually with an accuracy sufficient to place the transmission band of the filter within about 20 A. of the required wavelength.

The filters used in the work on which this paper is based were made of two partially reflecting silver films separated by a layer of zinc sulphide. It will be convenient to refer to silver and ZnS films, but the use of other materials is not precluded. It may be mentioned, in passing, that films of magnesium fluoride, a material commonly used for interference filters, were found to behave in an erratic manner after deposition; their optical thickness changed irregularly when air was admitted to the vacuum chamber and when a cover-glass was cemented to the filter. Zinc sulphide is not subject to these irregularities.

§ 2. PRINCIPLE OF THE METHOD

The transmission interference filter is also a highly reflecting mirror, but the spectrum of a white-light source reflected by the filter exhibits, in general, dark bands. These absorption bands are due to interference in the wave system set up between the silver films, and in a transmission filter they are approximately complementary to the transmission bands. Owing to the high reflectivity of the silver films, the absorption bands, like the transmission bands, are very sharply defined.

The transmission bands cannot, of course, be observed during the critical stage of construction, that is, while the ZnS is being deposited, because they do not appear until the second silver layer has been formed. Absorption bands, on the contrary, are observable at this stage because it is possible to direct the incident beam so that total internal reflection at the growing ZnS surface may perform the function of the absent silver film. If, then, the relation between the wavelengths of the absorption bands and transmission bands is known, the wavelengths of one or more of the absorption bands may be used as an accurate measure for the evaporation of the ZnS.

The essence of the method is the achievement of total internal reflection at the growing ZnS surface; without this the absorption bands are so broad that accurate estimation of their mean wavelength is impossible. This condition is realized by introducing the 'monitor' beam into the filter base through a right-angled prism, so that the angle of incidence on the filter itself is 45°.

For a thickness t of ZnS film, absorption bands will occur in the monitor beam with maximum absorption at wavelengths λ_a satisfying the condition

$$(2\pi/\lambda_a)nt\cos\theta+\phi=m\pi, \qquad \ldots\ldots(1)$$

where n is the refractive index of the ZnS film, θ is the angle of refraction in the ZnS, ϕ represents phase shifts due to reflection at the ZnS boundaries and transmission through the silver film, and m is the order of interference. The transmission bands of the complete filter, observed at normal incidence, will be centred on wavelengths λ_0 given by the condition

$$(2\pi/\lambda_0)nt+\phi_0=m\pi, \qquad \ldots\ldots(2)$$

where ϕ_0 represents the phase shift at the ZnS–silver boundaries. If the values of ϕ and ϕ_0 were known with sufficient accuracy, a filter having a transmission band centred at any desired wavelength λ_0 could be constructed by calculating from equations (1) and (2) the wavelength λ_a of the appropriate absorption band. As it is, these values for phase shifts are not yet known; the procedure is, therefore, to construct a number of filters for which both λ_a and λ_0 are measured and so to derive an empirical relationship between these two wavelengths. This does not require a knowledge of the phase shifts, but it is necessary that, for a given wavelength, they should not vary from one filter to another.

§ 3. CONTROL OF PHASE SHIFTS

As far as is possible we ensure that there is no variation in the experimental conditions, such as purity of materials, degree of vacuum, rate of evaporation and temperature of filter base; any of these factors may affect the quality of the silver films and hence alter the phase shifts. The only variables affecting the phase shifts which then remain to be controlled are the transmissivities of the silver films. The light in the monitoring beam must also be polarized in a suitable direction.

(i) *Transmissivity of the Silver Films*

The transmissivities of the silver films are set within fairly close limits by whatever transmission factor is required for the filter. For film transmissivities giving a filter transmission factor of 25% (a typical value) or less the value of the reflection phase shift is not very sensitive to small changes in transmissivity, so that control of transmissivity is not such a critical matter as control of the ZnS film thickness. The easiest way to obtain a measure of control over the transmissivity of the silver films is to evaporate completely a fixed weight of silver for each film. This was, in fact, the method finally adopted for the present investigation, and results have shown that a sufficient uniformity of transmissivity is usually, but not always, obtained. It is essential to ensure that the silver vapourizes smoothly without spitting molten metal.

An optical method was devised by one of us (C.B.) for matching the optical density of the silver film being deposited with that of a 'standard' film of the required density. This method was tried but abandoned owing to the difficulty of keeping the optical system, which was entirely within the vacuum chamber, free from deposits of ZnS, which disturb the essential optical 'balance' of the system.

(ii) *Polarization of the Monitor Beam*

The values of the phase shifts due to reflection of the monitor beam at the two boundaries of the ZnS film depend on the direction of polarization of the light relative to the plane of the filter. If the beam is 'unpolarized', the absorption bands will occur in pairs (which we shall call the p-absorption and s-absorption bands) due to the differing phase shifts for the p- and s-components. The bands will then be ill-defined through lack of contrast, because each band is seen against a bright background of light polarized at right angles to that being absorbed. It is therefore necessary to polarize the beam in either the 'parallel' or 'perpendicular' plane relative to the filter in order to remove this unwanted light. It is in practice convenient to be able to change the plane of polarization since, for filters of low order for certain wavelength regions, one or other of the absorption bands falls near or outside the limit of spectral visibility. There is, in fact, a small region for which filters of the first order cannot be monitored directly (this difficulty might be overcome by using a separate monitor prism and placing the filter blank at a greater distance from the evaporator than the prism; a special calibration would, of course, be necessary).

§4. OPTICAL SYSTEM FOR THE MONITOR BEAM

The optical system for observing the absorption bands consists of an illuminating beam and a spectrometer to analyse the light reflected from the films deposited on the filter base. The glass filter base is supported over a hole in a horizontal shield near the top of the vacuum bell-jar, vertically above the silver and ZnS evaporators. It is illuminated by light from a Pointolite lamp incident at an angle of 45° on the upper side of the filter base. In order that the angle of incidence at the ZnS–vacuum boundary may be high enough for total internal reflection a right-angled prism is placed with its hypotenuse face on the top surface of the filter base, with a film of high-vacuum oil between the surfaces to ensure optical continuity. The reflected beam is directed by a mirror and lens on to the slit of a plane grating spectrometer adjusted for the diffraction spectrum of first order. It is essential for good definition that the spectrometer slit should be at the principal focus of the lens. In front of the spectrometer slit is a rotatable 'Polaroid' polarizer.

§ 5. EXPERIMENTAL PROCEDURE

For the purpose of calibrating the instrument—that is, of determining the relationship between λ_a and λ_0—a number of filters are made with various thicknesses of ZnS film. The wavelength of the centre of either the *p*- or *s*-absorption band, λ_a, is read after the ZnS evaporation; the filter is then completed by evaporation of the second silver layer and removed from the vacuum chamber. A cover-glass is cemented on to the exposed silver surface and the wavelength of the centre of the transmission band, λ_0, measured at normal incidence.

§ 6. DISCUSSION OF RESULTS

We find that the relation between the experimental values of λ_a and λ_0 may generally be expressed in the form

$$\lambda_a = A\lambda_0 + B. \qquad \ldots\ldots (3)$$

Values of *A* and *B* for various orders are given in the Table. The figures relate to wavelengths measured in millimicrons and to λ_a measured for the *s*-absorption band.

Order	3	4	5
A	1·00	0·98	0·98
B	−6	−5	−15

The experimental results used in calculating the values of *A* and *B* for the fourth order are reproduced graphically in the Figure. These results were obtained from a series of 24 filters; four filters were rejected because of unevenness in the ZnS layer and the measurements from all the remainder were plotted (coincidence of values on the graph reduces the number of points to 13). The experimental values are indicated in the Figure by 'spots' having an equivalent diameter of approximately 20 A. It can be seen that, excepting two red filters, all the filters measured had values of λ_0 lying well within 20 A. of those satisfying the linear relationship of equation (3). Seven filters of this series were made with the monitor band wavelength λ_a adjusted to 526 mμ: the filters all had values of λ_0 lying between 544 and 546 mμ. It may therefore be said that control of λ_0 is possible within 20 A. for the fourth order.

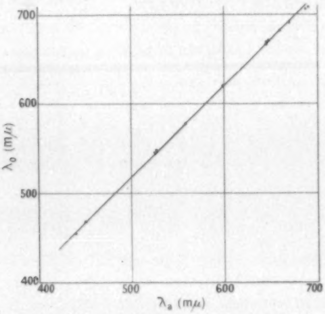

Calibration for fourth order.

The high concordance of results for the fourth order has, in our experience so far, not been quite so well maintained at lower orders; discrepant filters occur either singly or in a batch of successive evaporations. This may be the result of changes in the value of phase shift on reflection at the silver–ZnS boundaries, due to variations in the thickness and structure of the silver films. Experiments now in progress show that although the evaporation of a fixed weight of silver gives a reasonably consistent transmissivity in the majority of evaporations, there can be a very large deviation from the normal value.

§ 7. CONCLUSION

Determination of the relationship between the mean wavelength of an absorption band observable during the deposition of the ZnS *in vacuo* and the mean wavelength of the corresponding transmission band of the complete interference filter has made it possible to place the peak transmission of the filter within 20 A. of a predetermined wavelength. Greater discrepancies which sometimes occur may be due to an insufficient degree of control over the deposition of the silver films.

ACKNOWLEDGMENT

The authors desire to express their thanks to the Director and Council of the British Scientific Instrument Research Association for permission to publish this paper.

REFERENCES

Geffcken, W., 1942, German Patent No. 716,153; 1948, *Angew. Chem.*, **A60,** 1; 1949, *Ceram. Abstr.*, **32,** 87.

Hadley, L. N., and Dennison, D. M., 1947, *J. Opt. Soc. Amer.*, **37,** 451; 1948, *Ibid.*, **38,** 483.

Note on the Brightness Profile and Photometric Contrast of a Test-object having small Angular Dimensions and Silhouetted against the Twilight Sky *

BY D. R. BARBER
Norman Lockyer Observatory, of the University College of the South-west,
Sidmouth, South Devon.

Communicated by S. C. Goddard; MS. received 18*th July* 1949, *and in amended form* 6*th December* 1949.

ABSTRACT. Microphotometry of photographs of distant objects with small angular subtense has shown that inaccurate results are obtained if the apparent contrast is calculated on the assumption of uniform sky brightness. No evidence was found of any edge effect due to inward small angle scatter.

---

§ 1. INTRODUCTION

In the course of an investigation of the variation of brightness contrast of the sea-horizon an opportunity was taken to test the theoretical conclusions of H. Koschmieder (1924) regarding the physical basis of aerial perspective.

A long-focus camera was used to photograph a series of distant test-objects of different albedos at a range of 4,850 yards. Each exposure was calibrated by means of a supplementary exposure to a step-tablet of known brightness range, and the set of negatives was analysed by the aid of high-magnification (50 ×) microphotometer tracings of the photographic image of the test-object. Auxiliary exposures to a calibrated light source over a range of 2,000 yards were made concurrently with the main series in order to measure photographically the atmospheric transmission at the time of each observation.

Two separate objects were available for the experiments. One of these, marked T in Figure 1 (*a*) (Plate) †, had an angular subtense of about 3′ of arc as viewed from the camera site, and an albedo of 0·09, corresponding to a photometric contrast of 0·91. The second, marked H in the figure, had been specially painted so as to provide a composite object of known differential contrast: the panels, a, b, c (see Figure 1 (*b*)) had albedos of 0·80, 0·047 and 0·86 respectively corresponding to photometric contrasts, relative to the dark panel b, of 0·94 (a) and 0·95 (c).

The photographs used for the subsequent analysis were taken either in early twilight or in moonlight, under varying conditions of cloud-cover and visibility. Examples of the test-object profiles, plotted on an intensity scale from the microphotometer tracings, are reproduced in Figures 2 (*a*) and 2 (*b*). Brightness values are in c/ft^2 and the broken curve indicates in each diagram the measured profile when corrected for the limited resolution of the photographic record. The 'peak' of this profile is plotted at a level of intensity computed from the known albedo of the test-object, measured at close range, and the intensity of the sky background. In computing contrast values from intensity

---

* This work was carried out while with the Kodak Research Laboratories and is issued as Communication No. 1262H from these.

† Opposite p. 368.

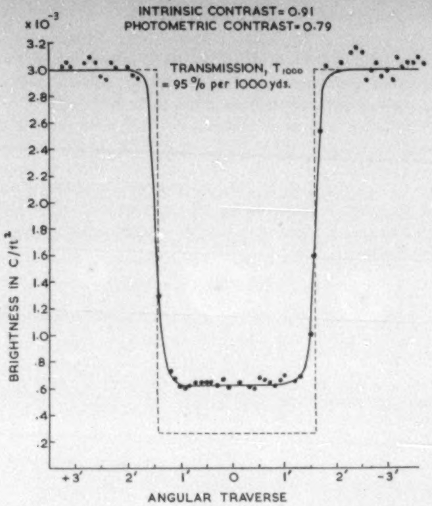

Figure 2 (*a*). Intensity profiles: ——— photometric, - - - - - computed from albedo, of low-albedo test-object. The shape of the photometric profile results from the limited resolution of the original photographic record.

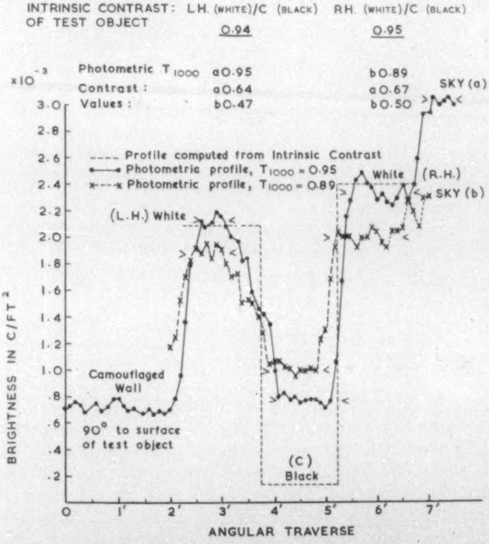

Figure 2 (*b*). Intensity profiles of composite test-object: ——— photometric, - - - - - computed from albedo measures. Plotted to same scale.

measures the expression, $C=(B-B')/B$ is used, where B and B' are brightness values for surround and test-object respectively; when the object appears lighter than its surround the contrast is taken to be negative.

§ 2. THEORETICAL TREATMENT

Considering now Koschmieder's argument, two conclusions emerge.

Firstly, the apparent brightness B_R of a test-object, albedo R, as observed from a distance l against the uniform background of horizon sky, brightness B_H, will be given by the expression,

$$B_R = RB_w e^{-\sigma l} + (1-e^{-\sigma l})B_H \qquad \ldots\ldots (1)$$

where σ is the generalized extinction coefficient of the atmosphere at the time of observation, and B_w is the intrinsic brightness of a perfectly white object ($R=1$).

On the assumption that the sky has uniform brightness in all azimuths, and that the brightness of the ground is zero, the value of B_w may be taken as $B_H/2$ so that the expression for the observed brightness of the test-object now becomes

$$B_R = R(B_H/2)e^{-\sigma l} + (1-e^{-\sigma l})B_H, \quad \text{or} \quad B_R = B_H[(R/2)e^{-\sigma l} + (1-e^{-\sigma l})]. \ldots\ldots (2)$$

Equation (2) may now be used to obtain the apparent contrast of the test-object, C_R where $C_R=(B_H-B_R)/B_H = 1-[(R/2)e^{-\sigma l}+1-e^{-\sigma l})]$ from (2) or

$$C_R = e^{-\sigma l}(1-R/2). \qquad \ldots\ldots (3)$$

This equation, among others, has been used to compute the apparent contrast of a test-object observed under different conditions of atmospheric transmission; and, for the purpose, values of the extinction coefficient σ have been calculated from the measured values of T_{1000}, the transmission per 1,000 yards. They appear in column (2) of Table 1.

Table 1

(1)	(2)	(3)	(4)	(5)	(6)	(7)	(8)	(9)	(10)
R	σ $\times 10^{-4}$	B_s (c/ft²)	C_{ob}		C_c			$(C_c-C_{ob})/C_{ob}$	
				$n=0$	$n=1$	$n=2$	$n=0$	$n=1$	$n=2$
0·05	1·20	Twilight 2·0	0·56	0·55	0·54	0·53	−0·018	−0·036	−0·054
0·80	1·20	,, ,,	0·19	0·32	0·21	0·10	+0·684	+0·105	−0·474
0·86	1·20	,, ,,	0·14	0·30	0·18	0·06	+1·142	+0·286	−0·571
0·09	0·81	Moonlight 8·0	0·63	0·64	0·62	0·61	+0·016	−0·016	−0·032
0·09	0·52	Twilight 12·0	0·72	0·75	0·72	0·70	+0·042	+0·000	−0·028
0·05	0·52	,, 3·0	0·75	0·76	0·74	0·73	+0·013	−0·013	−0·026
0·80	0·52	,, ,,	0·33	0·43	0·28	0·13	+0·303	−0·152	−0·606
0·86	0·52	,, ,,	0·23	0·40	0·25	0·09	+0·738	+0·087	−0·608
0·09	0·23	,, ,,	0·79	0·82	0·80	0·78	+0·038	+0·013	−0·013

Secondly, it is shown by Koschmieder that both the profile, and the apparent contrast of a distant object of very small dimensions viz. less than about 20′ of arc, should be influenced by inward small-angle scatter of light from the surrounding sky. Lohle (1929) has attempted a quantitative estimate of the 'edge effect' and finds that, for an object of 5′ angular radius, this inward scatter will amount to 10% of the sky brightness. Such an effect, if present, will diffuse the boundary of the object (ground-glass effect), and thus distort its angular dimensions, in addition to decreasing the apparent contrast, as computed from equation (3) above.

There remains some doubt as to the reality of this inward scatter. Recently Fry, Bridgman and Ellerbrock (1947) have made a detailed theoretical analysis of both effects for a low-albedo test-object, surrounded on all sides by a uniformly bright sky. They conclude that, for objects of angular width 0·01 radian, both 'edge' and 'ground-glass' effects are negligibly small. Thus the boundary profile will, for all practical purposes, be undistorted. In these circumstances, the contrast, as viewed from a distance, may be measured satisfactorily by means of the intensity drop at the boundary of object and sky-surround. The experimental results to be presented later support these conclusions.

Koschmieder further emphasizes the influence of the threshold contrast value for the observer on the observed contrast of a distant object. In daylight this lies between 0·01 and 0·02 for the average eye, when observing objects of angular dimensions greater than about 2 degrees. The value increases rapidly with decreasing angular dimensions: for an angular subtense of 0·2 degree the threshold contrast is increased five-fold. However, this particular complication will not enter into the present investigation so long as the dimensions of the object remain such that the image on the photographic record is adequately resolved. Moreover, it should be emphasized that the test-objects used in the present work have dimensions much smaller than those referred to above. It is therefore of considerable interest to compute (i) the computed and measured contrast values for various atmospheric transmissions, and (ii) the profiles obtained through varying amounts of haze or mist with those recorded under atmospheric conditions.

Koschmieder's assumption, in common with other early investigators (Föitzik 1932, Wright 1939, Middleton 1941), of a uniformly illuminated hemisphere of sky surrounding the test-object, and negligible ground reflectance in the vicinity of the object, may lead to appreciable errors if equation (3) is used to compute the apparent contrast values under very different atmospheric conditions; this is particularly so when the object considered has a relatively high albedo. This complication has been stressed by Moon and Spencer (1942) who show that the equation expressing the brightness, B_ξ, of an element of sky at a zenith angle ξ may be written

$$B_\xi = B_{\mathrm{h}}(1 + 2\cos\xi)$$

where B_{h} is the brightness of the horizon sky at $\xi = \pi/2$. This gives $B_{\mathrm{zenith}} = 3B_{\mathrm{horizon}}$, a value in line with that observed by Kimball and Hind (1921, 1922). More recently Middleton (1947) has extended the theoretical treatment by generalizing the above equation in the form,

$$B_\xi = B_{\mathrm{h}}(1 + n\cos\xi)$$

where n is an integer, the remaining quantities being defined as before.

From this relation it follows that the brightness, B_{w}', of a vertical white surface illuminated by skylight alone will no longer be given by the quantity $B_{\mathrm{h}}/2$, but by the expression,

$$B_{\mathrm{w}}' = B_{\mathrm{h}}(\tfrac{1}{2} + 2n/3\pi).$$

Further, if R' is the albedo of the ground in the immediate vicinity of the test-object, the resultant brightness, B_{w}'', due to ground reflectance, will be

$$B_{\mathrm{w}}'' = R' B_{\mathrm{h}}(\tfrac{1}{2} + n/3).$$

Thus the observed brightness of the test-object, due to the combined effects of sky and ground illumination, may be expressed as

$$B_w = B_w' + B_w'' = B_h[\tfrac{1}{2}(1+R') + (n/3)(2/\pi + R')]$$

and, if the white object is replaced by one of albedo R,

$$B_R = B_h[(R/2)(1+R') + (nR/3)(2/\pi + R')].$$

Hence the apparent contrast, C_R', of a grey object observed through an horizontal layer of atmosphere, thickness L and transmission coefficient σ, is given by the equation,

$$C_R' = [1 - \{(R/2)(1+R') + (nR/3)(2/\pi + R')\}]e^{-\sigma L}. \quad \ldots\ldots (5)$$

Equation (5) replaces (3) and enables a correction to be made for the combined effects of a non-uniform sky illumination, and of ground reflectance.

Table 1 illustrates the magnitude of the error which may result if the simple equation is used to compute the observed contrast for objects of high and low albedo values, when measured in a horizontal direction over a range of 4,840 yards, under varying atmospheric conditions and silhouetted against the twilight sky. Values of the transmission coefficient σ ranged from $1{\cdot}20 \times 10^{-4}$ to $0{\cdot}23 \times 10^{-4}$. A value of $R' = 0{\cdot}09$ has been taken for the average ground reflectance* around the test-object. Column (1) of the Table gives the true albedo of each test-object observed, and column (2) the value of the generalized extinction coefficient at the time of observation. In column (3) there are entered particulars of the atmospheric conditions, and the observed brightness of the sky. Column (4) contains the experimentally observed contrast value, whilst columns (5), (6) and (7) refer to values of contrast computed by the aid of equation (5) taking $R' = 0$, $n = 0$ (column 5), and $R' = 0{\cdot}09$, $n = 1, 2$ (columns 6 and 7). Finally, in columns (8), (9) and (10) there are given differences between computed and observed contrast utilizing the data of columns (4) to (7). In each instance, the difference is expressed as a fraction of the observed quantity.

§ 3. DISCUSSION

It will be seen that the contrast values computed for low-albedo objects agree well with those experimentally determined, so that the error involved in using the simplified equation (3) will, in general, be small. However, for high-albedo objects the error is in all cases appreciable. Indeed the computed value may be in error by as much as 100% of the observed contrast, as is illustrated by the case of the light-toned object ($R = 0{\cdot}86$) viewed against the twilight sky. In this particular instance, the contrast difference (computed minus observed) amounted to 0·16 but fell to 0·04 when account was taken of non-uniform sky and ground reflectance. For all the observations listed in Table 1 the object measured was illuminated by light received from a cloudless sky. It was found that, for this condition the computed values fitted observations best when equation (5) was entered with $n = 1$. Table 2 summarizes the contrast data for the low-contrast object ($R = 0{\cdot}09$) illuminated by a totally overcast twilight sky. Three values of C_c are found in adjacent columns: the first of these computed values is based essentially on equation (3) where $n = 0$, $R' = 0$, the remainder on equation (5) for $R' = 0{\cdot}09$, $n = 1$, $n = 2$ respectively. Under an overcast sky the

---

* The site of the test-object was at a cliff edge on rough grassland with red sandstone subsoil and coarse wild herbage on the surface.

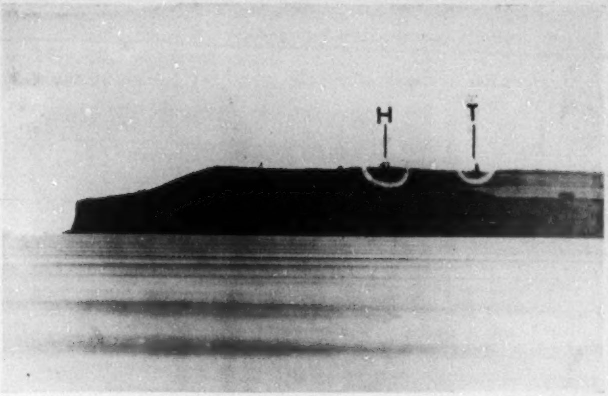

Figure 1 (*a*).

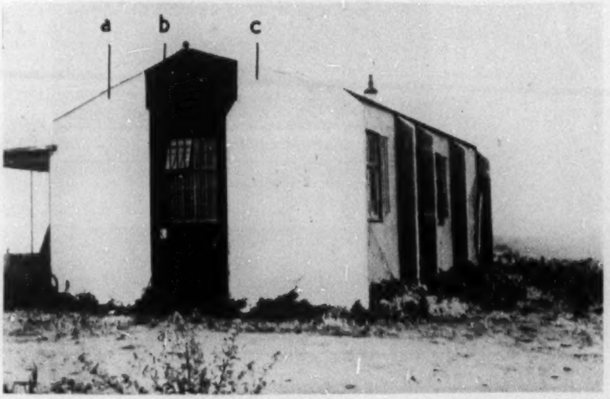

Figure 1 (*b*).

Figure 1. The test-objects (H and T) as seen from the camera site (*a*), and close-up view of composite test-object, H (*b*).

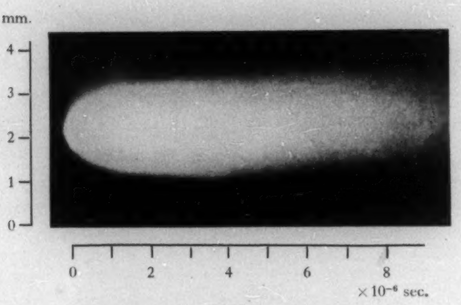

Figure 1.

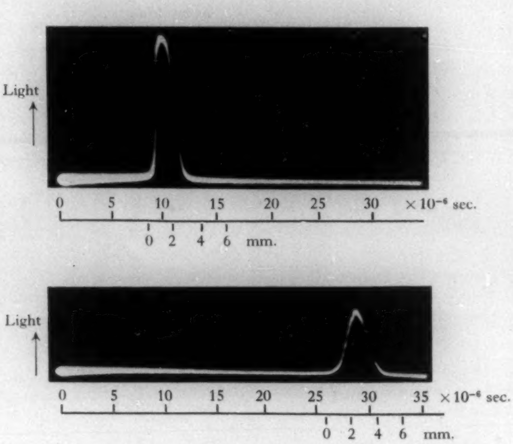

Figure 2.

computed contrast, using $n=2$, is found to fit experimental results rather better than that obtained from the use of equation (3) with $n=0$, or equation (5) with $n=1$.

It is evident that the simplified theoretical treatment based on a uniformly bright sky from horizon to zenith fails to yield results concordant with observation. By using Middleton's modification it is possible, however, to correct satisfactorily both for the sky effect and ground reflectance.

One other conclusion has emerged from a detailed study of the high magnification tracings of the brightness profiles of the low albedo test-objects. It is found that at high transmission values the profile, when properly corrected for the lack of resolution of the photographic lens-film combination employed in taking the original record, has a contour approximating very closely to that expected for a 'knife-edge' boundary. Further, the observed variations in the width of the object derived from the lower transmission records, made under conditions of light mist, or haze, exhibit no evidence of any 'edge-effect' due to inward light scatter, even when the object viewed has an angular width so small as 3 minutes of arc. These results support the theoretical arguments of Middleton (1942) and of Fry, Bridgman and Ellerbrock (1947).

Table 2

(1)	(2)	(3)	(4)	(5)	(6)	(7)	(8)	(9)	(10)
R	σ $\times 10^{-4}$	B_s (c/ft^2)	C_{ob}	C_c			$(C_c - C_{ob})/C_{ob}$		
				$n=0$	$n=1$	$n=2$	$n=0$	$n=1$	$n=2$
0·09	3·55	Twilight 30·0	0·16	0·17	0·17	0·16	+0·063	+0·063	+0·000
0·09	1·55	,, 4·0	0·42	0·46	0·45	0·43	+0·095	+0·071	+0·024

ACKNOWLEDGMENT

The experimental work forming the basis of the present paper was carried out as part of a general programme of marine photometry undertaken by the Kodak Research Laboratories under contract with the Admiralty, to whom acknowledgment is made for permission to publish this paper.

REFERENCES

Föitzik, L., 1932, *Met. Z.*, **49,** 134.
Fry, G. A., Bridgman, C. S., and Ellerbrock, V. J., 1947, *J. Opt. Soc. Amer.*, **37,** 635.
Kimball, H. H., and Hind, —., 1921–2, *Mon. Weath. Rev., Wash.*, **49,** 481; **50,** 616.
Koschmieder, H., 1924, *Beitr. Z. Phys. freien Atm.*, **12,** 33–53; 171–81.
Löhle, F., 1939, *Met. Z.*, **46,** 49–50.
Middleton, W. E. K., 1941, *Visibility in Meteorology* (2nd edn.) (Toronto: University Press); 1942, *J. Opt. Soc. Amer.*, **32,** 139; 1947, *Quart. J. R. Met. Soc.*, **73,** 456.
Moon, P., and Spencer, —., 1942, *Illum. Engng., N.Y.*, **37,** 707.
Wright, H. L., 1939, *Quart. J. R. Met. Soc.*, **65,** 411.

LETTERS TO THE EDITOR

The Measurement of Spark Channel Diameters

An attempt was made by Flowers (1943) to study the apparent optical diameters of spark channels, using a mechanical scanning camera. The results show that the optical diameter of the spark channel increases during the first few microseconds of its existence.

One of us (J.B.H.) has been extending this study in the course of work which will be published later. The technique used is essentially similar to that of Flowers, a rotating mirror being used to give the temporal resolution and a photographic emulsion for the recording. A record obtained in this way is shown in Figure 1 (see Plate opposite p. 368).

The light emission from a spark channel, and probably the distribution of light across the channel, varies rapidly. As little is known about the response of photographic emulsion subjected to the short exposures involved, it seemed desirable, as a check on the photographic method, to obtain spark-channel diameters using a different type of recording system. It was decided to use a photo-multiplier for this purpose.

The technique adopted involves a rotating mirror camera which scans the image of a spark across a slit, the length of which is parallel to the axis of the spark. The light passing through the slit is recorded by the photo-multiplier–amplifier–oscillograph unit described by Prime and Saxe (1949). The occurrence of the spark is synchronized with the position of the mirror, so that the image of the spark can be made to scan across the slit at any time relative to the initiation of the spark.

Figure 2 shows two typical records obtained in this way. The values of the spark-channel diameter are in good agreement with those obtained photographically. The records shown are slightly asymmetrical, principally because the Y-axis of the oscillograph is not quite normal to the X-axis. However, records taken during the earlier stages of the spark show a more pronounced asymmetry because of the change in the light distribution in the channel during the time of scan. For this reason no results have been obtained by this method during the first 5×10^{-6} second of the life of the spark channel.

The photographic method gives a continuous record of the variation with time of the diameter of a small portion of one particular spark channel, whereas the photo-multiplier technique gives only one cross section at a chosen time for each spark observed. However, the photomultiplier technique enables measurements to be made of the variation of light emission across the spark channel, and from these measurements it is possible to determine the radial distribution of light intensity in the channel. While the same result could be obtained photographically, there are difficulties involved because of the need for calibration of the photographic emulsion for the short exposures involved.

By using a higher mirror speed, a shorter and finer slit, and a greater amplification between the photo-multiplier and the oscillograph the new technique could be made to give a better temporal resolution and also to enable a greater range of light emission. In the examination of stable electrical discharges a slower scanning rate could be adopted, thus simplifying the amplifier design and enabling an ordinary oscillograph to be employed. The method may have applications in other fields.

This letter is published by permission of the Director of the Electrical Research Association.

Department of Electronics,
University of Liverpool.
January 1950.

* R. F. Saxe.
† J. B. Higham.

Flowers, J. W., 1943, *Phys. Rev.*, **63**, 225.
Prime, H. A., and Saxe, R. F., 1949, *J. Instn. Elect. Engrs.*, Part II, **96**, 662.

* Now at Armament Research Establishment, Fort Halstead, Sevenoaks, Kent.
† Now at Electrical Engineering Department, The University, Birmingham.

Crystal Diode and Triode Action in Lead Sulphide

Since the first publication on germanium crystal triodes by Bardeen and Brattain in 1948, it has been a matter of interest to investigate whether similar phenomena occur in other semiconductors. According to present theories of transistor action, the search should be directed towards materials which are *intrinsic* semiconductors at reasonably low temperatures and which have a high electron and hole mobility. These conditions are satisfied by PbS which also resembles Ge in other respects. For instance, both materials can occur as excess and deficit semiconductors, depending on the nature of the impurities present. Following this suggestion, selected samples of PbS were examined, using the usual arrangement as shown in Figure 1. These specimens were deficit semiconductors as inferred from the direction of rectification, which accounts for the polarity of the bias voltages shown. Transistor action was observed at some points of the material. A series of curves relating emitter voltage V_e and collector voltage V under dynamic conditions (load 10 kΩ) are given in Figure 2. It will be seen from the slopes that the voltage amplification is about 13 for 6 volts collector bias. Amplification factors as high as 25 have been recorded so far, though smaller values are more common on the existing samples. Power gains were in the neighbourhood of 4. Current gain has not so far been observed. The diode characteristics of emitter and collector are also of interest. Negative resistance may occur in both the forward and the reverse direction of current flow. Rectification ratios (at 1·5 volts) of 2000 : 1 have been obtained. All properties are appreciably affected by forming processes at the electrodes.

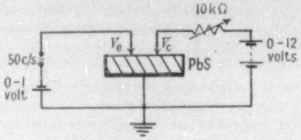

Figure 1. Schematic diagram of the circuit used for the detection of transistor action in lead sulphide.
(Distance between contact points is approx. 0·03 mm.)

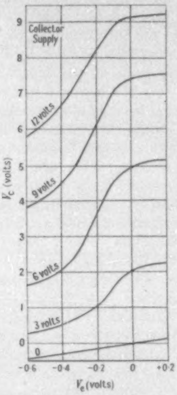

Figure 2. Dynamic characteristics of PbS transistor: relation between the emitter voltage V_e and collector voltage V_c for different values of the collector supply voltage. [Maximum gain = 13.] (Collector load = 10kΩ.)

The above performance of the present PbS transistors, considered as circuit elements, is, of course, inferior to that of Ge transistors. It is, however, of interest to note that the transistor effect can occur in a solid of the PbS type. A full report on these investigations will be published at a later date.

The authors would like to thank Professor R. W. Ditchburn for placing research facilities at their disposal and Dr. H. K. Henisch for much helpful advice. (One of us (H.A.G.) is a member of the Royal Naval Scientific Service.)

Department of Physics,
The University,
Reading, Berks.
23rd February 1950.

H. A. Gebbie.
P. C. Banbury.
C. A. Hogarth.

Bardeen, J., and Brattain, W. H., 1948, *Phys. Rev.*, **74**, 230.

REVIEWS OF BOOKS

Principles of Physics.—Part III. *Optics*, by F. W. Sears. Pp. 385. 3rd Edition. (Cambridge, Mass.: Addison Wesley Inc., 1948.) $4·50.

The subject matter of this excellently produced book corresponds roughly to what used to be understood by ' pass degree standard '. The treatment, notably the mathematical part of it, is rather more elementary; on the other hand, the text gains considerably from the direct physical approach which this implies. Explanation is a difficult thing: to succeed demands of the expositor both clarity in his own mind and experience. It is clear that the author of the present work has full measure of both of these qualities.

The first four chapters deal with the propagation of light (including the determination of **c**) and the Gaussian properties of mirrors and lenses. The latter are considered from the point of view of wave theory. Chapter 5 introduces the subject of aberration, regrettably in the basis of ray theory.

It is in Chapter 6 that errors abound. This is perhaps understandable in a chapter on optical instruments—a subject in which many supposed specialists seem to be so lacking. It is suggested that the " aberrations of a simple magnifier may be greatly reduced (in the case of a simple Ramsden eyepiece) since four refracting surfaces are available ". This is not the case. The additional two surfaces belong to a field lens, which increases most of the aberrations by a small amount and introduces very considerable field curvature. The important achromatized Ramsden is not mentioned. Again, on page 157, occurs the remarkable claim that " Most modern high speed short focal length lenses are modifications of the Zeiss ' Tessar ' lens ". In fact the ' Tessar ' was simply an obvious modification of the well-known ' Cooke Triplet ' lens due to the English designer H. D. Taylor. On page 144, Figure 6–15, it is the ' one ' on the left, not the right, which is an oil immersion objective.

Chapters 7, 8 and 9 treat polarization, interference and diffraction respectively. The approach is very clear, but almost qualitative. Chapter 10 deals with the limit of resolution and somehow manages to avoid all reference to Abbe's theory of the microscope. The electron microscope is described, and (rather pointlessly) one and a half pages are devoted to prints of the ' soda-fountain ' type of instrument. In the face of this, no mention is made of the very important topic of ultra-violet microscopy!

The remaining chapters deal conventionally, but adequately, with the elementary aspects of spectra, radiation, photometry and colour. Giving the whole gamut of terminology in these latter subjects will leave the student bewildered, but well-informed if he does stay the course.

There seems to be no attempt in the book to justify the addition of amplitudes or intensities according as the light is coherent or incoherent. That the intensity may be expressed by the square of the amplitude also seems to be stated rather than proved. One might have expected these two fundamental subjects to receive some discussion.

The standard of printing and the excellence of the diagrams should be singled out for special praise. The plates illustrating diffraction represent some beautiful experimenting. (It should be noted, that Figure 9–3 is described as Fresnel diffraction in the caption, but as Fraunhofer diffraction in the text, page 226. The text is correct.) Many of the diagrams revert to the practice of white-on-black, as an older generation will recall to have been used in Edser's *Light*.

The criticisms that have been given of this book should not detract from the general impression of considerable merit.

H. H. HOPKINS.

A Survey of General and Applied Rheology, by G. W. Scott Blair. Pp. xvi + 314. Second Edition. (London: Sir Isaac Pitman & Sons Ltd., 1949.) 40*s*.

Dr. Scott Blair is one of the pioneers of rheology in this country and has recently been elected president of the British Rheologists' Club. His survey of general and applied rheology was first published in 1943 and there now appears a second edition bringing the work up to date.

The book contains an historical and general introduction to rheology, followed by a wide survey of rheological phenomena. The survey is conducted under two main headings: (1) rheological phenomena and their measurement and (2) rheological interpretation and the evidence of psycho-physics, with the view to re-establishing " that association between our science and psychology which was so strongly emphasized by the early Indian rheologists ". The book is addressed primarily to the practical rheologist and the physicist will not find it easy reading. For example, how many physicists would identify the ideal liquid of hydrodynamics from the description that " it resists pantathenic stresses, but without change of volume and has no deviator components in its stress tensor " ? Presumably the practical rheologist understands this language. Any physicist contemplating an excursion into the field of rheology will, however, find certain sections of the book particularly useful. These are (1) the classification of methods of measurement where, under each method, there appears a list of materials to which the method has been applied, each material being followed by appropriate references; (2) the brief summaries indicating the scope of papers on certain subjects, e.g. viscosity of liquid mixtures, thixotropy, and dilatancy; and (3) the comprehensive bibliography. These three sections occupy some 70 pages of the book.

J. W. FOX.

CONTENTS FOR SECTION A

PAGE
Prof. A. O. RANKINE. Experimental Studies in Thermal Convection (33rd Guthrie Lecture) . . . 417
Dr. R. SHUTTLEWORTH. The Surface Tension of Solids . . . 444
Mr. OM PARKASH and Mr. P. L. KAPUR. On the Temperature Dependence of Counter Characteristics in Self-quenching Geiger–Müller Counters . . . 457
Dr. G. KORTÜM and Dr. H. VERLEGER. The Pressure Broadening of the Vibration Rotation Band of the HCN Molecule at 10380 A. . . . 462
Dr. S. M. NAUDÉ and Dr. H. VERLEGER. The Vibration–Rotation Bands of the Hydrogen Halides HF, $H^{35}Cl$, $H^{37}Cl$, $H^{79}Br$, $H^{81}Br$ and $H^{127}I$ . . . 470
Dr. M. S. PATERSON. Calculation of the Correction for Instrumental Broadening in X-ray Diffraction Lines . . . 477
Dr. B. BLEANEY and Dr. J. H. N. LOUBSER. The Inversion Spectra of NH_3, CH_3Cl and CH_3Br at High Pressures . . . 483
Mr. W. M. GIBSON and Dr. L. L. GREEN. The Neutrons Emitted in the Bombardment of ^6Li by Deuterons . . . 494
Dr. K. J. LE COUTEUR. The Relationship between the Size of Nuclear Disintegration Stars and the Mean Energy of the Emitted Particles . . . 498
Dr. A. B. BHATIA. On the Scattering of Polarized Neutrons by Protons . . . 502
Dr. L. MICHEL. Interaction between Four Half-Spin Particles and the Decay of the μ-Meson . . . 514
Mr. F. D. S. BUTEMENT. Radioactive Dysprosium Isotopes . . . 532

Letters to the Editor :

Dr. J. V. JELLEY. The Radioactivity of Fluorine 20 . . . 538
Miss P. ROTHWELL and Mr. D. WEST. Proportional Counters in a Magnetic Field ; an Investigation of the Nuclear Isomerism in ^{80}Br . . . 539
Miss P. ROTHWELL and Mr. D. WEST. The Calibration of Proportional Counters with X-rays produced by Radioactive Sources . . . 541
Dr. R. L. F. BOYD. He_2^+ in the Helium Discharge . . . 543
Dr. M. AFAF. Bands of ZrF . . . 544
Contents for Section B . . . 546
Abstracts for Section B . . . 546

ABSTRACTS FOR SECTION A

The Surface Tension of Solids, by R. SHUTTLEWORTH.

ABSTRACT. A distinction is made between the surface Helmholtz free energy F, and the surface tension γ. The surface energy is the work necessary to form unit area of surface by a process of division : the surface tension is the tangential stress (force per unit length) in the surface layer ; this stress must be balanced either by external forces or by volume stresses in the body.

The surface tension of a crystal face is related to the surface free energy by the relation

$$\gamma = F + A(dF/dA),$$

where A is the area of the surface. For a one-component liquid, surface free energy and tension are equal. For crystals the surface tension is not equal to the surface energy. The standard thermodynamic formulae of surface physics are reviewed, and it is found that the surface free energy appears in the expression for the equilibrium contact angle, and in the Kelvin expression for the excess vapour pressure of small drops, but that the surface tension appears in the expression for the difference in pressure between the two sides of a curved surface.

The surface tensions of inert-gas and alkali-halide crystals are calculated from expressions for their surface energies and are found to be negative. The surface tensions of homopolar crystals are zero if it is possible to neglect the interaction between atoms that are not nearest neighbours.

On the Temperature Dependence of Counter Characteristics in Self-quenching Geiger–Müller Counters, by OM PARKASH and P. L. KAPUR.

ABSTRACT. The effect of temperature on the counting rate–voltage characteristics of self-quenching Geiger–Müller counters with internal and external cathodes (in this paper denoted as counters Nos. 1 and 2) has been investigated within the temperatures ranging from 8° to 60° C.

It is found that the average counting rate remains independent of temperature (within the statistical error limits), and this constancy is better in the case of the external cathode counter than with the other. As counter No. 1 shows a greater increase in slope at higher temperatures, the rate appears to be greater at higher applied potentials. Further, it is noticed that the plateau decreases and disappears at lower temperatures in the case of counter No. 1, while counter No. 2 does not show this effect. This is partly explained by the formation of semiconducting paths between the central wire and the cathode, the discharges along which give rise to spurious counts in the case of counter No. 1, and the absence of these in the case of counter No. 2.

It is also observed that the slope of the plateau increases and the width decreases with rise of temperature in both cases, though the increase in slope is more marked with counter No. 1 than with counter No. 2. The increase in slope is probably due to the presence of a greater number of multiple discharges or spurious counts at higher temperatures, an important point which is under study.

The investigation also brings about the advantage of the external cathode in the construction and design of G–M counters, especially when reliable observations are desired with a counter under widely changing temperature conditions.

The Pressure Broadening of the Vibration Rotation Band of the HCN Molecule at 10380 A., by G. KORTÜM AND H. VERLEGER.

ABSTRACT. The relation between the line-width of the 0–3 vibration–rotation band of HCN at 10380 A. and the pressure of the HCN gas, as well as the pressure resulting from the addition of different extraneous gases, was investigated. In the P and R branches of the band a relation was found between the half-line width and the rotational quantum number, J, which differs for the broadening due to self-pressure and the broadening resulting from pressure of extraneous gases. The results could be explained, according to London's theory, in the former case as an effect due to the combined action of rotational resonance alignment, and in the latter case to alignment alone. Measurements made with the addition of DCN suggest that the chain association of the hydrogen bridge bonds also has an effect on the half-width value.

The Vibration–Rotation Bands of the Hydrogen Halides HF, $H^{35}Cl$, $H^{37}Cl$, $H^{79}Br$, $H^{81}Br$ and $H^{127}I$, by S. M. Naudé and H. Verleger.

ABSTRACT. The 2–0, 3–0 and 4–0 bands of ${}^1H^{19}F$, the 4–0 and 5–0 bands of ${}^1H^{35}Cl$ and ${}^1H^{37}Cl$, the 4–0 band of ${}^1H^{79}Br$ and ${}^1H^{81}Br$, and the 4–0 band of ${}^1H^{127}I$ were photographed under great dispersion in the infra-red. The molecular constants have been calculated and are summarized in a table.

Calculation of the Correction for Instrumental Broadening in X-ray Diffraction Lines, by M. S. Paterson.

ABSTRACT. A new numerical procedure, based on relaxation methods, for calculating the correction for instrumental broadening in X-ray diffraction lines has been evolved. The corrected integral breadth and the true line profile are obtained without restrictive assumptions. The calculations for a practical example are given.

The Inversion Spectra of NH_3, CH_3Cl and CH_3Br at High Pressures, by B. Bleaney and J. H. N. Loubser.

ABSTRACT. The absorption due to the inversion spectrum of ammonia has been studied at pressures up to 6 atmospheres between wavelengths of 8 cm. and 8 mm. The resonant frequency is found to shift downward from 0·78 cm^{-1} as the pressure rises, becoming substantially zero above 2 atmospheres. The line width rises less rapidly than the pressure in the transition region, but ultimately becomes proportional to the pressure with an effective ' collision diameter ' of 7·7 A. These effects are attributed to multiple collisions, which become dominant at the higher pressures; the resonant inversion is then destroyed by the molecular interaction.

In the methyl halides the inversion frequency is virtually zero owing to the low probability of tunnelling through the barrier, but the absorption line is spread out to the centimetre wave region by the collision process. The collision diameters are found to be 7·7 A. and 9·0 A. for methyl chloride and bromide respectively.

The Neutrons Emitted in the Bombardment of ${}^6Li$ by Deuterons, by W. M. Gibson and L. L. Green.

ABSTRACT. The neutrons from deuteron bombardment of a separated ^{6}Li target have been studied by the photographic plate method. The energy release for the reaction

$${}^6_3\mathrm{Li} + {}^2_1\mathrm{D} \longrightarrow {}^7_4\mathrm{Be} + {}^1_0\mathrm{n}$$

has been shown to be 3·40 ± 0·05 Mev., and evidence is given for the existence of a level in ^{7}Be at 450 ± 60 kev. This is identified with the level at 430 kev. found in work on the reaction ${}^{10}B(p\alpha){}^7Be$.

The Relationship between the Size of Nuclear Disintegration Stars and the Mean Energy of the Emitted Particles, by K. J. Le Couteur.

ABSTRACT. Nuclear evaporation theory predicts that the mean energy of the protons evaporated from disintegration stars should increase with star size. It is shown that the calculated rate of increase is in agreement with experimental results.

On the Scattering of Polarized Neutrons by Protons, by A. B. BHATIA.

ABSTRACT. The scattering and the consequent depolarization of a polarized beam of neutrons by an unpolarized proton gas is suggested as a means of obtaining information about the interaction potential between a neutron and a proton. It is found that the interaction, if it were spherically symmetrical, could be determined from a knowledge of the polarization and scattering differential cross sections. A similar analysis with non-central interaction has not yet been carried out. In this case, however, the polarization depends also on the azimuth ϕ of scattering. This dependence of polarization on ϕ is calculated for (*a*) very low energies, (*b*) very high energies. The maximum azimuthal variations for incident neutrons of energy 1 MEV. and 100 MEV. are about 1% and 50% respectively.

It is hoped that in future experimental techniques for the production and measurement of a polarized beam of fast neutrons will be developed, since these would give important information about the interaction potential between a neutron and a proton.

Interaction between Four Half-Spin Particles and the Decay of the μ-Meson, by L. MICHEL.

ABSTRACT. The general direct coupling between four fermions is studied. It is a linear combination of the five invariants used in β-decay theory. Altering the order of the particles in the Hamiltonian changes only the coefficients of the linear combination. The formalism of charge conjugation is used with the ordinary theory or the Majorana abbreviated theory for neutral particles. This is applied to the study of the decay of the μ-meson into an electron and two neutrinos.

Radioactive Dysprosium Isotopes, by F. D. S. BUTEMENT.

ABSTRACT. A new isotope of dysprosium, identified as ^{166}Dy, has been studied. It has been shown that it is formed by thermal neutron capture in the 140 minute isomer of ^{165}Dy, the capture cross section being about 1,200 barns. It decays with a half-life of 82 hours and is the parent of 27 hour ^{166}Ho. It emits beta-particles, the energy of which was found by absorption in aluminium to be 0·22 MEV., and gamma rays of less than 50 kev. energy.

Another new isotope, ^{159}Dy, has been made both by slow neutron irradiation of dysprosium and by deuteron bombardment of terbium. It decays by orbital electron capture, with a half-life greater than 50 days. It will be described in a later paper.